REFERENCE ONLY

UNIVERSITY OF LONDON THESIS

Degree MD   Year 2007   Name of Author ROBERTS, Elved Bryn

COPYRIGHT

This is a thesis accepted for a Higher Degree of the University of London. It is an unpublished typescript and the copyright is held by the author. All persons consulting this thesis must read and abide by the Copyright Declaration below.

COPYRIGHT DECLARATION

I recognise that the copyright of the above-described thesis rests with the author and that no quotation from it or information derived from it may be published without the prior written consent of the author.

LOANS

Theses may not be lent to individuals, but the Senate House Library may lend a copy to approved libraries within the United Kingdom, for consultation solely on the premises of those libraries. Application should be made to: Inter-Library Loans, Senate House Library, Senate House, Malet Street, London WC1E 7HU.

REPRODUCTION

University of London theses may not be reproduced without explicit written permission from the Senate House Library. Enquiries should be addressed to the Theses Section of the Library. Regulations concerning reproduction vary according to the date of acceptance of the thesis and are listed below as guidelines.

A.   Before 1962.   Permission granted only upon the prior written consent of the author. (The Senate House Library will provide addresses where possible).

B.   1962-1974.   In many cases the author has agreed to permit copying upon completion of a Copyright Declaration.

C.   1975-1988.   Most theses may be copied upon completion of a Copyright Declaration.

D.   1989 onwards.   Most theses may be copied.

This thesis comes within category D.

☑   This copy has been deposited in the Library of _University College London_

☐   This copy has been deposited in the Senate House Library, Senate House, Malet Street, London WC1E 7HU.

Assessment of Coronary Artery Stenosis using

Myocardial Contrast Echocardiography.

Elved Bryn Roberts

Division of Medicine, University College London.

Thesis submitted in accordance with the requirements of

The University of London for the degree of

Doctor of Medicine

2006

UMI Number: U593255

UMI

Dissertation Publishing

DECLARATION OF ORIGINALITY

This thesis is original, relates entirely to work undertaken by Elved Roberts, and has not been submitted previously in support of a degree qualification or other award.

....

Elved B Roberts, March 2006

ABSTRACT

The theoretical advantage of perfusion data over wall motion data for diagnosing coronary artery stenosis relates to the temporal sequence of these phenomena in the ischaemic cascade. Myocardial perfusion evaluation could thus provide earlier information than wall motion assessment, with important clinical consequences. This thesis examines myocardial perfusion assessment using ultrasound and micro-bubble contrast in stable coronary artery stenosis.

The first set of experiments were undertaken to establish both a means of infusing Optison™ (GE Healthcare, UK), and of displaying static frame contrast signal using Power Contrast Imaging™ (Acuson Sequoia™, Siemens Medical Solutions, Mountain View, CA, USA.). Three Optison™ concentrations, five infusion rates, and five trigger intervals were evaluated. This revealed an appropriate concentration and infusion rate for Optison™ and identified an ideal trigger interval of one in four cardiac cycles.

The second part of this study evaluated Power Contrast Imaging™ with Optison™ infusion in stable single or double vessel coronary artery stenosis. Perfusion assessment during Adenosine vasodilator stress was compared with standard wall motion assessment during Dobutamine stress, coronary angiography being the diagnostic standard. Among twenty-eight subjects and eighty-four coronary territories, Power Contrast Imaging™ had low sensitivity but equivalent specificity compared to wall motion assessment.

The third component of this research evaluated micro-bubble preserving real-time Coherent Contrast Imaging (Acuson Sequoia™, Siemens Medical Solutions) alongside Optison™ infusion in stable single or double vessel

coronary stenosis. Thirty-eight subjects and one hundred and fourteen coronary arteries were evaluated. Each subject underwent Dobutamine stress, during which standard wall motion, contrast wall motion, and contrast perfusion imaging were all assessed, the diagnostic standard being coronary angiography. This demonstrated that contrast wall motion evaluation is accurate and that combined contrast wall motion and perfusion imaging is at least equivalent to standard wall motion imaging alone for detecting underlying coronary stenosis.

ACKNOWLEDGMENTS

TABLE OF CONTENTS

CHAPTER THREE: INTERMITTENT POWER CONTRAST IMAGING™ IN STABLE CORONARY ARTERY DISEASE

CHAPTER FOUR: REAL-TIME COHERENT CONTRAST IMAGING™

IN STABLE CORONARY ARTERY DISEASE

INTRODUCTION

Coronary Heart Disease (CHD) is a leading cause of morbidity and mortality in the Developed World and is the main cause of death in Europe, accounting for 2 million deaths per annum. Approximately 2.6 million people in the United Kingdom have CHD [1], which accounted for 233000 deaths in 2003 [2]. Despite a promising reduction in Heart Disease deaths between 1997 and 2002, which was optimistically heralded as indicative of potential elimination of premature CHD death within a decade [3], trends in physical inactivity, Obesity, and Type Two Diabetes Mellitus are likely to offset these long term mortality improvements. To impact on CHD outcomes, primary prevention needs to be supported by early and accurate diagnosis of established disease, allowing appropriate symptomatic and prognostic therapies to be implemented in a timely fashion. While accurate diagnosis of CHD is achievable by means of coronary angiography, this is an invasive procedure with an associated mortality risk and it is not appropriate as a general means of investigating patients with symptoms that might have a cardiac origin. Non-invasive investigations are required for this purpose, at least as a first line approach.

Echocardiography has become integral to clinical cardiology and developments in stress techniques have broadened its scope to include functional assessment of coronary artery stenosis. Despite progress in computed tomographic, magnetic resonance and radionuclide imaging, there is a need for an inexpensive, efficient, mobile, non-radiological and non-invasive technique for assessment of coronary artery disease. Echocardiographic quantification of myocardial perfusion would

fit this requirement and would complement existing cardiac ultrasound capability, including stress echocardiography.

It has been evident for decades that it is possible to introduce certain substances into the vascular space and then visually display the interaction between incident ultrasound waves and the substance, effectively creating an intra-vascular tracer. These substances are typically composed of a fluid solution of micro-bubbles containing a gaseous core. The particular property that enables these substances to act as intra-vascular tracers is the ability to reflect ultrasound at harmonic frequencies such as double or triple the incident ultrasound wave frequency. If such tracers remain predominantly within the vascular space, they can theoretically be used to highlight cardiac cavities, coronary and other vessels, and the capillary bed of myocardial and other tissues. The myocardial contrast echocardiography research community has been aware of this fact for some time, but has been hindered by limitations in physical characteristics of ultrasound contrast agents, machine hardware, and processing software.

Recent developments in ultrasound contrast agent design have ensured sufficient stability that micro-bubbles can survive from venous injection through pulmonary circulation and the left sided cardiac chambers to the coronary arteries and myocardial vascular bed. Parallel advances in echocardiographic imaging, including harmonic and related capabilities, have allowed visual display of the effect of such agents on ultrasound backscatter. Considerable data exists on accuracy of contrast echocardiographic myocardial perfusion assessment under experimental conditions, especially by intra-coronary contrast injection.

Whether myocardial perfusion assessment using peripheral venous injection routes is reliable in clinical practice has been unclear and has been the subject of growing interest over recent years. In order for such a technique to be of clinical use, it would need to have a diagnostic efficacy at least equivalent to that of techniques such as stress echocardiography and nuclear perfusion assessment.

This Thesis is based on the feasibility and diagnostic utility of myocardial contrast echocardiographic perfusion assessment in clinical practice.

Chapter One begins with a review of other directly relevant assessment techniques, including basic clinical evaluation, Electrocardiography (resting and stress), Nuclear perfusion methods, Computed Tomography, Magnetic Resonance Imaging, and Stress Echocardiography. There follows a discussion of the dynamics of coronary and myocardial blood flow in health and disease, illustrated with reference to some of the physiological research enabled by early myocardial contrast imaging techniques. The next section deals with micro-bubble characteristics, design, and development. The final section of the first chapter reviews the major technical developments in ultrasound system design that have made echocardiographic myocardial perfusion assessment possible.

Chapter Two details a series of experiments designed to establish a means of infusing micro-bubbles such that supply to the myocardial vascular bed is constant. These experiments used Optison™ (GE Healthcare, UK) and the Power Contrast Imaging™ facility on the Acuson Sequoia C256 ultrasound system (Siemens Medical Solutions, Mountain View, CA, USA), a form of intermittent

high power ultrasound imaging capable of demonstrating myocardial perfusion. The technique involves intermittent image acquisition at between one and eight cardiac cycle intervals.

Chapter Three details a study of the feasibility and diagnostic efficacy of the Acuson Power Contrast Imaging™ system for detection of stenotic and non-stenotic coronary arterial supply during Adenosine hyperaemia, using the Optison™ infusion system described in Chapter Two. The technique is compared with Dobutamine Stress Echocardiography, X-ray Coronary Angiography being the reference standard for significant coronary artery stenosis.

The logical progression from intermittent perfusion imaging, which by definition cannot utilise wall motion data, is to real-time perfusion imaging. Chapter Four details a study of the feasibility and diagnostic efficacy of the Acuson Coherent Contrast Imaging™ real-time perfusion system for detection of stenotic and non-stenotic coronary arterial supply during Dobutamine stress. For this investigation, Dobutamine Stress Echocardiographic wall motion was used as the comparison technique, and X-ray Coronary Angiography was used as the reference standard for significant coronary artery stenosis.

The final Chapter is a summary of the major findings of this work, followed by a discussion of the implications for further research and clinical practice.

CHAPTER ONE

ESTABLISHED INVESTIGATIVE TECHNIQUES, UNDERLYING PHYSIOLOGY, AND EARLY DEVELOPMENTS IN ULTRASOUND PERFUSION ASSESSMENT

1. ESTABLISHED TECHNIQUES FOR FUNCTIONAL ASSESSMENT OF CORONARY ARTERY STENOSIS

(i) Clinical Assessment

Angina Pectoris was first described in 1772 by William Heberden (the elder), with details of his observations of twenty patients appearing in the Royal College of Physicians of London report *"Medical Transactions"* under the title *"Some Account of a Disorder of the Breast"* [4]. A more complete description appeared some years later, based upon his assessment of nearly one hundred patients, sometimes over as much as a sixteen-year period. The condition was described as a painful, disagreeable sensation in the chest initially brought on by exertion or stress, especially after meals, and eventually occurring at rest. Radiation of pain to the left arm was noted to be common. There was specific reference to the strangling sensation often characterising the condition, as well as accompanying anxiety and even the sense of imminent death during a prolonged attack. The observation that the discomfort would ease quickly with physical rest was clearly stated, as was the fact that symptom cessation would occur with less rapidity after a number of years with the condition. Heberden described a prolonged course of symptoms, often lasting more than a decade, with gradual increases in frequency and severity of attacks, but with apparently preserved health between

episodes. He not only described in considerable detail the main presenting features of the condition, but also highlighted variants such as pain extending to the right arm, epidemiological aspects such as preponderance among men aged over fifty years of age, and the absence of tachycardia during an attack. Perhaps the most noteworthy aspect of the account is a clear description of the condition's termination, which he noted to be characterised by abrupt collapse followed by almost immediate death. This description of Angina Pectoris has stood the test of time and remains to this day as thorough and detailed an evaluation of the symptoms and course of Angina Pectoris as can be found in most textbooks. However, there are deficiencies in Heberden's account that have been clarified over the subsequent two hundred years. For example, although use of the adjective "strangling" in relation to the character of ischaemic chest pain is common, it is also relatively frequent to find descriptions such as "aching", "dull", and "burning" in confirmed myocardial ischaemia. In addition, the site of discomfort can often include the neck, face, or upper back, and isolated exertion induced breathlessness may be the presenting feature. The latter two features appear to be more common in the very elderly [5]. Despite the relative ease with which typical symptoms can be labelled as Angina Pectoris, diagnosing less typical cases and confidently labelling certain symptoms as being of non-ischaemic origin can be difficult. In addition, clinical features do not usually give a reliable impression of the severity of underlying coronary disease, nor of prognosis. Furthermore, chest pain due to acute coronary plaque instability with associated spasm and thrombosis often presents with sudden onset of non-specific chest discomfort at rest. Incorporating certain other clinical features, including risk factors for CHD and physical findings such as obesity and

stigmata of Hyperlipidaemia, may help determine the likelihood of CHD in a population, but this approach is not particularly helpful when attempting to diagnose an acute episode in an individual. In addition to difficulties precisely defining the origin of symptoms such as chest pain, history and physical examination are unable to quantify silent myocardial ischaemia in patients with possible underlying CHD but without chest pain. The qualitative features and subtle clinical variations in Angina Pectoris do not lend the condition to easy quantitative measurement, and there is consequently relatively little published scientific data on diagnosis based on the history and physical examination alone. Despite the popular notion that cardiac pain is easy to diagnose, there is evidence that more experienced physicians are less likely to discharge patients presenting with acute onset chest pain than less experienced physicians [6], reflecting experience based appreciation of the above difficulties. Thus, a more sensitive and specific means of diagnosing myocardial ischaemia is needed.

(ii) The Electrocardiogram

The resting twelve lead electrocardiogram (ECG) can provide supporting evidence for CHD in the form of Q waves, ST segment and T wave abnormalities, left bundle branch block, and arrhythmia. Berger et al found that any ECG abnormality in patients presenting acutely with chest pain had a sensitivity of 98% for underlying coronary artery disease, while ST segment shift and T wave abnormalities had a sensitivity of 86% [7]. However, Gregoire et al found the sensitivity of ECG abnormality to be only 65%, with a specificity of 63% in similar circumstances [8]. It is important to note that these data relate to acute chest pain onset. Sensitivity and specificity values are significantly lower

in populations with stable Angina Pectoris without previous myocardial infarction, as these patients usually have normal resting myocardial perfusion.

Certain electrocardiographic changes provide evidence of previous manifestations of coronary artery disease. For example, pathological Q waves suggest previous myocardial infarction, which can be taken as additional evidence that ongoing symptoms may be of ischaemic origin. In addition, previous myocardial infarction, especially if extensive and anterior characterised by anterior electrocardiographic Q waves, suggests adverse long-term prognosis. Left bundle branch block may also be due to previous myocardial infarction, although other causes such as hypertension and left ventricular impairment are frequent. Indeed, numerous electrocardiographic abnormalities can relate to non-coronary conditions. Typical examples in clinical practice include abnormalities of ST segments and T waves being secondary to left ventricular hypertrophy, digitalis therapy, and electrolyte disturbances. Furthermore, such changes can be normal variants.

A theoretical advantage of ECG over history and physical examination alone is the possibility of localising the region of ischaemia to a certain vascular territory. While some data suggests anterior ST segment and T wave abnormalities are associated with Left Anterior Descending coronary artery stenosis [9], the territorial correlation between ST segment abnormality and underlying coronary stenosis in stable Angina is generally weak and cannot be relied upon to make clinical judgements.

The inability of resting electrocardiography to detect underlying coronary disease with sufficient accuracy to enable clinical decision-making has led to the suggestion that provision of ECG recordings for patients with recent onset chest pain should be replaced by full clinical assessment in a Cardiology setting [10]. Evidence of general acceptance of this notion can be seen in National Service Framework format as the current recommended United Kingdom model for assessing patients with new cardiac symptoms [11].

(iii) Stress Electrocardiography

Increased cardiac workload generates increased metabolic demand, which in turn is met by increases in myocardial blood flow, provided there are no restrictions to normal physiological responses. When coronary artery disease limits the necessary augmentation in coronary arterial flow, ischaemia develops. This sequence of events gives rise to electrocardiographic changes such as T wave inversion and ST segment shift. This principle is used in stress electrocardiography, the usual stressor being treadmill exercise and the usual protocol being that of Bruce and Hornsten [12]. Treadmill stress electrocardiography is undoubtedly the most widely used form of stress testing in the United Kingdom, where virtually every Cardiac department is set up to process a significant inpatient and outpatient caseload by means of this tool.

The accuracy of exercise electrocardiographic ST segment depression for presence of coronary artery disease is very variable, and resulting predictive values depend on the prevalence of coronary artery disease as well as other specific characteristics in the population under investigation [13,14]. Previous

studies suggest sensitivities of 40%, 66%, and 75% for single, double, and triple vessel disease respectively [15,16], but a meta-analysis of use of exercise electrocardiographic ST segment depression to diagnose coronary artery disease reported a mean sensitivity of 68%, range 23-100%, standard deviation 16%, and a mean specificity of 77%, range 17 to 100%, standard deviation 17% [17]. When used in the common clinical setting characterised by mixed pre-test coronary artery disease probability, co-morbidity, and age, the diagnostic effectiveness of stress electrocardiography starts to fall. In elderly patients, relatively limited exercise capacity and the high prevalence of baseline electrocardiographic abnormalities significantly limits the usefulness of this investigation [18-20], while there are diagnostic and prognostic limitations in female populations due to a combination of factors such as limited exercise capacity, baseline electrocardiographic changes, and a high false positive rate [21]. In general, the electrocardiographic territory in which ST segment change occurs does not correlate well with the territory of angiographic stenosis [14,15,22-24], although there may be specific situations in which ST depression in lead V1 or the right precordial leads improves the sensitivity of the test [25,26]. Specific factors likely to give false positive results include digitalis therapy [27,28], hypokalaemia [29,30], pulmonary hypertension [31], left ventricular hypertrophy [32,33], mitral valve prolapse [34,35], bundle branch block [36], and pectus excavatum [37]. Despite problems with the accuracy of exercise electrocardiography, prognostic information can be obtained. For example, studies concur in the suggestion that those with significant ST segment depression have a relatively high likelihood of experiencing cardiac events in subsequent years [38-44]. In addition, incorporating factors beyond the degree of ST segment depression appears to confer prognostic

information. Those incapable of exercising to 6 minutes of the Bruce protocol or unable to achieve a heart rate of at least 85% of their predicted maximum have an increased risk of cardiac events, while those capable of exceeding the equivalent of ten metabolic equivalents are thought to have a good prognosis [45-47]. The Duke treadmill score [45] and Long Beach Veteran's Administration score [48] allow prognostic stratification by incorporating clinical, electrocardiographic, and exercise capacity data. However, prognostic stratification based on treadmill exercise tests is heavily based on exercise capacity as a whole, which is more likely to be limited in those with co-morbidity, a group who are in turn more likely to suffer cardiac and other events during follow up.

Summary: Exercise Electrocardiography

Despite its wide availability and routine clinical use, there are major limitations to exercise electrocardiography including limited sensitivity and specificity and lack of territorial correlation.

(iv) Nuclear Perfusion Imaging

Nuclear cardiac imaging can be achieved using a Gamma Camera or Positron camera. Gamma cameras allow planar or tomographic imaging by detection of single photons (Single Photon Emission Computed Tomography, SPECT), while Positron cameras allow imaging by detection of paired photons emitted by tracer material and rejection of single scattered photons, thus improving spatial resolution and minimising tissue attenuation (Positron Emission Tomography, PET).

Single photon approaches include Radionuclide angiography and Myocardial perfusion imaging. The former method allows assessment of ejection fraction and regional wall motion using agents such as Technetium-99m, while the latter allows assessment of myocardial perfusion itself using Thallium-201 or Technetium-99m based agents. Nuclear perfusion methods rely on the fact that certain tracers are extracted by viable myocardial tissue, resulting in spatial distribution in proportion to regional blood flow and volume. For detection of ischaemia and infarction, images acquired shortly after physical stress or pharmacological hyperaemia are compared to those acquired a number of hours later, after redistribution of tracer has taken place. Infarction is represented by a fixed defect and ischaemia is represented by a reversible defect. In addition, by using protocols and tracers suited to delayed post-redistribution image acquisition, markedly under-perfused but viable tissue representing hibernating myocardium can be detected. Certain differences between Technetium-99m and Thallium-201 based imaging account for minor differences in applicability, but in general the methods are comparable in terms of sensitivity and specificity for coronary artery disease [49-53].

Positron Emission Tomography utilises agents such as Rubidium-82, oxygen-15 water, and Nitrogen-13 ammonia to depict perfusion. The short half-life of such agents allows serial imaging within a short time period, which is ideal for protocols involving stress or hyperaemia. Metabolic activity, estimated using F-18 fluorodeoxyglucose, and associated perfusion information can be used together to assess viability in regions of wall motion abnormality. Using this approach, metabolically active tissue can be identified as hibernating

myocardium. Some studies suggest PET scanning may be more accurate than Thallium-201 SPECT [54,55].

The accuracy of SPECT imaging for diagnosis of coronary artery disease is variable. Diagnostic effectiveness depends, like exercise electrocardiography, on certain patient characteristics and the overall population disease prevalence. Thallium-201 SPECT scintigraphy has, in general, been more accurate than planar techniques [56]. In addition, computer coding of regional perfusion signal derived from numerous tomographic planes allows three-dimensional perfusion maps to be generated, which can be automatically compared to normal control regions for a quantitative assessment of perfusion [57-63]. Using such techniques, a sensitivity of 90% and specificity of 70% has been suggested [64], although previous non-quantitative analysis had already been shown to have a mean sensitivity of 89% and specificity of 76% [65,66]. However, specificity in this range is disappointing and problematic in clinical practice. In a bid to minimise the impact of this moderate degree of specificity, the same authors "qualify" it by stating a "normalcy rate" of 89% for patients who have not undergone cardiac catheterisation and have no clinical or stress electrocardiographic evidence of coronary artery disease [64]. This represents the proportion of patients without other clinical or exercise electrocardiographic evidence of coronary artery disease who can be expected to have a normal Thallium-201 perfusion study. Hence, 11% of patients with no other evidence of coronary artery disease who have not undergone cardiac catheterisation, will have a positive Thallium-201 SPECT study. While some of these will have otherwise latent epicardial coronary artery disease, a significant proportion will not.

25

Despite problems with specificity, the territory and size of a Thalium-201 perfusion defect relates to the site and functional significance of coronary artery disease. For example, prevalence of Thallium-201 perfusion defects among patients with significant left main stem disease is very high [51,67-70], while large severe defects correlate well with severe proximal vessel disease [71-74]. To some extent, coronary artery stenosis location and severity correlate with perfusion defect size [75-79], but most importantly number of reversible defects has been shown to be a very reliable predictor of future cardiac events [80-82].

While it is true that Thallium-201 SPECT scintigraphy is sensitive and prognostically useful, specific clinical situations reduce its' accuracy. For example, there is evidence to suggest that the sensitivity of the technique is reduced in women [83,84]. Another factor limiting the usefulness of SPECT imaging is Obesity due to adipose tissue related photon attenuation. This can be significantly overcome by using Technetium-99 based methods or PET. In addition, left bundle branch block increases the likelihood of a false defect in the septal region, especially during exercise stress [85-87]. Such artefact may be minimised by using pharmacological hyperaemia rather than exercise stress [88,89].

Summary: Nuclear Perfusion Methods:

Nuclear perfusion methods have a definite role in the diagnosis, localisation, and prognostic stratification of coronary artery disease. These techniques have an extremely valuable complementary role alongside other investigational approaches. However, certain drawbacks can be a limitation in clinical practice. Firstly, despite being "non-invasive", nuclear methods by definition rely upon

nuclear isotope exposure, with albeit small associated risks. In addition, nuclear methods for assessment of coronary artery disease are not portable, are relatively time consuming, and remain expensive compared with other methods such as stress electrocardiography and echocardiography. Furthermore, the specificity of nuclear perfusion techniques in certain situations can be a significant problem in clinical practice.

(v) Computed Tomographic Imaging

Cardiac imaging by Computed Tomography is achieved by Electron-Beam (EBCT) or Multidetector-Row CT (MDCT). The EBCT method involves a focused electron beam being swept across the target structure, while the MDCT method uses a rotating X-ray source and detector that allow data acquisition in a spiral fashion. EBCT has a higher temporal resolution and lower spatial resolution than MDCT.

Computed Tomographic Assessment of Coronary Calcium:

Coronary calcification is part of the atherosclerotic condition, and is found in a variety of coronary artery plaques [90,91]. While many imaging modalities can detect the simple presence or absence of coronary calcification, quantification can only be achieved using computed tomography, and there are a number of specific methods for this within the field [92,93]. For purposes of diagnosis, high coronary calcium levels are sensitive but not specific markers of significant coronary stenosis [94]. However, EBCT appears to have high prognostic value, with high coronary calcification burden being strongly linked to future cardiac events [95]. Indeed, it has been suggested that the technique might prove useful in

targeting prognostically beneficial therapies to high risk individuals [96]. MDCT

has been shown to be capable of differentiating soft, intermediate, and calcified

coronary plaques [96], and may allow imaging of segments of non-calcified

coronary disease at the expense of motion artefact relating to a relatively poor

temporal resolution [97]. EBCT has been considered the best way to assess

calcification within atherosclerotic plaques for some time [92], and has been

advocated as a means of non-invasive diagnosis and follow-up among certain

patient groups [94].

Computed Tomographic Coronary Angiography:

- Both EBCT and MDCT have been evaluated in conjunction with intravenous

contrast for the assessment of coronary artery stenosis, with variable stated

accuracies and proportion of cases affected by insufficient visualisation. For

example, Achenbach et al reported 92% sensitivity and 94% specificity [98], while

Budoff et al published an EBCT series with 78% sensitivity and 91% specificity

for identification of significant coronary artery stenosis against the gold standard

of quantitative X-ray angiography [99]. However, the former study excluded 25%

and the latter 11% of vessels on grounds of poor visualisation. In another study,

32% of imaged vessels had to be excluded before reaching a sensitivity of 85%

and specificity of 76% [100]. On the other hand, excellent specificity (98%) and

moderate sensitivity (78%) has been achieved with exclusion of only 6% of

segments by utilising good beta-blockade to minimise motion artefact before

image acquisition [101]. MDCT advances over recent years have continued, with

ever-greater spiral rotation speed and increasing detector numbers, with

consequent improvements in resolution.

Summary: Computed Tomographic Techniques:

Both EBCT and MDCT have roles in the diagnosis and prognostic assessment of coronary artery disease by means of detecting stenosis angiographically and by coronary calcium quantification. Image acquisition is fast and entirely non-invasive. However, a significant proportion of the coronary arterial tree may be poorly imaged, radiation is involved, and these techniques are not portable. Despite the outstanding recent advances in computed tomographic techniques, it would appear that there is still a niche for an alternative, non-radiation based, and portable technique of coronary artery disease assessment.

(vi) Magnetic Resonance Imaging

Magnetic resonance images are created by detecting changes in proton alignment after application of magnetic field and radio-frequency pulses. Proton realignment during this process is dependent upon relaxation time, proton density, molecular diffusion, and tissue motion, among other variables. Images are constructed by encoding proton realignment, which can be taken as a marker of tissue characteristics. Certain processing steps and contrast enhancement can be used to help delineate coronary vessels and other moving structures, although there are definite limitations to the technique when it is used to image small moving structures.

Three types of Coronary Magnetic Resonance Angiography (CMRA) have been investigated. Firstly, 2-dimensional breath-hold techniques were evaluated, with sensitivities for significant coronary stenosis from 63% to 90% and specificities from 89% to 92% in the first published studies [102-104]. The next "generation"

CMRA technique was 3-dimensional retrospective respiratory navigator-gated imaging. This was expected to improve accuracy, but in fact made no real difference to published results, which included sensitivities from 38% to 83% and specificities from 54% to 95% for coronary stenoses in excess of 50% luminal diameter [105-113]. Later work, using 3-dimensional prospective respiratory gating, demonstrated successful imaging of the proximal and middle sections of 84% of coronary vessels in one hundred and nine patients referred for coronary angiography. CMRA accuracy for diagnosing coronary artery disease was 72%, while not a single case of left main stem or proximal triple vessel disease of ≥50% luminal diameter was missed [114]. Specificity for left main or proximal triple vessel disease in this study was 85%. Accuracy has continued to improve as second generation methods requiring long acquisition times, hence lengthy breath holding, have given way to third generation techniques that are capable of multiple slice imaging in a single breath-hold. While accuracy with this method is still variable, two experienced groups have shown sensitivities of 86% and 68%, and specificities of 91% and 97%, with and without contrast enhancement respectively, for coronary stenosis in excess of 50% luminal diameter [115,116]. A potential role for CMRA, even if lower sensitivities for distal vessels remains, might be to stratify patients according to the existence of left main stem or proximal triple vessel disease, on the basis that prognostically beneficial treatments such as coronary artery bypass surgery might only apply in these groups. This concept has some validity, but it should be noted that percutaneous revascularisation is increasingly undertaken for patients with coronary artery disease patterns that do not strictly require surgical revascularisation. If non-invasive imaging strategies were only capable of determining patterns such as

proximal triple vessel or left main stem disease, many patients would eventually undergo X-ray coronary angiography regardless of the results of initial imaging, with a view to percutaneous interventional therapy.

Summary: Magnetic Resonance Techniques:

The first clinical results of CMRA demonstrating excellent sensitivity of 90% and specificity of 92% against standard radiographic coronary angiography [102], were met with enthusiasm and expectation in 1993. Despite major advances in the technique in the decade since, these results have not been matched. Optimistic expectations that CMRA would be the major non-invasive coronary imaging technique have dwindled and are replaced by the hope that it will help complement existing non-invasive and invasive means of assessing coronary disease, and might perhaps be used to stratify patients into low and high likelihood of having major coronary disease prior to invasive investigation. CMRA techniques capable of sub-millimetre imaging resolution are currently being assessed [117], and it is likely that such developments coupled with improved contrast agent design will lead to this safe, non-radiation based method of cardiac imaging being used increasingly in clinical settings. However, for the time being CMRA is expensive, moderately accurate, and not widely available. It is also nowhere near as portable a tool as echocardiography.

(vii) Stress Echocardiography

The central tenet of stress echocardiography relates to the series of events depicted by the ischaemic cascade [118,119]. The first event is ischaemia induced by increased cardiac workload, which is followed sequentially by diastolic

dysfunction, systolic dysfunction, electrocardiographic changes, and symptoms such as chest pain (Figure 1.1). Furthermore, regional ischaemia gives rise to regional systolic dysfunction, which in turn can be assessed echocardiographically [119]. It was clear that wall motion abnormalities could be induced by ischaemia long before stress echocardiographic assessment of this phenomenon was possible [120], but advances in echocardiographic image acquisition and processing over the last ten to fifteen years, especially the ability to digitise images, have resulted in this technique becoming a standard clinical investigative tool. The required stress can be achieved by exercise or pharmacological means. The most widely used form of exercise stress is treadmill testing, while the most widely used pharmacological approach is Dobutamine infusion. However, bicycle exercise stress, Arbutamine, Dobutamine-Atropine, Dipyridamole, and Adenosine have been used with success.

Evidence for the ability of stress echocardiography to accurately diagnose coronary artery disease is overwhelming [121-129]. A review of published data up to 1997 showed sensitivity of 80%, specificity of 84%, and accuracy of 81% among 2246 patients [130] while head to head comparison with nuclear perfusion estimation has revealed either equivalent or superior sensitivity of nuclear perfusion methods and equivalent or superior specificity of stress echocardiography [126,131-133]. Prognostic value of stress echocardiography for prediction of future cardiac events has been found to be strong among various populations [134-137], although it is true that nuclear perfusion has been studied in a wider set of population types. Perhaps the most practically useful and clinically

relevant aspect of Stress Echocardiography is that the technological requirements for it are entirely in keeping with the technological requirements for modern clinical echocardiography in general. Stress Echocardiography can therefore be part of a General Echocardiographic laboratory set up, without the need for extensive provision of additional equipment, space, data storage, archiving facilities, appointment systems, insurance and maintenance contracts, and administrative time. This tremendous capacity of a single system to generalise for multiple functions is especially impressive when one considers that myocardial perfusion might soon be added to the capabilities of clinical echocardiography. In addition, the hardware required is entirely portable and does not require special provision of lead lined screening for radiation protection.

However, Stress Echocardiography does demand specific investment in skilled personnel, ongoing training, and quality assurance [138]. The United Kingdom has been relatively slow to take up Stress Echocardiography widely, although centres of excellence and leading research are based here. Furthermore, despite advances in ultrasound such as second harmonic imaging, wall motion interpretation is sometimes misleading. False negative stress echocardiographic studies may occur if stress levels are sub-optimal, with poor image quality, and in single vessel stenosis. False positive studies may also occur if images are sub-optimal. Although the rate of non-interpretable studies has fallen with the use of second harmonics and ultrasound contrast (for cavity / endocardium delineation), the fundamental limitation for this technique is a poor echocardiographic window, which seems less of a problem with nuclear, Computed Tomographic X-ray, and Magnetic Resonance based methods.

Summary: Stress Echocardiography

Stress Echocardiography is a non-invasive, non-radiation based, portable technique that allows assessment of the full spectrum of cardiac haemodynamics as well as myocardial ischaemia. As such, it is well suited to routine clinical practice. However, as illustrated by the ischaemic cascade, perfusion defects occur before systolic wall motion abnormalities, and development of echocardiographic techniques to enable perfusion to be assessed would strongly complement current echocardiographic capability. This would allow haemodynamic, wall motion, and perfusion information to be derived from a single non-invasive and non-radiation based technique.

2. MYOCARDIAL PERFUSION DYNAMICS

(i) Vascular Anatomical Factors

As with all vasculature, vessel types supplying myocardium start with arteries and sequentially involve arterioles, capillaries, venules, and finally veins (Figure 1.2). All of these share an endothelial inner layer, while arteries, arterioles, venules, and veins share variable amounts of elastin, smooth muscle, and collagen in respective outer layers towards the vessel's external surface. The major difference between capillaries and other vessel types is therefore the lack of smooth muscle, and consequently lack of the typical vasoconstrictive properties found elsewhere. Similarly, absence of elastin results in almost no capillary distensibility [139]. These anatomical differences have important consequences for auto-regulation of blood flow.

(ii) Micro-bubbles as Flow Tracers

Both physiological and patho-physiological understanding of myocardial perfusion has been clarified using Myocardial Contrast Echocardiography. The micro-bubbles comprising ultrasound contrast material behave as pure intravascular tracers. Hence, signal intensity from reflected ultrasound relates to myocardial micro-bubble concentration in the ultrasound field, which has in turn been shown to depict myocardial blood volume [140]. When imaging during steady state contrast agent infusion, signal enhancement in the myocardium is due to the micro-bubbles that are in the capillaries at the moment of imaging, which can then be used as a marker of capillary blood volume. This constitutes 90% of the total myocardial blood volume [141-144].

(iii) Myocardial Blood flow in Health

Auto-regulation of blood pressure within the microvascular compartments can be divided into intrinsic and extrinsic components.

While intrinsic auto-regulation in the brain and kidney depend on *myogenic* factors to maintain constant perfusion pressure irrespective of fluctuations in arterial pressure, the Heart depends much more on *intrinsic metabolic autoregulation*, mediated by local factors such as temperature, nitric oxide, adenosine and related compounds, lactate, pyruvate, and potassium concentration. *Intrinsic humoral autoregulation*, involving kallikrein, bradykinin, and histamine also play a role in local alteration of blood supply, although more so in exocrine, cutaneous, and gastrointestinal tissue than in the heart.

Extrinsic *sympathetic and parasympathetic nervous* and *adrenergic humoral* factors are involved in auto-regulation, but again less so in myocardium compared to systemic tissues [139].

Myocardial tissue extracts a large proportion of available substrates for metabolic function from supplying vasculature, such that there is little residual capacity to meet greater metabolic demand. Consequently, myocardial blood flow must increase dramatically to meet the metabolic requirements of increased cardiac workload. Under physiological conditions, this is believed to occur by means of vascular dilatation and capillary recruitment.

Determination of capillary flow is complex, and depends on a mixture of intrinsic and extrinsic factors affecting arteries, arterioles, and venules without actual vasoconstriction or dilatation of the capillaries themselves. There has been considerable debate as to the site of myocardial blood flow autoregulation. Some data has suggested predominant vasomotor control of overall blood flow at an arterial and arteriolar level, involving vessels of 100um to 150um diameter [145,146], while other findings have suggested autoregulation predominantly by means of *"recruitment and decruitment"* of unutilised capacity at the capillary level [147-151]. The notion behind capillary recruitment is that, at basal levels, a significant proportion of a capillary network does not participate in blood circulation, while at levels of increased work, capillary networks saturate with blood. The gatekeepers of this variable capillary blood saturation are smooth muscle components in the walls of pre-capillary arteriolar tissue, the so-called pre-capillary sphincters. It is suggested that during basal non-hypoxic conditions,

pre-capillary sphincters are capable of diverting blood away from capillaries through "thoroughfare channels" directly to venules, thereby bypassing the major network through which cellular metabolic function occurs. Under conditions requiring additional metabolic capacity, pre-capillary sphincters are thought to alter the supply of capillary networks such that maximal use is made of capillary surface area, thus enhancing nutrient and oxygen supply. However, this concept is not entirely supported by myocardial contrast echocardiographic perfusion data. In reality, it may be that arteriolar vasomotor and capillary recruitment and decruitment co-regulate tissue blood flow, as evidenced by discrepancies between measured and predicted variables according to models based exclusively on either one or other assumption [152].

(iv) Myocardial Blood Flow in Disease

Myocardial ischaemia occurs if myocardial blood flow is insufficient to meet myocardial oxygen demand. The resulting switch from aerobic to anaerobic metabolism, accompanied by a number of biochemical changes, leads to contractile impairment, electrophysiological changes, and varying clinical features. Adenosine produced during ischaemia leads to arterial and arteriolar dilatation as well as stimulation of sensory afferent nerves, resulting in the patient suffering noxious effects such as chest pain. Disease dependent local abnormalities in collateralisation, cellular respiration and microvascular function greatly complicate the model of normal coronary haemodynamics derived from the controlled and standardised conditions necessary for animal experiments, which constitute much of the published findings relating to microvascular physiology. Gould and Lipscomb are credited with the original demonstration of

dynamics of myocardial blood flow in coronary artery stenosis. They showed that normal perfusion is maintained under basal conditions at up to 85% coronary artery stenosis, while a normal hyperaemic response occurs at stenoses of <50% luminal diameter, and a blunted hyperaemic response at between 50 and 85% coronary stenosis [153]. This led to the widespread assumption that inter-territory relative myocardial blood flow mismatch was responsible for the perfusion defects seen in territories supplied by stenotic coronary arteries on scintigraphic myocardial perfusion imaging. Subsequent work has cast doubt on this as an isolated mechanism, suggesting that there is an absolute reduction in myocardial blood volume in stenotic territories subjected to exogenous hyperaemia.

To understand the mechanism of reduced blood volume and flow rate in such circumstances, it is necessary to consider how blood flow is affected by flow-limiting stenoses as well as non flow-limiting stenoses with and without exogenous hyperaemia. A number of investigators have found that, in the absence of stenosis, drug induced hyperaemia increases mean myocardial blood velocity without affecting myocardial blood volume significantly [144,148,154]. A proposed mechanism by which this phenomenon occurs is through reductions in arteriolar and venular resistance. These changes were quantified by Professor Sanjiv Kaul's group at the University of Virginia, who demonstrated constant baseline to peak hyperaemic myocardial contrast video intensity but changing rate of microbubble replenishment after their destruction within the ultrasound field by high power pulses [144]. In non flow-limiting stenosis, myocardial blood flow is maintained under basal conditions by means of an increase in myocardial blood volume, with flow and volume reductions occurring during coronary

hyperaemia [141,155,156]. Furthermore, it has been shown that the extent of hyperaemia induced myocardial blood volume reduction, as measured by myocardial contrast echocardiography in open-chest dogs, is very closely related to the degree of coronary artery stenosis [157]. This may be mediated by decruitment of capillaries in order to maintain constant intracapillary perfusion pressure. This hypothesis gave rise to further work which demonstrated, using myocardial contrast echocardiography and radiolabelled microsphere techniques, that 99mTc-sestamibi perfusion defects occurring during drug induced hyperaemia are largely secondary to reductions in myocardial blood volume in the territory of a stenosis rather than simple myocardial blood flow disparity caused by marked blood flow increase in non-stenosed vascular beds. However, this is very much an oversimplification of the likely dynamics of hyperaemia in non-experimental conditions. For example, most hyperaemia inducing methods also induce myocardial ischaemia or systemic arterial blood pressure reduction, which will in turn result in a combination of coronary arterial, arteriolar, and venular dilatation, and coronary capillary recruitment. The auto-regulatory responses during such systemic changes are likely to have similar effects on myocardial blood flow and volume to exogenous hyperaemia, although differing in degree and proportion. It is worth noting that recent data comparing the effects of Adenosine and Dobutamine, in a rigorous and well-controlled experimental design, confirm that both agents induce perfusion defects as well as reduced rate of contrast agent replenishment after destructive ultrasound pulses in a model of coronary stenosis [158]. This again suggests reduction in capillary blood volume and myocardial blood flow velocity, which is in keeping with other data.

It is unrealistic to think of the effects of hyperaemia or ischaemia as being confined within the territory of a stenotic coronary artery, as microvascular networks of different coronary territories interact with each other by means of collateral vessels. The resultant myocardial blood flow and volume distribution, hence markers of perfusion, will depend not just on the capillary network in the myocardium supplied by a stenotic coronary artery, but on intra and inter regional diversion of blood [159]. These phenomena will tend to complicate the changes in myocardial blood flow and volume described thus far. Indeed, there is canine experimental evidence to suggest that double vessel coronary stenosis reduces the capacity for collateralised perfusion in a neighbouring stenotic territory [160]. This may explain why sensitivity of stress techniques increase with increasing number of stenosed vessels.

In summary, Myocardial Contrast Echocardiography has been used to clarify myocardial perfusion physiology and pathophysiology, and has specifically characterised variation in myocardial blood volume and velocity with differing degrees of stenosis during hyperaemic or ischaemic stress.

3. ULTRASOUND CONTRAST AGENTS

(i) History and Overview

The first report of echo contrast in 1968 [160], and later work by Feigenbaum et.al. [161] formed the basis for dramatic subsequent development of ultrasound contrast agents. Initially, saline or dextrose was agitated with a small amount of air between two syringes in an attempt to form a solution of suspended air micro-bubbles. While this approach, subsequently modified by using sodium

bicarbonate with ascorbic acid [162], hydrogen peroxide [163,164], and Renograffin®
[165,166], provided good ultrasound back-scatter, it did not reliably produce
solutions with micro-bubbles small enough to behave like red blood corpuscles
or stable enough to survive pulmonary circulation after peripheral venous
injection. Although left heart opacification was partly successful after venous
injection of related lipid emulsion based agents, the earliest contrast agents were
essentially limited to delineation of right heart cavities or right-left shunts by
venous injection and to early work on myocardial perfusion assessment by intra-
coronary or aortic root injection.

Significant advances in contrast agent design came in the form of sonication,
whereby micro-bubbles in solution are made to undergo a number of ultrasound
induced alterations in physical characteristics that ultimately result, after
separation and re-suspension, in small and stable micro-spheres. Initially
Renograffin® (sodium diatrizoate) was sonicated in this way, but the process
was also used for other substances such as saline, dextrose, galactose, and
albumin. Feinstein and colleagues were the first to demonstrate reliable left heart
opacification after venous injection of insonicated human albumin solution [167].
This solution was developed into Albunex ® (Mallinkrodt pharmaceuticals, later
incorporated into Amersham Healthcare / GE Healthcare, United Kingdom),
which became the first such agent to receive United States Food and Drug
Administration approval and product licences for clinical use. A large amount of
data supported the notion that Albunex was safe and had neutral haemodynamic
effect. However, users found the reliability and duration of contrast effect to be
limited and generally insufficient to assess myocardial perfusion, despite

excellent left ventricular opacification. The reason for this is the unfortunate fact that opposite physical characteristics are required for vascular transit and ultrasound scattering. Contrast agent ultrasound scattering ability is related to the sixth power of bubble radius [168]. Although larger bubbles produce greater scatter, the ability to pass through capillaries without becoming trapped requires smaller micro-bubbles [167,169]. The earliest contrast micro-bubbles were either large enough that rapid decay would still leave enough size to scatter ultrasound intensely yet too large to traverse capillaries, or they were so small and unstable that air diffused out of them to a point at which ultrasound scatter intensity was too low. Hence, the search for newer ultrasound contrast agents centred on developing stable but small bubbles (<10um diameter). This lead to two types of micro-bubble: those with durable shell components (Optison™, Sonovue™); and shell-less bubbles stabilised with palmitic acid (Levovist™) or surfactant (Imavist™). The so-called second generation contrast agents such as Optison™ were variations on the theme of gaseous cored micro-bubbles, but contained synthetic gases rather than air, which are less likely to diffuse outward and reduce particle size. Choice of contrast agent depends on the intended use and individual ultrasound machine type and settings. Some examples of these micro-bubbles preparations available for clinical or research use are detailed in Table 1.1.

Safety of ultrasound contrast agents could not be taken for granted. At high power, ultrasound can damage blood or tissue structures by means of "cavitation". This phenomenon occurs when cavities in fluid generated by ultrasound bombardment collapse, releasing high concentrations of energy which

result in free radical and electromagnetic radiation emission [170]. Theoretically, micro-bubble solutions might increase the chances of this process. However, previous work has suggested that such problems only occur with ultrasound doses far greater than those used in diagnostic imaging, and that there is no significant deleterious effect with the micro-bubble concentrations and ultrasound intensity used during contrast echocardiography [171-174].

(ii) Optison™

This thesis is based on a series of studies using Optison™, an agent consisting of micro-bubbles of Perfluoropropane in a shell of human albumin with a mean particle diameter of 3.9 μm. Optison™ has been found to have no significant effect on gas exchange or haemodynamics, and is safe in humans [175,176]. Optison™ is presented as a 3-millilitre suspension of micro-bubbles, which are ready to use after aspiration from a vial using a special device to avoid destruction by the negative pressure of suction. It is usually given in small bolus doses to highlight the left ventricular cavity walls.

4. ULTRASOUND CONTRAST MYOCARDIAL PERFUSION: EARLY RESULTS

Myocardial contrast echocardiography has a well established role in endocardial border delineation for purposes of ejection fraction calculation [176-179], stress echocardiography [180], and pulmonary vein Doppler flow signal enhancement [181,182]. Other research has investigated use of contrast to improve Left Anterior Descending coronary flow detection [183]. The series of studies detailed in this

thesis deal with myocardial perfusion assessment, which will be the theme of all further discussion.

In theory, if myocardial contrast agents could behave as pure intravascular tracers, quantification of the relative ultrasound backscatter intensity generated by an agent in different myocardial regions could be taken as a surrogate marker of relative myocardial perfusion in those regions. In addition, if accurate quantification of myocardial vascular bed contrast input were possible, contrast backscatter parameters could also be used to calculate actual regional myocardial blood flow. These assumptions depend heavily on the design of contrast agents themselves as well as the ability of ultrasound machines to detect and display different backscatter intensities in a proportionate fashion.

The first published report of myocardial contrast echo demonstrating myocardial perfusion showed that autoradiographic evidence of blood flow deficit distal to coronary occlusion correlated with myocardial contrast echo score [184]. At a similar time, radio-labelled microsphere and electromagnetic flow probe evidence of perfusion and flow were shown to correlate well with various echo contrast indices of perfusion [163,185-188]. Many such reports relate to highly experimental conditions whereby the ultrasound probe was fixed against an exposed canine heart and contrast was injected directly into the aorta or coronary arteries. While such protocols continue to this day to contribute to our understanding of myocardial perfusion physiology, myocardial perfusion contrast echocardiography required significant advances in micro-bubble design and ultrasound machine hardware and software before clinical use could be

considered. Contrast agents suitable for peripheral venous administration were the immediate priority.

5. PERIPHERAL VENOUS CONTRAST DELIVERY

Contrast echocardiographic estimation of perfusion after peripheral venous injection became more of a reality with the advent of contrast agents capable of not only surviving pulmonary circulation after peripheral venous injection, but of generating a detectable echocardiographic signal after penetrating myocardial vasculature. Animal experimental work subsequently enabled demonstration of myocardial vascular penetration [175], coronary flow reserve [180], and risk area in myocardial infarction [189] after venous injection. The importance of these highly experimental studies was that they confirmed myocardial perfusion could be assessed after venous injection of micro-bubbles in animal models. Subsequent research on human subjects, including developments relevant to intermittent Stimulated Acoustic Emission and low Mechanical Index real-time perfusion imaging, will be discussed in the relevant chapters.

6. ULTRASOUND SYSTEM CAPABILITY

(i) Ultrasound Power and Micro-bubble Response

The various ways in which ultrasound and micro-bubbles interact must be understood in order to appreciate the principles underlying design of contrast echocardiographic hardware and software. The most important single determinant of this interaction is the power of transmitted ultrasound pulses. This is expressed as the Mechanical index, an estimate of the maximum amplitude of a pressure pulse in tissue (Mechanical index = P / f^{-2} where P = peak negative

pressure in and f = ultrasound frequency). Conventional low power ultrasound (<100kPa, Mechanical index <0.1) tends to result in linear backscatter [190] with signal intensity largely proportional, within a certain range, to micro-bubble concentration. Linear backscatter depends on micro-bubbles being of a certain size, stability, and concentration. Providing these conditions are satisfied, a marked contrast effect is seen in the large cavities of the heart with such imaging. However, the myocardial vascular bed cannot be identified easily using linear backscatter. This is due to the resulting mix of tissue and micro-bubble grey-scale data within the same image, making it difficult for the human eye to differentiate the two. New low power techniques are discussed in relation to real-time imaging in section (iii) "Real-Time Myocardial Perfusion Imaging".

When higher power ultrasound is used (100 kPa to 1 MPa, Mechanical index 0.1 to 1), micro-bubbles start to exhibit harmonic behaviour. This is due to an inherent physical characteristic of bubbles that leads to them reaching a resonant state when bombarded with certain power and frequency ultrasound. When this occurs, reflected ultrasound waves with frequencies that are multiples of the incident wave frequencies are generated [191,192]. Ultrasound systems have been designed to detect these so-called harmonic frequencies, which are mainly double the transmit frequency (second harmonics), while suppressing display of fundamental frequencies. This improves the contrast to background signal ratio, since micro-bubbles are much more able to behave in this fashion at conventional transmit frequencies than surrounding tissue. Despite the fact that interrupted static frames and extensive post-processing are necessary if attempting to assess myocardial perfusion with second harmonic imaging, there have been

demonstrations of successful perfusion imaging using such methods. For example, Porter et al showed excellent correlation between nuclear perfusion and intermittent harmonic ultrasound perfusion with intravenous PESDA during Dipyridamole stress tests [193]. Similarly, Kaul et al also demonstrated outstanding segmental concordance between intermittent harmonic contrast echocardiography with Optison™ and Tc-99 sestamibi SPECT, again in a Dipyridamole stress protocol [194]. However, extensive post-processing of images was used in both of these studies, and such success has not been widely replicated by others.

A variation on the theme of harmonic imaging is Pulse Inversion Imaging, which theoretically improves the ability to selectively represent contrast signal. This technique, also occurring at relatively low ultrasound power, relies on the fact that blood and tissue structures resonate symmetrically while micro-bubbles resonate asymmetrically under ultrasound exposure. Hence, when dual pulses of ultrasound of identical but directionally opposite waveform are transmitted into a region of myocardium supplied by contrast micro-bubbles, blood and tissue signal is minimised through cancellation effects, while micro-bubble signal is enhanced through summation effects. Although theoretically useful, Pulse Inversion Imaging still results in cluttered echo signal combining tissue and micro-bubble data, in part due to tissue motion being encoded as harmonic signal artefact.

At still higher ultrasound power (>1 Mpa, mechanical index > 1MPa) micro-bubbles are destroyed. In the process of destruction, they emit ultrasound waves

over a range of frequencies, causing a Doppler shift, which can then be represented in image form. This phenomenon is called Stimulated Acoustic Emission, and is utilised in such techniques as Harmonic Power Doppler and Power Contrast Imaging™. These methods rely on subtraction of reflected ultrasound after transmission of dual pulses along the same scan line separated by a short delay [195-197]. The major problem with this approach is the necessity for intermittent imaging to allow the vascular space to be replenished with micro-bubbles in time for the next pulse of destructive ultrasound.

The above techniques were not able to show myocardial perfusion in real-time. Even when intermittent imaging was used, with the exception of stimulated acoustic emission methods, significant post processing was necessary to reliably detect perfusion. Despite the technical difficulties, the end of the last decade saw a number of claims that myocardial perfusion echocardiography might be ready for routine clinical use. These hopes proved too optimistic. While the techniques were successful to a degree in a handful of research laboratories, there was a distinct lack of replication of such success elsewhere. Marwick et al published one of the largest series of the late 1990s in the form of a multi-centre study of contrast echocardiography compared to SPECT imaging in 200 patients with previous myocardial infarction [198]. Partly due to methodological differences from previous work, including lack of post-processing and use of fundamental imaging for a significant proportion of cases, Marwick's results indicated a poor correlation between contrast echocardiography and nuclear perfusion. Nevertheless, this was a very useful reminder that better ultrasound capability, with or without specific post processing of images, was necessary before

myocardial contrast echocardiography could be used for perfusion analysis in a clinical setting.

(ii) Intermittent Myocardial Perfusion Imaging

The discovery that ultrasound destroys micro-bubbles and that intermittent imaging leads to improved micro-bubble backscatter was serendipitous. Porter and Xie were the first to report increased myocardial opacification secondary to micro-bubble signal after brief interruption to harmonic imaging following venous contrast injection [199]. Meanwhile, Sanjiv Kaul and colleagues at the University of Virginia confirmed that real-time imaging was responsible for micro-bubble destruction, as evidenced by gradual linear decline in video-intensity signal during contrast echocardiography at conventional frame rates [200]. Furthermore, it was noted that larger intra-myocardial vessels such as septal perforators could be seen during contrast echocardiography even at conventional frame rates, the implication being that high velocity flow would be sufficient to continuously replenish the ultrasound beam area and allow continuous signal, whereas low velocity flow such as occurs at the capillary level would not. These observations lead to intentional interruption of imaging as a means of improving micro-bubble signal. Such an approach is no more pertinent than during high power Stimulated Acoustic Emission, which results in transient harmonics at the expense of almost complete micro-bubble destruction. The interruption to ultrasound allows micro-bubbles to replenish the myocardial vascular bed, a process that is more complete the higher the concentration and rate of flow of contrast agent and the longer period of the interruption. Hence, if images are acquired at pre-specified points in the cardiac cycle and contrast micro-bubbles

are infused at a steady rate, intermittent imaging can be set at the cardiac cycle frequency that best displays myocardial opacification. Furthermore, if non flow-limiting stenoses could be unmasked by stress or hyperaemia during intermittent imaging, differential micro-bubble flow rates and signal intensities could be detected, allowing functional assessment of stenosis in coronary artery disease.

The question of how to move on from demonstration of myocardial capillary bed micro-bubble signal in an experimental setting to assessment of perfusion defects in the clinical practice has been a focus for numerous investigators for several years. Most early research quantifying myocardial micro-bubble signal under various imaging conditions used highly experimental models, often with exposed canine hearts and ultrasound probes fixed against a pre-determined point for the perfect 2-dimensional image slice. However, in the clinical environment it becomes impossible to control for many factors that can adversely affect image quality. Firstly, intermittent imaging does not give the subtle visual clues required by the sonographer to perfect the image plane, resulting in loss of ideal ultrasound probe position and image slice. Thus, it can be very difficult to acquire two or more perfectly comparable images, especially for detection of perfusion at baseline and peak stages of exercise, Dobutamine, Adenosine, or Dipyridamole stress protocols, where tachycardia and deep breathing become factors. Secondly, Stimulated Acoustic Emission based methods tend to result in wall motion artefact being represented as perfusion. One way around the latter problem is to employ two closely spaced pulses of ultrasound (within approximately 50 milliseconds). The first pulse destroys micro-bubbles and creates a perfusion image. The second pulse is used to verify that signal from the

first pulse is due to perfusion and not wall motion – the entire myocardium should be devoid of signal as micro-bubble destruction will have been complete after the first pulse. If signal is present within the myocardium on the image generated by the second pulse, it must be due to wall motion and not perfusion. Hence, the interpreter does not falsely label myocardial segments devoid of perfusion as normal. The third significant problem with intermittent imaging is the fact that real-time data, perhaps the most dramatic triumph of echocardiography over other non-invasive imaging modalities, is completely lost. Wall motion is not assessable unless a separate echocardiographic imaging protocol is employed in addition to Stimulated Acoustic Emission Myocardial Contrast Echocardiography. Finally, artefacts caused by contrast agent shadowing and the inherent problems with ultrasound dynamics in the lateral image plane serve to further limit the accuracy of the displayed image as a true representation of myocardial perfusion level.

These physiological variations, the nature of ultrasound itself, and technical problems such as limited acoustic window and tissue or contrast agent blocking of ultrasound signal mean that comparing different regions with one another may not be an ideal way to assess perfusion. This can be overcome to an extent in stress test situations, where the same myocardial segments are compared with each other before and after stress.

Stimulated acoustic emission was briefly the method of choice for myocardial perfusion imaging, but has since been largely replaced by low mechanical index

real-time myocardial perfusion imaging. Research undertaken during this era is detailed in Chapter 3.

(iii) Real-time Myocardial Perfusion Imaging

There had been a degree of success at visualising wall motion and perfusion in what was effectively real-time using Accelerated Intermittent Harmonic Imaging [201,202]. In this technique, mechanical index is reduced to approximately 0.3, allowing relatively micro-bubble conserving frame rates of 10 to 12 Hz. However, few were able to show this method to be effective. In order to solve the problem of image clutter with standard harmonic imaging and the constraints of intermittent imaging with Stimulated Acoustic Emission based methods, a technique capable of selectively imaging micro-bubbles rather than tissue during real-time imaging was required.

A number of such methods for real-time imaging began to appear in prototype form in 1999. Different techniques evolved in line with slightly different research strategies and partnerships in various sectors of the ultrasound imaging industry. For example, some groups worked almost exclusively with a single ultrasound contrast agent, while others attempted to broaden the applicability of their technique to a number of different agents. The main outcomes of this phase of real-time perfusion ultrasound development were Power Pulse Inversion / Pulse Inversion Doppler™ (ATL, Phillips Medical Systems, Eindhoven, the Netherlands), Power Modulation Imaging™ (ATL, Phillips Medical Systems), and Coherent Contrast Imaging™ (Acuson Sequoia, Siemens Medical

Solutions). The first demonstration of the new generation of real-time imaging systems was in 1999, in the form of ATL's Power Pulse Inversion [203].

Power Pulse Inversion™ is, to some extent, a fusion of Harmonic Power Doppler and Pulse Inversion imaging. Here, Doppler processing of returning ultrasound from alternating standard and inverted waveforms is used to separate linear (symmetrical) and non-linear (asymmetrical) signal, allowing highly selective colour coded display of micro-bubble signal to be superimposed on two-dimensional grey-scale tissue signal [204]. Early work demonstrated that this technique did not destroy micro-bubbles to any significant degree and that it allowed simultaneous display of both wall motion and perfusion [203]. Subsequent research went further, suggesting that the agreement between territory of stenosis according to quantitative coronary angiography and echocardiographic myocardial perfusion was greater than the agreement between angiography and wall motion assessment during stress echocardiography [205].

The principle underlying Power Modulation Imaging™ is again that micro-bubbles resonate asymmetrically, while tissue behaves in a symmetrical fashion. For contrast imaging, two identically shaped but different amplitude pulses (single versus double amplitude) are emitted, followed by subsequent multiplication of the smaller returning wave by a factor of two and subtraction of it from the higher amplitude returning wave. Symmetrically behaving tissue results in identical transmitted and returning waveforms, the latter of which are cancelled out by the type of mathematical processing detailed above. Asymmetrically behaving micro-bubbles result in return of two waves of

53

differing amplitude and shape, such that simple multiplication and subtraction processes do not cancel the signal. In common with certain other methods, signal amplitude is then colour coded and superimposed for display purposes.

The real-time imaging technologies described above require multiple ultrasound pulses to ensure separate display of tissue and micro-bubble signal. There are two potential problems with multiple pulse generation. Firstly, despite some evidence to the contrary, it theoretically increases the risk of bubble destruction. Secondly, it reduces the capacity for high frame rate imaging. Acuson Corporation designed a real-time contrast imaging system that avoids the need for multiple pulses and such associated problems. The system is based on shaping emitted pulses such that ultrasound waves returning from micro-bubble and tissue naturally fall into separate spectra. The tissue signal is then suppressed at a given spectrum with single ultrasound pulses rather than numerous "cancellation pulses". Grey scale signal is then used to display presence of micro-bubbles. While this theoretically allows greater frame rates and minimal bubble destruction, it is clear that certain actual or theoretical advantages could be claimed for each system. Certainly, no single technique was thought to be significantly better than any other. Acuson pioneered pulse shaping and single pulse cancellation technology and launched it in prototype form under the name Coherent Contrast Imaging™ in 1999. Research conducted into this technique is detailed in Chapter 4.

The arrival of micro-bubble sensitive low mechanical index imaging techniques allowed simultaneous assessment of perfusion and wall motion in real-time. Thus, perfusion assessment could at last be obtained without discarding wall

motion data, which had long been a clear advantage of echocardiography over other imaging techniques. An obvious application for real-time perfusion assessment is stress echocardiography, which conventionally relies on detection of wall motion and thickening abnormality alone. According to the ischaemic cascade, one would expect perfusion abnormalities to be more sensitive than wall motion abnormalities for detecting coronary artery disease [118,119]. Given that the sensitivity of (Dobutamine) Stress Echocardiography is approximately 80% overall, and lower in single vessel coronary artery disease [206], a significant clinical benefit could result if perfusion assessment were able to provide additional diagnostic information beyond that which is conventionally obtained by wall motion analysis alone. The only standard means of assessing myocardial perfusion at present are nuclear imaging modalities. Such methods should theoretically be more sensitive for coronary artery disease than wall motion assessment during stress echocardiography. However, a combination of artefact and technical limitations mean that nuclear perfusion methods are only slightly more sensitive than stress echocardiography when it comes to clinical practice. If real-time low mechanical index myocardial perfusion assessment with ultrasound contrast agents is to become a clinical tool for use in chronic coronary artery disease, it needs to overcome the technical limitations of nuclear imaging techniques while retaining valuable wall motion data.

With all of these phenomena and the techniques that have been derived from them, far-field image problems can occur due to shielding from incident ultrasound by excessive near-field micro-bubble concentration. In addition, myocardial capillary density is not necessarily uniform across all myocardial

regions. It is therefore important to be aware that there may be variations between contrast signals originating from different myocardial segments, even in normal myocardium.

CHAPTER TWO

DEVELOPING AN OPTISON™ INFUSION METHOD AND IDENTIFYING THE IDEAL TRIGGER INTERVAL FOR POWER CONTRAST IMAGING™

1. BACKGROUND

(i) Rationale for Ultrasound Contrast Infusion

In order to compare myocardial perfusion at baseline and peak stages of a stress protocol, the rate of delivery of contrast agent to the coronary arteries should ideally be even. Bolus injection of a contrast agent results in a steep rise in contrast effect followed by a brief plateau and rapid fall to minimally detectable levels of agent. Infusion at an appropriate constant rate should theoretically result in a steady rise to a plateau effect that will persist as long as infusion is continued [207], although this is not strictly the case according to in-vivo results, which suggest an exponential association [144]. Figures 1.3 and 1.4 show the type of micro-bubble signal response following contrast bolus and infusion respectively. A steady rise in contrast effect with subsequent plateau, or an exponential variation on this, could potentially be mimicked by repeated small boluses or slow manual injection, but the resulting contrast signal is unlikely to be smooth and would not represent a true steady state. Aside from failure to provide a smooth steady state contrast signal, it is clear that bolus dosing often results in too high a concentration of micro-bubbles in the image plane during maximal effect. This leads to an excessive ultrasound signal in and around the region nearest to the ultrasound probe and signal dropout beyond this region, a phenomenon known as contrast shadowing. Related to this is the phenomenon of

blooming, whereby signal is saturated by such an excess of micro-bubble scattered ultrasound that there is an impression of strong contrast effect in nearby myocardial regions despite lower actual micro-bubble concentration within them. These phenomena not only lead to difficulty in visualising certain myocardial regions adequately, but significantly distort quantification based assessment of contrast effect and hence perfusion. For example, if one myocardial region is subject to contrast shadowing while the other is subject to blooming effect, any attempt to compare perfusion between the two, based on intensity of contrast signal, would be subject to major error.

(ii) Previous Studies of Ultrasound Contrast Infusion

The earliest comparison of bolus and infusion methods of ultrasound contrast delivery confirmed prolonged steady state Doppler profile enhancement in arterial and venous circulation of a number of small animals after venous infusion of a galactose based agent [208]. It has since been demonstrated in humans that, compared to bolus dosing, infusion of Levovist® (Schering AG, Berlin, Germany) provides sustained and even femoral artery pulsed and colour Doppler signal while minimising saturation artefact [209]. Elsewhere, canine experimental work with Imagent® infusion (now known as Imavist®, Alliance Pharmaceutical Corp., San Diego, USA) confirmed prolongation of signal and reduction of saturation artefacts, with the additional finding that calculations incorporating video intensity and pulsing interval during intermittent imaging allowed quantification of myocardial signal [143]. Subsequent work with Optison™ infusion, published after the technique established here, will be discussed in the context of the experimental findings later in this chapter.

(iii) Problems Associated with Optison™ Infusion

Some ultrasound contrast agents are better suited to infusion than others. It is true that Optison™, while best choice for use alongside the Ultrasound System employed in this study (Acuson Sequoia C256 with Power Contrast Imaging™), is not ideally suited to infusion. The main problem encountered with infusion of this agent is related to the relative buoyancy of the contained micro-bubbles compared to the solution in which they are suspended. If left to stand for more than a few seconds, the micro-bubble fraction begins to float to the top of the container. This leads to uneven infusion unless it is somehow ensured that complete mixture of micro-bubbles and carrier solution is maintained. The phenomenon of micro-bubble and carrier solution separation is not only confined to syringes or vials but also to infusion lines. However, this protocol required steady state contrast effect throughout each perfusion study for the sake of baseline and peak stage comparisons, and an infusion method was needed.

(iv) Trigger Intervals

All Stimulated Acoustic Emission based imaging systems allow alteration of the image trigger interval, based on either a fixed time period (time triggered) or a certain cardiac cycle frequency (ECG triggered). The period between triggers allows the vascular space within the ultrasound field to replenish with micro-bubbles after a destructive ultrasound pulse, while the next triggered image displays the resulting pattern of vascular replenishment. Different ultrasound contrast agents will suit different trigger intervals, depending on their individual physical properties and behaviour under incident ultrasound waves. Furthermore, the rate of delivery of ultrasound contrast micro-bubbles to the myocardial

vascular bed will affect how rapidly the ultrasound field is replenished, and will therefore impact on the ideal trigger interval. In other words, under conditions of increased cardiac output and high micro-bubble infusion rate, the trigger interval may not need to be so long, while at low cardiac output and low infusion rate, a longer ultrasound field replenishment time would be necessary, requiring longer trigger intervals. Because a number of variables affect the time needed for micro-bubble replenishment, there is no predetermined ideal trigger interval. It is therefore necessary to set a trigger interval appropriate to the particular study being undertaken, making an allowance for factors such as micro-bubble infusion rate and dilution, heart rate, Stimulated Acoustic Emission imaging system type and settings, and ease of image acquisition and interpretation.

(v) Power Contrast Imaging™

Power Contrast Imaging™ (PCI) (Acuson, Siemens Medical Solutions USA), is a contrast specific imaging modality designed to assess myocardial perfusion. It relies on the acoustic properties of micro-bubbles when bombarded with high-energy ultrasound, namely stimulated acoustic emission. Details of this process are described in Chapter 1. The Acuson system is designed in such a way that Doppler energy from stimulated acoustic emission is displayed as a colour image superimposed on the standard grey scale two-dimensional echocardiogram. This allows visual assessment of myocardial perfusion without resorting to offline digital subtraction techniques. Because high-energy ultrasound destroys micro-bubbles, imaging must be intermittent and at low frame rate, and contrast agent must be infused at a constant rate.

(vi) Outline of Investigation: Infusion Methods and Trigger Intervals

At the commencement of this research, there was no accepted best method of Optison™ infusion, and there were no clear recommendations for trigger interval in such a protocol as Adenosine Power Contrast Imaging™. The first stage of the study was therefore to identify a reliable means of infusing Optison™ and a suitable ECG trigger interval for the purposes of such protocols. This was undertaken in the context of Adenosine Power Contrast Imaging™ Studies using visual interpretation of contrast effect. These cases were not included for subsequent analysis of the accuracy of Adenosine Power Contrast Imaging™, as the protocol for this section was designed to address issues of infusion and trigger interval. Assessment of the accuracy of Adenosine Power Contrast Imaging™ per se is discussed in Chapter 3.

2. AIMS

1. To identify the most appropriate method of infusing Optison™ for the purpose of Power Contrast Imaging™ during an Adenosine vasodilator stress protocol.

2. To ascertain which trigger intervals are most appropriate for the combination of the Acuson Power Contrast Imaging™ technique and Optison™ infusion.

3. METHODS

(i) Ethical Approval

The study was approved and registered by the Royal Free Hospital medical ethics committee (Reference: Royal Free Hampstead NHS Trust Ethics code 161-99,

research and development reference number 3810). All subjects gave written informed consent.

(ii) Subjects

Twelve patients with >50% stenosis affecting one or two coronary arteries, but without occlusion or sub-total occlusion, were recruited (Table 2.1). These patients had been scheduled for percutaneous coronary intervention. Inclusion criteria were diagnostic coronary angiography within one month and informed consent. Exclusion criteria were previous transmural myocardial infarction (clinical, electrocardiographic, or echocardiographic evidence), unstable angina or symptomatic deterioration within the previous month, sensitivity to albumin products, previous adverse reaction to Dobutamine or Adenosine, valvular heart disease, asthma, second or third degree atrio-ventricular block, and caffeine or methylxanthine related product ingestion during the 24 hours preceding each study.

(iii) Echocardiography

Contrast Echocardiography was performed with subjects in the left lateral decubitas position. The Acuson Sequoia C256 ultrasound machine was used, incorporating the Power Contrast Imaging™ facility (PCI). Baseline standard two-dimensional echocardiography was used to confirm normal myocardial resting function and wall thickness. For perfusion imaging, machine settings were as per the recommendations of the manufacturer, adjusted to optimise the contrast echocardiographic image (Table 3.1). Power Contrast Images were acquired using intermittent electrocardiographic triggering in the apical four-

chamber view at end diastole. Acquisition intervals of once in every cardiac cycle, one in two, one in four, one in six, and one in eight cardiac cycles were used. If myocardial segmental perfusion was not clearly seen at end diastole, triggers were reset to end systole. Images were stored on optical disc and VHS videotape. The best trigger interval, as established by visual assessment of the quality of myocardial contrast effect during baseline imaging, was then selected for imaging during the final minute of Adenosine infusion.

(iv) Optison™ Infusion

Two 18G peripheral venous cannulae (Vygon, Ecouen, France) were placed in large antecubital fossa and forearm veins. A three-way tap was connected to the most proximally sited cannula, which was reserved for infusing Optison™. The second cannula was used for Adenosine infusion. Optison™ was drawn into a 50 ml syringe and either left undiluted or diluted to one of two concentrations with 0.9% saline (see below). Extension tubing (1ml priming volume, length 19cm, Alaris Medical Systems ®, San Diego, Ca, USA) was connected to the syringe, primed with 1ml of syringe contents, and then connected at the other end to the three-way tap.

Optison™ was left undiluted in four cases and was diluted to two concentrations with 0.9% saline in two further sets of four cases each. The following three Optison™ preparations resulted:

1. Non diluted Infusion (4 subjects):

   Six millilitres of Optison™ (2 vials) was drawn into a 50 ml syringe, using the manufacturer's recommended vial aspiration unit, designed to minimise

negative pressure induced micro-bubble disruption. Infusion tubing was connected and primed with Optison™ from the syringe. The syringe was then inserted into a 50 ml syringe driver (Graseby 3400, Graseby Medical Limited, Smiths Industries plc, Watford, UK), which was set to infuse at 72 ml/hr initially, followed by stages at 36, 24, 18, and 14 ml/hr, during which baseline images were acquired. The rates of 72 to 14 ml/hr corresponded to infusion durations of 2.5, 5, 7.5, 10, and 12.5 minutes per vial of Optison™, excluding the 1 ml volume contained in the connection tubing. The syringe driver was rotated continuously by hand in horizontal and vertical planes to prevent separation of micro-bubbles from solution. Infusion was halted for 4 minutes during Adenosine infusion at 140 mcg/kg/min, with the 3-way tap turned so that Optison™ in the connection tubing could not ascend the intravenous line into the vein. Manual rotation of the syringe driver was continued throughout. Optison™ infusion was recommenced for peak imaging during the fifth minute of Adenosine stress at the rate and trigger interval that resulted in best myocardial perfusion during the first part of the Optison™ infusion. If more than one infusion rate and trigger interval appeared equally suitable, they were each used during the peak stage.

2. Diluted Infusion A (4 subjects):

   Six millilitres of Optison™ was drawn into a 50 ml syringe as previously described. Nine millilitres of 0.9% saline was drawn into the same syringe to make a diluted 15ml solution. Subsequent priming of the extension tubing and connection of devices was as above. The Syringe driver was to infuse at 180 ml/hr initially, followed by stages at 90, 60, 45, and 36 ml/hr, during which baseline images were acquired. These rates corresponded to infusion

durations of 2.5, 5, 7.5, 10, and 12.5 minutes per vial of Optison™, excluding the 1 ml volume contained in the connection tubing. Image acquisition, manual rotation of the syringe driver, Adenosine infusion, and peak stage imaging were as above.

3. Diluted Infusion B (4 subjects):

Six millilitres of Optison™ was drawn into a 50 ml syringe. Twenty-four millilitres of 0.9% saline was drawn into the same syringe to make a diluted 30 ml solution. Subsequent priming of the extension tubing and connection of devices was as above. The Syringe driver was to infuse at 360 ml/hr initially, followed by stages at 180, 120, 90, and 72 ml/h. Once more, these rates corresponded to infusion durations of 2.5, 5, 7.5, 10, and 12.5 minutes per vial of Optison™, excluding the 1 ml volume contained in the connection tubing. Image acquisition, manual rotation of the syringe driver, Adenosine infusion, and peak stage imaging were as above.

In all cases, an assistant was assigned the task of continuous manual rotation of the Optison™ charged syringe driver.

(v) Adenosine Infusion

Adenosine infusion was commenced at a dose of 140mcg/kg/min through a separate intravenous cannula after baseline imaging had been completed and continued for five minutes. Peak stage images were acquired during the final minute of infusion. Adenosine was supplied in a solution with 0.9% saline to a total volume of 125ml and was delivered by standard intravenous infusion using an Ivac® 572 volumetric infusion pump (Alaris Medical Systems®). Clinical and

65

electrocardiographic monitoring was carried out continuously and blood pressure was checked every two minutes during the infusion. Adenosine was stopped if the following occurred: horizontal or down-sloping electrocardiographic ST segment depression of $>0.2mV$ 80 ms beyond the J point; electrocardiographic ST segment elevation; severe angina; fall of systolic blood pressure of > 40 mmHg from baseline or to < 90 mmHg systolic; significant brady-arrhythmia; intolerable Adenosine related side effects, or at the patient's request.

(vi) Image Analysis

After review and selection, baseline and peak images were placed on screen side by side for comparison. Each set of images was assessed for the presence of myocardial contrast effect, blooming, and contrast shadowing.

(vii) Dobutamine Stress Echocardiography

Dobutamine Stress Echocardiography was carried out in a separate sitting in accordance with standard techniques and guidelines in the cases that had a valid and successful contrast echocardiogram. Only three such cases occurred, so Dobutamine Stress Echocardiography was only carried out for these three cases.

4. RESULTS

There were four females and eight males in the group.

Mean age was 64.8 years, standard deviation 7.6 years.

All patients had stable coronary artery disease but no clinical, electrocardiographic, or echocardiographic evidence of myocardial infarction.

Heart rates during image acquisition were between 50 and 90 beats per minute in all cases.

Adenosine infusion was terminated prematurely in four cases due to dyspnoea or chest pain (Table 2.1).

Dyspnoea and associated deep breathing contributed to inadequate image clarity in at least two cases (cases seven and eight) (Tables 2.1 and 2.5).

During Adenosine infusion, electrocardiograms were negative for inducible ischaemia in five cases, inconclusive in five cases (minor T wave abnormalities in three cases and normal electrocardiogram with early termination of Adenosine infusion in two cases), and positive for inducible ischaemia in two cases (ST segment depression > 1.5 millimetres). Both the cases with ST segment depression had non-interpretable peak stress Power Contrast Images due to technical problems with Optison™ infusion (Case 1 with undiluted Optison™ and case 8 with Optison™ in dilution A) (Table 2.5).

(i) Non-diluted Infusion

At 24 ml/hr, adequate myocardial contrast signal was visualised in all cases at a trigger interval of 1 in 4 cardiac cycles and in three cases at a trigger interval of 1 in 6 cycles.

At 18 ml/hr, adequate myocardial contrast signal was visualised in all cases at a trigger interval of 1 in 6 cycles and in three cases at trigger intervals of 1 in 4 and 1 in 8 cardiac cycles (Table 2.2).

Blooming and shadowing effects occurred at all trigger intervals in all cases at 72 ml/hr and 36 ml/hr. Myocardial contrast effect was deficient in all cases at 14 ml/hr, irrespective of the trigger interval (Table 2.2).

Image quality was best at trigger intervals of 1 in 4 cardiac cycles at 24 ml/hr in two cases (cases 1 and 2) and at 1 in 4 cycles at 18 ml/hr in two cases (cases 3 and 4), so these trigger intervals and infusion rates were selected for resumption of imaging after Adenosine infusion (Table 2.5).

Upon resumption of imaging during the final minute of Adenosine infusion, non-uniform myocardial contrast effect with associated artefact such as blooming or shadowing occurred in all cases. Furthermore, inspection of the connection tubing, three-way tap and cannula hub after completion of the infusion revealed deposits of Optison™ in every case.

(ii) Diluted Infusion A

At 90 ml/hr, adequate myocardial contrast signal was visualised in two cases at trigger intervals of 1 in 6 and in two cases at intervals of 1 in 8 cardiac cycles (Table 2.3).

At 60 ml/hr, adequate myocardial contrast signal was visualised in two cases at a trigger interval of 1 in 4 cycles and in all four cases at a trigger interval of 1 in 6 cycles (Table 2.3).

At 45 ml/hr, adequate myocardial contrast signal was visualised in three cases at a trigger interval of 1 in 6 cardiac cycles (Table 2.3).

Blooming and shadowing effects occurred at all trigger intervals in all cases at 180 ml/hr and in all cases at 1 in 1, 2, and 4 cardiac cycles at 90 ml/hr. Myocardial contrast effect was deficient in all cases at 36 ml/hr, irrespective of the trigger interval.

Image quality was best at trigger intervals of 1 in 6 cardiac cycles at 90 ml/hr in one case (case 7), 1 in 4 cycles at 60 ml/hr in two cases (cases 5 and 6), and at 1

in 6 cycles at 60 ml/hr in 1 case (case 8). These trigger intervals and infusion rates were selected for resumption of imaging after Adenosine infusion (Table 2.5).

Upon resumption of imaging during the final minute of Adenosine infusion, non-uniform myocardial contrast signal with associated artefact such as blooming or shadowing occurred in two cases. Inspection of the connection tubing, three-way tap and cannula hub after completion of the infusion revealed deposits of Optison™ in both of these cases. In the remaining two cases, good myocardial contrast effect was seen at peak stage in all except the basal-lateral segments in the apical four-chamber image.

(iii) Diluted Infusion B

At 180 ml/hr, adequate myocardial contrast signal was visualised in all cases at trigger intervals of 1 in 6 and 8 cardiac cycles (Table 2.4).

At 120 ml/hr, adequate myocardial contrast signal was visualised in all cases at trigger intervals of 1 in 4 and 6 cycles and in three cases at 1 in 8 cardiac cycles (Table 2.4).

At 90 ml/hr, all cases demonstrated adequate myocardial contrast signal at a trigger interval of 1 in 8 cycles while only one case demonstrated good myocardial contrast signal at a trigger interval of 1 in 6 cycles (Table 2.4).

Blooming and shadowing effects occurred at all trigger intervals in all cases at 360 ml/hr and in all cases at 1 in 1, 2, and 4 cardiac cycles at 180 ml/hr. Myocardial contrast effect was deficient in all cases at 72 ml/hr, irrespective of the trigger interval.

Image quality was best at a trigger interval of 1 in 4 cardiac cycles at 120 ml/hr in all four cases, so this rate of infusion and trigger interval were selected for peak stress image acquisition after Adenosine infusion (Table 2.5).

Upon resumption of imaging during the final minute of Adenosine infusion, good myocardial contrast signal was seen in all cases. Inspection of the connection tubing, three-way tap and cannula hub after completion of the infusion did not reveal evidence of concentrated Optison™ deposits in any case (Table 2.5). An example of image quality using this infusion with 1 in 4 cardiac cycle image acquisition is shown in Figure 2.1.

5. DISCUSSION

(i) Infusion Technique

At the time this series of studies was commenced (November 1999), there was little published data regarding bolus injection or continuous infusion of ultrasound contrast agents. Specifically, there had been no practical demonstration of the actual means by which continuous infusion of an agent such as Optison™ could be achieved. The central problem with this agent, namely that of separation of micro-bubbles from the carrying solution, has made infusion a very awkward undertaking and has been partly responsible for more recent development of infusible contrast agents such as Definity™ (DuPont Pharmaceutical Co., Wilmington DE, USA) [210,211]. Optison™ was not the only ultrasound contrast agent available at the time this study was undertaken, however. It had previously been demonstrated that femoral artery flow signal could be enhanced very effectively for prolonged periods without technical difficulty using an intravenous infusion of Levovist® (Schering AG, Berlin,

Germany) [212], so one might assume Levovist® should have been used in this study. It should be noted, however, that simply switching to an alternative ultrasound contrast agent is not necessary an appropriate way to overcome problems of agent delivery, as most ultrasound systems incorporating contrast imaging were originally developed to complement the specific acoustic properties of a single "partner" agent. For the Acuson Power Contrast Imaging™ system, Optison™ was the specific agent of choice at the time.

This data suggests that infusion of undiluted Optison™ is effective as long as infusion is not interrupted. If interruption occurs, significant quantities of contrast agent become lodged in tubing and connection taps, rendering the second stage infusion uneven. This becomes less of a problem with a dilution of 6 ml Optison™ to 9 ml 0.9% Saline, and the problem disappears with a dilution of 6 ml Optison™ to 24 ml 0.9% Saline. It is most likely that this relates to the relative quantities of micro-bubbles contained in the syringe, connection tubing, intravenous cannula, and three way taps. To infuse 6ml of Optison™ using the stated equipment requires approximately 1.5ml of the agent to be contained in parts of the infusion system that it is not possible to subject to continuous rotation. Hence, unless the rate of infusion is rapid, these relatively static parts will allow separation of Optison™ micro-bubbles from the carrying solution. This in turn allows aggregation of micro-bubbles in certain parts of the system. This effect will be minimised with continuous moderate to high flow rates, but will be exacerbated by either flow interruption or very low flow rates. The physical effect of this on delivery of contrast agent would be infusion of collections of micro-bubbles interspersed with columns of carrier solution, while

the imaging consequence would be periods of excess micro-bubble signal alternating with periods of insufficient signal. However, a larger volume of contrast agent with the same number of contained micro-bubbles would result in a relatively small proportion of micro-bubbles separating within the static components connecting the syringe to the vein. As long as the infusion rate is increased in proportion to the dilution factor, the uneven delivery of micro-bubbles arising in the connection system (in these cases developing during interruption to infusion) will last for a brief period only, allowing resumption of infusion of adequately mixed Optison™ micro-bubbles from the agitated syringe after a very brief period of time. This explains the finding that undiluted Optison™ infusion worked well until interruption for Adenosine delivery, while dilution A worked well after interruption in only two cases and dilution B worked well in all cases despite interruption. Further tests on greater dilutions of Optison™ were not carried out, as dilution B provided the necessary properties and image quality.

(ii) Accuracy of Myocardial Contrast Effect Assessment

It could be reasoned that assessment of the accuracy and appropriateness of various trigger intervals and Optison™ infusion methods should incorporate some type of quantitative contrast echocardiographic signal analysis. While this implies a certain methodological rigour, image analysis needs to be seen in the context of the eventual use of the technique. One of the theoretical strengths of Power Contrast Imaging™ in myocardial perfusion assessment is its suitability for visual analysis in a clinical setting. As such, it is equally appropriate for visual analysis of contrast effect to be used for defining standardised aspects of

the protocol such as infusion method and trigger interval. In other words, the margin of error for the accuracy of visual assessment of myocardial perfusion according to Power Contrast Imaging™ will not exceed the margin of visual error for assessment of the effects of various trigger intervals and infusion methods. However, if quantitative methods of perfusion assessment had been employed, matters of protocol and technique would need to have been pre-determined by quantitative means. Such an approach has been adopted elsewhere, requiring video intensity analysis to interpret evidence of perfusion level during an intermittent second harmonic imaging protocol [213].

(iii) Triggering Intervals

The ideal triggering intervals for optimal myocardial contrast signal were one in four or six cardiac cycles, at heart rates of between 50 and 90 per minute. This suggests that, with the Acuson Power Contrast Imaging™ system and Optison™ infusion, four or more cardiac cycles are required to fully replenish the myocardial vascular bed with contrast material after destruction by high power ultrasound. Shorter intervals result in an incomplete perfusion image, while longer intervals gain little additional perfusion effect and occasionally result in blooming. The reason for patchy perfusion defects at lower intervals is not entirely clear, but possible explanations were discussed by Kolias et al after they found patchy perfusion signal in a very similar imaging protocol to the one used in this study [214]. Particular explanations might be variable intensity of ultrasound incident power at different locations in myocardial tissue and myocardial capillary density variability as a normal physiological phenomenon.

It is important to note that the rate of micro-bubble replenishment is unlikely to be constant at all times under all conditions. One might expect more rapid replenishment, hence the need for a shorter triggering interval, during tachycardia and high cardiac output, as occurs in exercise or pharmacological stress. Therefore, a vasodilator induced perfusion deficit could theoretically "fill in" in the time taken for four cardiac cycles to pass, making it inappropriate to apply a one in four triggering interval to the peak stage of a stress protocol simply on the basis of this frequency being ideal at rest. This theoretically becomes problematic if one is attempting to derive perfusion information by comparing baseline and peak stage images from an Adenosine vasodilator protocol. However, alternative approaches such as reducing the trigger interval at peak stage until evidence of perfusion defects appears are open to strong criticism. For example, it is clear that reducing the trigger interval at rest to one in one or two cardiac cycles results in patchy myocardial contrast effect, despite complete contrast "fill-in" at less frequent trigger intervals with no other reason to expect impaired resting myocardial perfusion. According to this data, all cases showed variable myocardial contrast deficit at rest using trigger intervals of one in one or two cardiac cycles, despite absence of other manifestations of impaired resting myocardial blood flow and normal perfusion image at frequencies of one in four, six, or eight. There are therefore limitations to the validity of comparing perfusion at baseline and peak stress using different triggering interval. Some would contend that reduction of peak stress trigger interval is still valid, on the basis that it is possible, in some cases at least, to differentiate contrast signal deficit due to perfusion impairment from physiological perfusion variability or artefact related contrast signal deficit. However, the decision as to which defects

are "genuine" can be very subjective, and the concept of altering trigger intervals at peak stress was so significantly problematic that it was decided to keep triggering intervals constant throughout each Power Contrast Imaging™ investigation. While this work was being undertaken, Heinle et al published data confirming myocardial perfusion could be assessed without resorting to low trigger intervals such as one in one or two cardiac cycles [215]. In fact, their reason for not using such frequent triggering stemmed from a pilot study they had previously undertaken which concurred with the above stated effect; namely, that lower triggering intervals result in inadequate representation of myocardial perfusion in otherwise normal regions.

(iv) Other data relating to Optison™ infusion

Research published after this work had been completed identified a means of infusing Optison™ by specifically utilising the buoyant properties of its contained gaseous micro-bubbles [213]. Essentially, the technique involves saline being "infused through" a vertically oriented extension tube containing Optison™, which then travels to the patient at a rate and dilution determined by the saline infusion rate. It was demonstrated using the vertical extension line technique that steady microsphere concentration as well as excellent myocardial opacification were possible, while diluted infusions were less effective. Others have since found that such an infusion of Optison™ is superior for detecting myocardial opacification in direct comparison with bolus dosing [216]. There has been little progress in infusion techniques since, and it had remained the case until after completion of this study that some researchers used diluted infusions while others preferred the vertical extension line technique. In general, the

consensus would appear to be that infusions are preferable to boluses for the sake of stress protocols, and this is reflected in the subsequent development and promotion of ultrasound contrast agents specifically designed for ease of infusion.

(v) Comparison of Power Contrast Imaging with Dobutamine Stress Echocardiography

Clearly, the lack of success with all but a smallest number of Power Contrast Imaging cases means that comparison with Dobutamine Stress Echocardiographic wall motion analysis is meaningless in this part of the study.

6. CONCLUSIONS

1. Optison™ infusion is feasible during an Adenosine vasodilator protocol.

2. Non-diluted infusion of Optison™ works well until interruption occurs. This results in the relatively large static fraction of remaining micro-bubbles contained in the connection tubing, intravenous cannula, and three way tap separating into components and either remaining trapped or travelling as a bolus into the vein upon resumption of infusion, leading to inadequate subsequent myocardial contrast effects. The dilution most likely to result in high quality second phase images after interruption was 6 ml Optison™ in 30 ml total volume saline solution.

3. The most suitable triggering intervals for this protocol are 1 in 4 or 1 in 6 cardiac cycles.

4. Blooming and contrast shadowing tend to occur at high infusion rates, while incomplete myocardial contrast effect tends to occur at low infusion rates.

7. LIMITATIONS

1. The main limitation of this part of the study is the small sample size. Although carried out according to a pre-specified and rigorous protocol, this work should be regarded in essence as a pilot study.

2. Of the three Optison™ concentrations tested, the most dilute provided the best imaging characteristics. Theoretically, higher dilutions could also have provided adequate or better imaging characteristics. However, this possibility was not tested.

3. It should be noted that Optison™ infusion is in fact an awkward and labour intensive process, requiring the dedicated attention of an assistant throughout the examination. Further development in contrast agent and ultrasound system design will eventually render this work on infusion obsolete.

CHAPTER THREE

INTERMITTENT POWER CONTRAST IMAGING™ IN STABLE CORONARY ARTERY DISEASE

1. REVIEW OF STIMULATED ACOUSTIC EMISSION BASED IMAGING

(i) Background

The technical aspects relating to image formation using these techniques have been outlined in Chapter 1. Previous research in perfusion assessment will be discussed in relation to such methods.

While intermittent harmonic imaging allowed for enhanced micro-bubble signal by utilising harmonic back-scatter and avoiding excessive bubble destruction, a significant amount of post-processing, typically off-line video intensity and digital subtraction techniques, was necessary in order to selectively display micro-bubble signal superimposed on tissue signal. The post-processing stage was recognised as being very important in intermittent harmonic imaging after the publication of the results of a large series of myocardial contrast echocardiography cases by Marwick's group [198]. This series demonstrated limited sensitivity for SPECT derived resting perfusion defects of standard, harmonic, and intermittent harmonic myocardial contrast echocardiography. Post-processing was not used in the study. However, much better results were reported by Kaul and colleagues using video intensity quantification techniques to identify presence of resting perfusion impairment in a series of patients who

had also undergone nuclear perfusion imaging [194]. Unfortunately, the post-processing stage is very time consuming and, in general, needs to be specifically designed to meet the requirements of single laboratories. Hence, it became clear that a more clinically appropriate and widely applicable method of micro-bubble display was necessary. This appeared in the form of Stimulated Acoustic Emission techniques. However, even after these methods had matured, off-line video intensity assessment remained necessary in certain highly experimental protocols, and desirable in some clinical studies.

(ii) Tissue Models

It has been shown that micro-bubble flow can be quantified accurately in a tissue model by a variety of stimulated acoustic emission methods coupled with infusion of Levovist® [217] and Definity™ [218], and with bolus doses of Optison™ [219]. While in vitro work is obviously important as a precursor to animal and human studies, in vivo work is vastly different. Biological factors such as variable capillary density, distance of object from ultrasound source, movement artefact, and interference with image caused by adiposity, lungs, and ribs make the assumption that in vitro studies are transferable to and comparable with in vivo work almost invalid.

(iii) Animal Experimental Data

Animal experiments have been conducted to assess Stimulated Acoustic Emission based methods in settings of normal perfusion, variable coronary artery stenosis, coronary occlusion, and myocardial infarction. Broillet et. al. published results of experiments with a combination of such a technique (Harmonic Power

Doppler, ATL HDI 3000) and intravenous Sonovue™ (Bracco Diagnostics, Princeton, NJ 08540, USA) in both a tissue model and in mini-pigs [220]. Variable echocardiographically derived contrast flow rates were detected in keeping with actual flow in the tissue model and in keeping with the dynamics of coronary vascular bed flow during and immediately after occlusion of the left anterior descending coronary artery in the mini-pigs. Others, using Optison™ infusion coupled with the ATL HDI 5500 ultrasound machine, have found a strong correlation between Intermittent Harmonic Power Doppler (IHPD) derived video intensity and fluorescent micro-bubble flow ratios in open chest dogs subjected to variable coronary artery stenosis [221]. Grey scale background subtracted video intensity in the same animals was also found to be inferior to IHPD in terms of ability to demonstrate reduced video signal at all grades of stenosis except total occlusion. Meanwhile, visually appreciable myocardial contrast signal was demonstrated without offline processing by using IHPD imaging coupled with Levovist® injections in dogs with normal coronary arteries [222]. More recently, two and three-dimensional IHPD has been shown to accurately predict nuclear perfusion defect size and subsequent post mortem verified myocardial infarction size during and after coronary occlusion in dogs injected with the new agent AI 700™ (Accusphere Inc., Watertown, MA, USA) [223]. Interestingly, however, grey scale harmonic imaging undertaken on the same series of dogs was more sensitive for perfusion defects than Harmonic Power Doppler. This finding is not in keeping with the results of most comparisons, and it should be noted that the sensitivity of Harmonic power Doppler was still high at 80%.

(iv) Human studies

In 1997, using IHPD and peripheral venous injection of Levovist®, Becher et al. demonstrated patchy reticular contrast signal representing the myocardial capillary bed in three healthy volunteers and two patients with ischaemic heart disease [196]. The primary aim of their study was to show delineation of left and right ventricular cavities from myocardium rather than to quantify myocardial perfusion, so stressors were not used and detailed assessment of Power Doppler signal was not carried out. However, the results did suggest that IHPD imaging could be used to display myocardial vasculature with sufficient clarity for visual appreciation without off-line post-processing. The next step for similar imaging modalities was to be able to demonstrate resting perfusion defects, and this capability was soon confirmed. For example, Nanda et al. demonstrated an apical contrast deficit using Power Contrast Imaging™ in a single patient with prior myocardial infarction and an associated apical nuclear perfusion defect [224]. A careful and more systematic study by Roxy Senior et al used blinded observers to rate presence or absence of myocardial perfusion by Harmonic Power Doppler after injections of Sonovue™ among fifteen patients with known coronary artery disease and Tc99m-SPECT resting perfusion defects [225]. In the latter study, excellent mean territorial concordance of 92% was demonstrated between SPECT and Harmonic Power Doppler. However, caution is still necessary in interpreting perfusion images, as evidenced by the findings of Kolias et al. using video intensity analysis of images generated by the Acuson Sequoia Power Contrast Imaging™ package coupled with Optison™ infusion [214]. This study confirmed significant regional variation in percentage contrast signal intensity

reduction between perfusion and post-destruction frames, implying regional variation in ultrasound effect, capillary density, or artefact.

The first major published study exploring the ability of Harmonic Power Doppler imaging to detect Adenosine stress induced perfusion defects in a clinical setting used Optison™ micro-bubbles and a Hewlett-Packard Sonos 5500 ultrasound system in patients who also underwent nuclear myocardial perfusion assessment [215]. The results, published while the series of investigations detailed in this thesis was underway, were encouraging but did not establish a significant clinical role for perfusion myocardial contrast echocardiography, with agreement between SPECT and HPD of 81%, 76%, and 72% for the left anterior descending, right, and circumflex coronary territories respectively. Only 15 out of 103 patients underwent combined Harmonic Power Doppler Imaging, SPECT, and angiographic assessment, as the authors felt coronary angiography was not a valid comparator for myocardial perfusion imaging. While this assumption about angiographic imaging is true in physiological terms, coronary angiography is without doubt the gold standard for diagnosing and quantifying epicardial coronary artery disease in clinical practice and it is still informative to include it as a comparator, especially given the fact that nuclear perfusion estimates have a significant false positive rate. However, when the results from this subgroup of 15 patients is scrutinized, it becomes clear that Harmonic Power Doppler imaging was less sensitive (62% vs. 73%) although more specific (89% vs. 79%) than SPECT for significant coronary artery disease (>50% luminal diameter stenosis). In fact, Harmonic Power Doppler and SPECT correlated only moderately with one another (Phi=0.526, Cohen's Kappa=0.513, p=0.001).

Taking all 103 patients into consideration, if one assumes SPECT to be accurate for significant underlying coronary artery stenosis and fixed defects are excluded on the basis that they represent either artefact or infarction (i.e. the investigation is designed to detect impaired perfusion secondary to coronary artery stenosis rather than scar tissue), reversible defects on Harmonic Power Doppler imaging were present in 12 out of 24 coronary territories with similar SPECT defects, and 15 out of 174 territories without such defects. This gives a sensitivity of only 44%, a specificity of 93%, positive predictive value of 50% (95% confidence interval 31% to 69%), negative predictive value of 91% (95% confidence interval 86% to 95%), and a Cohen's Kappa score of 0.39 (p<0.001) for stenotic coronary arteries supplying non-infarct myocardium. If both fixed and reversible defects are assumed to be valid (i.e. the investigation is designed to detect impaired perfusion secondary to coronary artery stenosis or scar tissue), sensitivity rises to 68% and specificity falls to 81%, with a Cohen's Kappa score for agreement between the two techniques of 0.48 (p<0.001). Given published sensitivity of conventional stress echocardiography of at least 74% and specificity of 69% to 100%, it is unclear if the above degree of accuracy is of any practical use. However, it remained the case that each individual method, with its specific combination of hardware, software, micro-bubble type, and stress protocol, needed to be considered on its own specific merits. It was premature to make generalisations of poor performance of such a new technique, and there was certainly a need to quantify accuracy in other clinical circumstances. Furthermore, it should perhaps be regarded as very promising that one of the earliest forms of modern ultrasound perfusion analysis demonstrated even moderate correlation with nuclear perfusion imaging results.

(v) Rationale for this Study

The case for further investigation of Stimulated Acoustic Emission based imaging remained at the outset of this study, in many respects because of, rather than despite, the moderate accuracy of such techniques declared previously. There was a clear need to assess the clinical role of these imaging technologies in combination with a variety of technical modifications, micro-bubble contrast agents, and imaging protocols. This study deals with Adenosine Power Contrast Imaging™ using the Acuson Sequoia ultrasound system and Optison™ micro-bubbles in patients also assessed by conventional Dobutamine Stress Echocardiography and Coronary Angiography.

2. HYPOTHESES

Regarding detection of coronary artery stenosis of greater than 50% luminal diameter:

Null Hypothesis 1 (Sensitivity):

The sensitivity of Adenosine Power Contrast Imaging™ is NOT SUPERIOR to the sensitivity of Dobutamine Stress Echocardiography.

Alternative Hypothesis 1 (Sensitivity):

The sensitivity of Adenosine Power Contrast Imaging™ is SUPERIOR to the sensitivity of Dobutamine Stress Echocardiography.

Null Hypothesis 2 (Specificity):

The specificity of Adenosine Power Contrast Imaging™ is INFERIOR to the specificity of Dobutamine Stress Echocardiography.

Alternative Hypothesis 2 (Specificity):

The specificity of Adenosine Power Contrast Imaging™ is NOT INFERIOR to the specificity of Dobutamine Stress Echocardiography.

3. AIMS

To compare the ability of Dobutamine Stress Echocardiographic wall motion assessment (DSE) and Adenosine Power Contrast Imaging™ perfusion assessment (PCI) to detect one or two vessel coronary artery stenosis in excess of 50% luminal diameter.

4. METHODS

(i) Ethical Approval

The study was approved and registered by the Royal Free Hospital medical ethics committee. (Reference: Royal Free Hampstead NHS Trust Ethics code 161-99, research and development reference number 3810). All subjects gave written informed consent.

(ii) Assumptions and Sample Size Calculations

Analysis of a series of Dobutamine Stress Echocardiograms carried out at the local institution in which this study was undertaken revealed a Sensitivity of 70% and Specificity of 80% in a population with >50% stenosis of one or two

coronary vessels, the overall ratio of stenotic to normal vessels being approximately 1:1 (Operator E Roberts). It should be noted that these figures are slightly lower than mean sensitivity and specificity quoted in many published series. This presumably relates to the fact that the cases concerned were a mixture of relatively simple single and double vessel stenosis.

To be clinically useful, Adenosine Power Contrast Imaging™ would need to be no less specific but significantly more sensitive than current techniques. A clinically relevant improvement would probably require sensitivity of approximately 90%, which coincidentally matches or exceeds stated sensitivity values for certain nuclear perfusion methods and approximates experimental sensitivity using certain echocardiographic myocardial perfusion methods [226]. At the time this work was undertaken there were no directly comparable studies from which to draw conjectured sensitivity and specificity values.

Sample sizes were calculated using the principles and formulae of CA Beam [227] and WC Blackwelder [228]. These formulae were specifically designed to allow sample size estimation for sensitivity and specificity data.

For Sensitivity

Null Hypothesis: Sensitivity PCI not > Sensitivity DSE.

Alternative Hypothesis: Sensitivity PCI   >   Sensitivity DSE.

Conjectured Sensitivity of DSE = 70% (from Royal Free Hospital DSE series).

Conjectured Sensitivity of PCI = 90% (conservative from work of Moraes et al [226]).

Conjectured threshold for superior sensitivity of PCI = 90%.

Alpha = 5%.

Power = 80%.

Minimum number of stenotic territories required = 29 (assuming absolute correlation between DSE and PCI).

Maximum number of stenotic territories required = 50 (assuming non-correlation between DSE and PCI).

For Specificity

Null Hypothesis: Specificity PCI < Specificity DSE.

Alternative Hypothesis: Specificity PCI not < Specificity DSE.

Conjectured Specificity of DSE = 80% (from Royal Free Hospital DSE series).

Conjectured Specificity of PCI = 90% (conservative from work of Moraes et al [226]).

Conjectured threshold for inferiority of PCI = 75%.

Alpha = 5%.

Power = 80%.

Minimum number of non-stenotic territories = 25 (assuming absolute correlation between DSE and PCI).

Maximum number of non-stenotic territories = 69 (assuming non-correlation between DSE and PCI).

Thus, the target sample size was approximately 50 stenotic and 50 non-stenotic coronary arteries among a population of patients with one or two vessel disease. Recruitment of 33 patients with an equal proportion of single and double vessel

disease would result in approximately 50 stenotic vessels and 50 non-stenotic vessels in total.

(iii) Subjects

Thirty-five patients with >50% stenosis, affecting one or two coronary arteries and without occlusion or sub-total occlusion, were recruited. These patients had been scheduled for percutaneous coronary intervention. Inclusion criteria were diagnostic coronary angiography within one month, and informed consent. Exclusion criteria were previous trans-mural myocardial infarction, acute coronary syndrome or symptomatic deterioration during the previous month, unstable angina, sensitivity to albumin products, previous adverse reaction to Dobutamine or Adenosine, valvular heart disease, asthma, second or third degree atrio-ventricular block, and caffeine or methylxanthine related product ingestion during the 24 hours preceding each study. Each patient underwent Power Contrast Imaging™ using Adenosine vasodilator stress and echocardiographic wall motion assessment using Dobutamine stress. Investigations were carried out on separate days within a two-week period.

(iv) Dobutamine Stress Echocardiography Protocol

Dobutamine Stress Echocardiography was performed according to standard protocols, using the segmental model recommended by the American Society of Echocardiography [229]. Baseline electrocardiogram, blood pressure and two–dimensional echocardiogram were recorded at rest. Two-dimensional images of the parasternal long and short axes and apical four and two-chamber views were obtained with the patient in the left lateral decubitus position. Images were

acquired with an R–wave trigger to obtain a continuous loop using the Stress Echocardiography program of the Sequoia C256 echocardiography machine. Image loops from baseline, low, intermediate and peak stress stages were displayed in a quad screen format for analysis. Dobutamine was infused through a peripheral intravenous line using a mechanical pump starting at a dose of 5 mcg/kg/min and increasing to 10, 20, 30, 40 and 50 mcg/kg/min at intervals of 3 minutes until an end point was reached. If significant wall motion abnormalities were absent and the target heart rate had not been achieved ($\geq$85% of maximum predicted for age and sex of the patient) the final stage was prolonged to a maximum of 5 minutes, and/or atropine was added in bolus doses of 300 mcg, up to a maximum of 1500 mcg.

Electrocardiograms and two–dimensional echocardiograms were monitored continuously and blood pressure was measured at three-minute intervals. Continuous clinical monitoring was also undertaken throughout. Test end points included $\geq$85% of maximum predicted heart rate, development of severe and/or extensive new wall motion abnormalities, horizontal or down-sloping electrocardiographic ST segment depression of >0.2mV 80 ms beyond the J point, ST segment elevation, severe angina, fall of systolic blood pressure of > 40 mmHg from baseline or to < 90 mmHg systolic, blood pressure of > 230/120 mm Hg, significant tachyarrhythmia, and intolerable side effects secondary to Dobutamine.

(v) Power Contrast Imaging™ Protocol

For Power Contrast Imaging™, Optison™ was infused as a diluted solution of 3ml in 15 ml solution with 0.9% saline via an 18 gauge intravenous cannula placed in a large antecubital fossa vein. A 50ml syringe driver was used to infuse the solution at a constant rate, starting at 120 ml/min and increasing as necessary until good baseline perfusion was seen. This is the same concentration and infusion rate that was found to be ideal in previous work detailed in Chapter 2. However, only half the quantity of Optison™ was used for each study, reflecting the fact that the required period of Optison™ enhanced was brief. The syringe driver was rotated continuously by hand in horizontal and vertical planes. Optison™ infusion was started one minute prior to acquisition of baseline images, discontinued during the first three minutes of Adenosine infusion, and then recommenced for peak imaging during the fourth minute of Adenosine stress. Peak stress images were acquired during the fifth minute.

Triggers were set to acquire end diastolic images every fourth cardiac cycle. If end diastolic imaging resulted in poor visualisation of perfusion effect during Optison™ infusion at baseline, triggering was adjusted to acquire end systolic images before image acquisition. The ultrasound machine settings were according to the recommendations and pre-sets of the Power Contrast Imaging™ (PCI) mode of the Acuson Sequoia C256 echo machine (see table 3.1). Focus depth was set during baseline PCI at the level of the mitral valve. If contrast signal was not seen in the apical myocardium during baseline PCI, the focal depth was moved toward the apex until signal was evident. If apical signal was absent despite this adjustment, it was assumed a fixed perfusion defect was

present. Contrast image settings were established during baseline PCI and maintained constant throughout each study. Imaging frame rate was kept at 1:4 cardiac cycles throughout each study. Apical four and two chamber images were acquired at baseline and repeated during the fifth minute of "stress", which was achieved by infusing Adenosine at 140mcg/kg/min for five minutes, through a separate intravenous cannula. Patients were re-warned about possible sensations of flushing, dyspnoea, and faintness due to Adenosine and were asked to hold their breath for each peak stress image acquisition at the point of the respiratory cycle allowing the best echocardiographic view.

Clinical and electrocardiographic monitoring was carried out continuously throughout the investigation and blood pressure was checked every two minutes during Adenosine infusion. Adenosine was stopped if the following occurred: horizontal or down-sloping electrocardiographic ST segment depression of >0.2mV 80 ms beyond the J point; ST segment elevation; angina pectoris; fall of systolic blood pressure of > 40 mmHg from baseline or to < 90 mmHg systolic; significant brady-arrhythmia; and intolerable Adenosine related side effects.

(vi) Echocardiographic Image Interpretation

Images were acquired digitally and stored in digital format on magneto-optical discs and in analogue format on VHS video. Interpretation of images was done in a blinded fashion in order that the observer had no knowledge of the angiographic data.

Dobutamine Stress:

The 16 segment model was used for interpretation of Dobutamine Stress Echocardiograms, in line with previous widely accepted recommendations [229]. Images were placed in quad screen format, enabling baseline, low, intermediate, and peak stages of stress to be compared in phase with each other. If peak stress occurred at a dose other than 40 mcg/kg/min, the relevant images were placed in the 40mcg/kg/min screen slot. DSE was regarded as positive if there was evidence of new or worsening wall motion or thickening abnormalities, with more than one segment needing to be involved to confirm ischaemia in the basal segments of the posterior circulation.

Adenosine Power Contrast Imaging™:

After completion of each PCI investigation, the highest quality images were selected from baseline and peak stress and placed in a dual screen format for comparison. Presence or absence of perfusion was assessed visually, using the model for coronary territories depicted in figure 3.1. Perfusion was graded as full or impaired. PCI signal defects were interpreted as genuine perfusion deficit or artefact using comparator segments as detailed in table 3.2 and the general principles outlined in previous recommendations [230]. A reversible perfusion defect was deemed present if a clearly demarcated contrast signal deficit appeared at peak stress in a segment characterised by good signal at baseline. If a segment was not visualised at baseline, it was not included in analysis.

(vii) Angiographic Image Interpretation

All patients had undergone X-ray coronary angiography according to standard techniques [231] less than one month prior to echocardiographic studies. An experienced interventional cardiologist (Dr DP Lipkin) analysed each coronary angiogram to give a visual estimate of the percentage reduction in luminal diameter. Coronary stenosis was deemed significant if this figure exceeded 50%. Cases with evidence of distal vessel collateralisation were excluded, as were cases with occluded or sub-totally occluded vessels, or evidence of transmural Myocardial Infarction. If a patient agreed to participate, he/she was entered into the study with angiographic details omitted from the data sheet. After echocardiographic image analysis and reporting, angiographic data was recombined with the relevant echocardiographic and clinical data.

(viii) Statistical Analysis

Parametric variables are expressed as mean plus standard deviation. Non-parametric variables are expressed as median with inter-quartile range.

Sensitivity, specificity, negative and positive predictive values, and accuracy were calculated for DSE and PCI, using angiography as the reference standard. Sensitivities, specificities, and accuracies of each investigation were compared using McNemar's test for dependent proportions. Fisher's Exact Test was used for comparison of categorical values for heterogeneous groups and when it was not feasible to calculate McNemar's Test due to sample size. Correlation of DSE and PCI results with angiographic coronary stenosis territory were calculated using Chi square-based statistics (Phi). Statistical significance was set at a p value of ≤ 0.05 (2-sided).

Interobserver variability was tested for DSE and PCI on an individual territory basis and for all territories combined. For this, presence or absence of a peak stress territorial wall motion abnormality or reversible contrast deficit were rated independently by two operators, with subsequent Kappa score calculation.

5. RESULTS

Thirty-five patients were recruited to the study. Four patients were excluded after they declined further investigation following DSE. Three patients with poor baseline image quality, uninterpretable PCI images, and left anterior descending coronary artery stenosis were excluded. In two of these cases, DSE was successful and suggested left anterior descending territory ischaemia. The remaining twenty-eight patients had stenoses of greater than 50% luminal diameter in forty-one out of eighty-four coronary arteries, while there were forty-three normal or minimally stenosed coronary arteries. The mean age of this group was 62.6 years (standard deviation 9.9 years). All patients had a history of stable exertional Angina Pectoris but none had experienced Myocardial Infarction. For baseline characteristics and coronary stenosis territories, see Tables 3.3 and 3.4.

All patients reached a suitable end-point for DSE (wall motion abnormality or 85% target heart rate). All patients completed five minutes of Adenosine infusion. Chest pain occurred during 6 DSE and 13 PCI studies. Dyspnoea occurred during 10 PCI studies. There were no significant haemodynamic problems or cardiac rhythm disturbances.

For details of wall motion abnormality and PCI result against angiographic stenoses, see Table 3.10, 3.11, and 3.12.

(i) Diagnostic Effectiveness for Combined Territories

Among the 28 cases in whom both DSE and PCI were conclusive (Tables 3.5 and 3.10):

DSE correctly identified significant coronary artery disease in 18 out of 20 left anterior descending territories (LAD), 11 out of 12 right coronary territories (RCA), and 6 out of 9 circumflex territories (Cx). DSE correctly identified all 8 non-stenosed left anterior descending territories, 14 out of 16 non-stenosed right coronary territories, and all 19 non-stenosed circumflex territories. Overall sensitivity of DSE was 85.4% (95% Confidence Interval 70.1% to 93.9%), specificity was 95.4% (95% Confidence Interval 82.9% to 99.2%), negative predictive value was 87.2% (95% Confidence Interval 71.3% to 95.4%), positive predictive value was 94.6% (95% Confidence Interval 80.5% to 99.1%), and accuracy was 90% (95% Confidence Interval 81.6% to 95.5%).

PCI correctly identified significant coronary artery disease in 14 out of 20 LAD territories, 6 out of 12 RCA, and 4 out of 9 Cx territories. PCI correctly identified 7 out of 8 non-stenosed left anterior descending territories, all 16 non-stenosed right coronary territories, and 15 out of 19 non-stenosed circumflex territories. Overall sensitivity of PCI was 58.5% (95% Confidence Interval 42.2% to 73.3%), specificity was 88.4%, (95% Confidence Interval 74.1% to 95.6%), negative predictive value was 69.1% (95% Confidence Interval 49.2% to 84.1%),

positive predictive value was 82.8% (95% Confidence Interval 63.5% to 93.5%), and accuracy was 73.8% (95% Confidence Interval 62.9% to 82.5%).

The difference in sensitivity between DSE and PCI among the 28 cases for whom both imaging modalities were interpretable is statistically significant (McNemar based p value = 0.003), implying that PCI has inferior sensitivity to DSE. The difference in specificity is statistically non-significant. The difference in negative predictive value is statistically significant (Fisher's exact p value = 0.034), implying PCI has inferior negative predictive value compared to DSE. The difference in positive predictive value is statistically non-significant. The overall accuracy of DSE was greater than that of PCI, in terms of both statistical and clinical significance, at 90% compared to 73.8% (McNemar based p value = 0.003). For an example of a reversible apical contrast defect in a patient with stenosis in the mid left anterior descending coronary artery, see Figure3.2.

Among the 30 cases for whom DSE was successful, including 2 cases for whom PCI was unsuccessful (Tables 3.6, 3.10, 3.12):

Overall sensitivity of DSE was 86.1% (95% confidence interval 71.4% to 94.2%), specificity was 95.7% (95% confidence interval 84.3% to 99.3%), positive predictive value was 94.9% (95% confidence interval 81.4.1% to 99.1%), negative predictive value was 88.2% (95% confidence interval 73.0% to 95.8%), and accuracy was 91.1% (95% confidence interval 82.7% to 95.8%). When diagnostic effectiveness of DSE among these 30 cases was compared with diagnostic effectiveness among the 28 interpretable PCI cases, DSE was superior

in terms of sensitivity (p value = 0.007), negative predictive value (p value = 0.02), and accuracy (p value = 0.004).

Among 26 patients with good or fair echocardiographic images, after exclusion of all those with poor images (Tables 3.7 and 3.11):

Overall sensitivity of DSE was 84.6% (95% confidence interval 68.8% to 93.6%), specificity was 94.9% (95% confidence interval 81.4% to 99.1%), positive predictive value was 94.3% (95% confidence interval 79.5% to 99.0%), negative predictive value 86% (95% confidence interval 69.3% to 94.8%), and accuracy was 90.4% (95% confidence interval 80.3% to 95.2%). Overall sensitivity of PCI was 61.5% (95% confidence interval 44.7% to 76.2%), specificity was 92.3% (95% confidence interval 78.0% to 98.0%), positive predictive value was 88.9% (95% confidence interval 69.7% to 97.1%), negative predictive value was 70.6% (95% confidence interval 49.9% to 85.7%), and accuracy was 76.9% (95% confidence interval 65.8% to 85.4%). Among these cases, PCI was inferior to DSE in terms of sensitivity (p value = 0.012) and accuracy (p value = 0.021).

(ii) Diagnostic Effectiveness for Individual Coronary Territories

(See Tables 3.8, 3.9, 3.10, and 3.12).

Sample size was too low for meaningful subgroup analysis by coronary territory. However, for completeness, results are shown in the tables specified above.

(iii) Reproducibility

Interobserver variability testing was possible among 21 cases, one of whom had poor image quality, five of whom had fair image quality. Intraobserver variability was not systematically tested, as it was apparent that repeat interpretation was influenced by recollection of images that had been analysed previously.

Agreement between raters for presence or absence of DSE wall motion abnormality was 90.5% in the left anterior descending coronary territory, with a Kappa score of 0.80 ($p=0.001$). For the right coronary artery territory, agreement was also 90.5%, with a Kappa score of 0.80 ($p<0.001$). For the circumflex territory, agreement was again 90.5%, with a Kappa score of 0.62 ($p=0.029$). Overall agreement between raters for presence or absence of DSE wall motion abnormality was 90.5%, with a Kappa score of 0.80 ($p<0.001$)

Agreement between raters for presence or absence of PCI reversible contrast deficit was 85.7% in the left anterior descending coronary territory, with a Kappa score of 0.70 ($p=0.002$). For the right coronary artery territory, agreement was 95.2%, with a Kappa score of 0.83 ($p=0.003$). For the circumflex territory, agreement was 81.0%, with a Kappa score of 0.57 ($p=0.017$). Overall agreement between raters for presence or absence of PCI reversible contrast deficit was 87.3%, with a Kappa score of 0.73 ($p<0.001$).

6. DISCUSSION

The acid test for Myocardial Contrast Echocardiography in diagnosis of stable coronary artery disease is whether it is any better than Dobutamine Stress

Echocardiography in routine clinical practice. This data suggests that the particular PCI technique under investigation here, using Adenosine as the stressor, is not as diagnostically effective as conventional DSE in a clinical setting. The results concur to a degree with the work of Heinle et al.[215], in that sensitivity of such echocardiographic perfusion techniques is low, while specificity is high. In many respects, the fact that the specificity of the technique is so high is a very promising finding. As with any diagnostic test, the balance of sensitivity and specificity are the determinants of their clinical usefulness. It is frequently the case that a high specificity is accompanied by a low sensitivity, and vice versa. When techniques are in their design and development phase, it may be possible to adjust the threshold at which the test is said to have produced a positive result, thereby shifting the balance between sensitivity and specificity in a more favourable direction. These findings suggest there may be scope for reducing the stringency of criteria required to label a myocardial segment as having a perfusion defect, or to alter the ultrasound system settings such that micro-bubble contrast effect is less intense, increasing the chance of detecting underlying impairment.

(i) Choice of Stress Agent for Power Contrast Imaging™

As previously discussed, coronary stenoses of between 50% and 85% luminal diameter are likely to result in perfusion abnormalities under stress or hyperaemic conditions, while more severe stenoses may cause resting hypoperfusion in the associated coronary artery territory.

The methods of "stress" for echocardiographic or radionuclide imaging protocols depend on a number of variables and essentially fall into one of two categories – those that cause vasodilatation and those that directly increase cardiac work. Vasodilators, such as Adenosine and Dipyridamole, predominantly cause changes in myocardial perfusion dynamics such that perfusion defects appear in ischaemic regions. Inotropic agents such as Dobutamine increase cardiac work thereby causing perfusion supply and demand mismatch and ultimately ischaemia. Exercise is certainly the most physiological stressor, as it exactly replicates the local conditions likely to produce ischaemia while also increasing non-cardiac work with consequent increases in tissue metabolism and respiration.

Adenosine is a purine nucleoside with a complex set of cardiac effects, including potent vasodilatation mediated via coronary smooth muscle and endothelial relaxation. Wilson et al demonstrated that an intravenous infusion of Adenosine at 140 mcg/kg/min achieved full coronary vasodilatation 84 +/- 46 seconds after starting the infusion, while cessation of effect occurred 145 +/- 67 seconds after termination of infusion [232]. Haemodynamic effects of this Adenosine dose include a modest rise in heart rate, increased pulmonary capillary wedge pressure, a fall in systolic blood pressure and a reduction in systemic vascular resistance [233]. However, ischaemia does not necessarily become simultaneously manifest during Adenosine infusion according to non-perfusion based assessment methods [234]. Dipyridamole has similar effects mediated by inhibition of endogenous Adenosine uptake at the cellular level, thereby mimicking the effects of exogenous Adenosine.

Dobutamine is a synthetic catecholamine capable of producing a marked inotropic and chronotropic response, the overall balance of effect being determined by a mixture of alpha and beta-adrenergic stimulation. While the degree of coronary hyperaemia associated with Dobutamine infusion is nearly as pronounced as with intracoronary Adenosine, the latter drug induces less contractility and rate rise than the former, during either coronary or intravenous infusion [235]. Theoretically, this makes Dobutamine more likely to induce ischaemia than Adenosine. Dobutamine, in common with other stressors, has a short half-life, which makes it suitable for short-term induction of stress during echocardiography, its half-life being approximately 2 minutes [236].

Conventionally, Stress Echocardiography is carried out during exercise or Dobutamine / Dobutamine-Atropine infusion, although some would advocate use of Dipyridamole [237-240], Arbutamine [241-243], or high dose Adenosine (200mcg/kg/min) [244]. There is some evidence suggesting, perhaps counter intuitively, that Dipyridamole and Dobutamine stress echocardiography are similarly accurate [245], despite the different modes of action of these stressors [246]. Adenosine is seldom used in clinical practice of stress echocardiography, as evidence of its effectiveness is lacking for all but high dose infusions, which produce more unpleasant side effects than the standard dose. For nuclear perfusion assessment, however, Adenosine [233,247-249] and Dipyridamole [250,251] have a very large body of evidence behind their use. Despite a general preference for vasodilator stress during nuclear perfusion assessment, there is data to suggest that Dobutamine is just as suitable, with acceptable sensitivity, specificity, and safety [252-254]. Preference for one form of stress over another is

ultimately dictated by practical and technical considerations. It remains the case that Dobutamine (with or without Atropine) is predominantly used for stress echocardiography, and Adenosine or Dipyridamole are predominantly used for nuclear myocardial perfusion studies, and there is some data to support such an approach [233,255].

Using Power Contrast Imaging™ puts certain limitations on the choice of stress agent. It should be appreciated that it is very difficult to keep the same echocardiographic section through the heart when the subtle visual clues of continuous high frame rate imaging are lost. Triggering at one in four cycles often results in slightly different frame-to-frame image sections despite no conscious alteration of probe position relative to the heart. Physical exercise stress simply exacerbates this problem and is therefore extremely unlikely to provide accurate information, making pharmacological agents necessary. Although there are a number of reasons for using Dobutamine in this type of investigation, this drug does cause significant tachycardia. This becomes important when intermittent imaging parameters, such as electrocardiography based image triggers as per the Acuson PCI system, need to be set at baseline. It is not easy to re-set these at peak stress and inaccurate setting can result in wall motion artefact being mistaken as perfusion. In addition, the inotropic effect of Dobutamine can markedly alter the cross sectional profile of myocardium at end systole, making it difficult to be sure if an appropriate and representative image has been acquired, as well as making comparison of baseline and peak perfusion images difficult. It is therefore important to use an agent that does not cause significant tachycardia or major inotropism, such as Adenosine. This agent does

cause a sense of dyspnoea, which can impair the echocardiographic window due to deep and rapid breathing. However, it is possible to minimise this effect to some extent by careful reassurance and by asking the patient to breath hold or take shallow breaths at crucial imaging points.

While Adenosine is at least theoretically more practicable than Dobutamine or other stressors for intermittent stimulated acoustic emission based methods, there is no data directly comparing stressors for such imaging methods. However, recent work by Lafitte et al demonstrates that Adenosine and Dobutamine are able to induce perfusion impairment that is detectable by real-time low mechanical index myocardial contrast echocardiography, even without coexisting wall motion abnormality [158]. Laffite's findings also suggest that, while Dobutamine results in perfusion impairment and wall motion abnormality at less severe grades of stenosis than Adenosine, the latter drug yields more interpretable contrast echocardiographic images than Dobutamine. Whether the superiority of Adenosine over Dobutamine for real-time imaging is as marked for Power Contrast Imaging™ remains unclear in terms of the available evidence, although it is plausible that this is the case.

Considering the above discussion and previous published data, it would seem that Adenosine is the most suitable agent for pharmacological vasodilatation during Power Contrast Imaging™. The precise mode of administration is also an issue, as the drug can be introduced into venous circulation as a continuous infusion or as a bolus dose (direct coronary injection is not within the remit of the study). Most investigators have tended to use infusions, mirroring experience

with nuclear perfusion methods, but there is data to suggest Adenosine is effective when introduced in bolus doses of 6 to 18 mg, albeit during intermittent second harmonic myocardial contrast echocardiography [256,257]. Moreover, a well-designed study has recently shown that, among 64 patients undergoing Myocardial Contrast Echocardiography and Dipyridamole Thallium SPECT, Adenosine bolus and infusion are equivalent in terms of diagnostic accuracy, practicality, and safety [258]. It must be recognised, however, that such high bolus doses can be extremely unpleasant for the patient. Beyond this, and despite the above studies, such an approach might result in image acquisition during different stages of Adenosine response from one patient to the next, depending on when during Adenosine build up, peak, or decay phases the images were captured. In addition, an infusion offers the advantages of steady state vasodilatation and controlled conditions. It was therefore decided not to use bolus doses of Adenosine, and the standard infusion of 140mcg/kg/minute was chosen.

(ii) Choice of Dobutamine Stress Echocardiography and Coronary Angiography as Comparators

While others have validated a number of echocardiographic perfusion techniques against radionuclide methods [198,215,225,259-261], it is clear that ultrasound myocardial perfusion estimation needs to be at least as clinically useful as conventional stress echocardiography. This requires excellent diagnostic accuracy in an equivalent or broader population group to that for which stress echocardiography is currently used. Comparison of echocardiographic perfusion

estimation with conventional stress echocardiographic parameters is therefore appropriate.

Coronary Angiography is by no means a functional assessment of perfusion and ischaemia. Territories supplied by a significantly stenotic coronary artery can also be supplied by good collateral vessels, making perfusion normal or near normal. To reduce the chances of this phenomenon, cases of angiographically detectable collateralisation were excluded from the study. In addition, normal epicardial coronary arteries do not preclude perfusion impairment, presumably due to unrecognised small vessel disease [262]. Despite this, angiographic measures of coronary disease type and severity remain the ultimate determinant of treatment strategy and have powerful prognostic value.

Because of these issues, diagnostic efficacy of Adenosine PCI was compared with that of conventional DSE in a cohort of patients with angiographically determined coronary artery disease.

(iii) Mechanism of Reduction in Peak Stress Contrast Intensity

In theory, the intensity of micro-bubble signal in a myocardial region relates to the concentration of micro-bubbles in that region, which in turn relates to its contained Myocardial Blood Volume. In terms of two dimensional imaging, as evidenced by a series of careful experiments conducted at the University of Virginia School of Medicine, a similar relationship holds for the myocardial cross sectional area in a two-dimensional image plane [144]. While normal coronary vessels can supply increased flow demand under hyperaemic conditions, thus

allowing for an increase in myocardial blood flow with or without a limited expansion of myocardial blood volume, the same conditions in a stenotic myocardial bed result in a reduction in the myocardial blood volume. This is probably mediated by an increase in the capillary bed gradient and collapse or compensatory decruitment of capillaries in order to maintain constant pressure. Thus, reduced micro-bubble signal video intensity during peak hyperaemia in regions supplied by a stenotic coronary artery can be expected.

(iv) Trigger Interval Settings

Some researchers recommend using variable trigger interval during intermittent Harmonic Power Doppler studies. While it is theoretically possible to quantify myocardial micro-bubble replenishment rate and hence myocardial blood flow with this approach, the intention here was to allow display of impaired contrast signal at fixed trigger intervals. It may be that sensitivity could have been improved using triggering intervals such as one in two instead of one in four cardiac cycles at peak stress. The one in four interval used in this study may have been too high, allowing capillary replenishment with micro-bubbles between triggers despite impaired myocardial perfusion in the stenotic vascular territory. However, there are problems with reducing trigger intervals at peak stress, as discussed in Chapter 2. Others agree that triggering intervals should be at least one in four cardiac cycles at peak Adenosine stress using such imaging techniques, based on their findings of contrast deficit as part of normal physiology at lower intervals [215].

Dual trigger imaging and wall motion artefact:

Another possible reason for the low sensitivity demonstrated here could have been false interpretation of wall motion Doppler signal as perfusion. One way to negate such a problem is to use dual trigger intermittent imaging, whereby a second pulse of ultrasound shortly after the main imaging pulse is used to verify complete micro-bubble destruction. If a "perfusion signal" is present on the second pulse, it must logically be due to wall motion and not perfusion. This approach, utilised by Grayburn's group and others [214,215], allows the interpreter to make an allowance for wall motion artefact when comparing pre and post stress images, therefore reducing the chance of false attribution of Doppler signal to perfusion. This problem is more pronounced if tachycardia occurs, such as with Dobutamine or exercise stress, as this makes identification of the ideal trigger point within the cardiac cycle prone to error. Dual triggering was not used in this study because previous local experience was that the second trigger made it difficult to assess during the study whether or not an adequate perfusion effect had been displayed at the time of the first trigger. Such an assessment is important because it allows for minor but crucial alteration of the image plane during baseline and peak imaging as well as alteration of infusion rate and machine settings prior to commencing Adenosine. It was reasoned that minimal tachycardia, as per Adenosine infusion, would allow very precise selection of triggering point, thereby avoiding wall motion signal as much as possible.

End-systolic and End-diastolic Triggering:

There is no consensus as to which of these trigger points is most suitable. The end-diastolic period has the advantage of being relatively easy to accurately

identify and end-diastolic images may be less prone to wall motion artefact. However, the broader the "object" to be interrogated by an ultrasound beam, the more problematic the displayed image. This is partly related to rib and lung induced lateral dimension image loss and partly due to inherent problems with ultrasound in the lateral plane at depth. In addition, end diastolic frames tend to have a relatively thin rim of myocardium and relatively strong mitral annular and epicardial signal, especially toward the basal wall segments. Previous local experience of this technique revealed that this thinness occasionally made visual interpretation of myocardial contrast signal very difficult. End-systolic triggering is not without its problems, however. Firstly, the precise point at which "end-systole" occurs may be difficult to identify, despite careful attention to the electrocardiographic signal. This makes wall motion artefact very difficult to avoid. Secondly, the inotropic effect of the "stressor", even Adenosine rather than Dobutamine, is such that the myocardial thickness at peak stress is greater than at baseline imaging. This incomparability of images will certainly affect interpretation and could conceivably reduce its accuracy. However, there are two specific advantages to end-systolic imaging: firstly, the relatively narrow "object" allows better imaging in the lateral plane at depth; secondly, the relatively high myocardium to epicardium ratio allows good visualisation of myocardial contrast signal. To analyse accuracy among subgroups according to which technique was used in this study would introduce bias due to the small numbers involved. For this reason, this was not formally investigated.

The decision to use a combination of end-diastolic and end-systolic triggering, maintaining the most suitable method for each individual patient constant

between baseline and peak stress imaging, reflects a pragmatic approach based on the fact that different patients have different echocardiographic features which render one or other technique more suitable. Purists might suggest only systolic or diastolic frame imaging should have been used, but this does not take account of the inherent biological variability for which a clinically relevant tool must cater.

(v) Subendocardial and Transmural Contrast Effect

Trans-myocardial perfusion is not necessarily evenly distributed, especially under hyperaemic conditions with underlying coronary stenosis. There is evidence that relative endocardial perfusion deficit can be detected by Myocardial Contrast Echocardiography using detailed quantitative analysis of myocardial blood volume and flow [142,263]. However, demonstration of this effect has tended to require selective imaging of a specific region of myocardium, often to the exclusion of other regions. Transmural gradients in contrast signal were not evident in any consistent pattern during visual assessment in this study, although their detection was not a specific part of the experimental protocol. The same imaging system could have been set up to detect Adenosine induced trans-myocardial micro-bubble signal gradients, albeit at the expense of losing other relevant data.

(vi) Optison™ Infusion

Optison™ was designed for bolus injection rather than infusion. Although others have used Optison™ boluses to quantify myocardial perfusion, comparison between baseline and peak stress images in this protocol required steady state

micro-bubble concentration. Boluses would probably have caused shadowing and blooming artefact at peak signal. In addition, boluses could have resulted in mistaken attribution of "decay phase contrast defects" to perfusion impairment, as discussed in Chapter 2. The notion that infusion is ideal has been generally accepted within the field of contrast echocardiography, as evidenced by the fact that many other investigators have used infusion for Optison™ administration, albeit with slightly different methods.

(vii) Image Quality

Three cases were excluded from the study on the basis that the PCI image quality was very poor. A number of other myocardial wall segments could not be visualised, although this did not affect an entire coronary territory in the remaining 28 patients. This remains a limitation of PCI perfusion assessment, especially when one takes into account that parasternal windows are not generally suitable for PCI, while being eminently suitable for DSE. This allows up to twice the number of opportunities to image myocardial segments during DSE than during PCI. It is important to note that many demonstrations of PCI imaging have involved a high degree of subject selection, mainly for image quality. This study assessed applicability of the technique to clinical practice without heavy case selection, with purposeful inclusion of patients who might normally be considered for stress echocardiography, irrespective of baseline image quality. Justification for this is strong when one considers that ultrasound based perfusion assessment should ideally be at least as applicable and accurate as conventional stress echocardiography, which often provides valuable information in cases of less than perfect image quality. Indeed, the other main

application for ultrasound contrast agents, namely endocardial border delineation in sub optimal echocardiography, has allowed greater accuracy in precisely such cases, making the standard for perfusion assessment even more rigorous. The only patients excluded in this series were the three with such poor echocardiographic windows that PCI was virtually impossible to interpret. Stringent selection of cases based on baseline image quality may have resulted in better accuracy, but this would have undermined any suggestion that the technique could be used as a clinical tool. It is noteworthy that DSE was successful in two of the three cases excluded from PCI on the basis of poor image quality, and the diagnostic effectiveness of Dobutamine Stress Echocardiography among the 30 patients for whom images were interpretable still exceeded that of Adenosine Power Contrast Imaging™ among the 28 patients for whom contrast images were interpretable.

(viii) Single, Double, Triple and Complex Coronary Artery Disease

The coronary lesions included in this study were simple in that they were between 50% and 95% luminal diameter, affected the main vessel only, and did not have angiographically evident distal collateralisation. In addition, only patients with one or two such vessels were included as this enabled non-stenotic territories to be used as controls. These results cannot therefore be extrapolated to more complex or widespread coronary artery disease. Even with the simple coronary disease patterns described, control territories could have been affected by unrecognised small vessel disease.

(ix) Visual Assessment

Purely visual assessment of myocardial perfusion was used in this study. It is possible to quantify signal intensity, mainly by off-line video intensity analysis [200,214,219]. It may have been possible to improve the accuracy of contrast echocardiographic perfusion estimation using such techniques, and perhaps even to quantify degrees of perfusion impairment. These techniques have generally been applied to the open chest canine model, with near perfect image quality at baseline. Although post processing of imperfect images in clinical investigation of humans might compound errors originating prior to the image acquisition phase, it is certainly worthy of investigation. However, the Acuson PCI system was designed as an entity, with visual interpretation in mind. Later versions of perfusion imaging systems, from a variety of manufacturers, have since incorporated on-line quantification.

7. CONCLUSIONS

Regarding detection of single or double vessel coronary artery stenosis of greater than 50% luminal diameter using visual assessment during Power Contrast Imaging™:

1. Dobutamine Stress Echocardiography is superior to Adenosine Power Contrast Imaging™ in terms of sensitivity, accuracy, and negative predictive value.

2. The specificity and positive predictive value of Dobutamine Stress Echocardiography and Adenosine Power Contrast Imaging™ are not significantly different.

3. There is evidence to reject Alternative Hypothesis 1. Null Hypothesis 1 is therefore accepted.

4. There is insufficient evidence to reject Alternative Hypothesis 2. Alternative Hypothesis 2 is therefore accepted.

5. Exclusion of cases with less than ideal image quality did not make any significant difference to the diagnostic effectiveness of Power Contrast Imaging™ in this series.

6. Power Contrast Imaging™ may be better suited to detecting underlying coronary artery stenosis in certain myocardial regions than in others.

8. LIMITATIONS:

1. Greater accuracy may have been achieved using a quantitative measurement technique such as video-intensity analysis.

2. The Power Contrast Imaging™ protocol relied on Optison™ infusion. As previously discussed, this contrast agent is not ideally suited to infusion.

3. Adenosine and Dobutamine are not directly comparable means of hyperaemia and stress induction.

4. Coronary Angiography is an imperfect means by which to assess coronary artery stenosis and therefore has limitations as a reference standard for flow-limiting disease.

5. The possibility that small vessel coronary disease could have been present in some cases is acknowledged, as all patients had documented epicardial coronary stenosis in at least one major vessel.

6. The sample size is relatively small. Thus, small differences in diagnostic efficacy between imaging techniques could have been overlooked.

CHAPTER FOUR

REAL-TIME COHERENT CONTRAST IMAGING™ IN STABLE

CORONARY ARTERY DISEASE

1. REVIEW OF LOW MECHANICAL INDEX REAL-TIME PERFUSION IMAGING TECHNIQUES

(i) Background

As previously alluded to, the fact that perfusion impairment precedes wall motion abnormality in the ischaemic cascade implies that myocardial perfusion assessment should be more sensitive than wall motion assessment for underlying coronary artery disease. Despite demonstration of this in humans using relatively outdated intermittent harmonic imaging techniques [264], evidence of early perfusion impairment was not apparent during the Adenosine Power Contrast Imaging™ study described in the previous chapter. Among a number of reasons for the limited accuracy of the technique was difficulty holding an exact and specific image plane between triggered images. It is difficult to circumvent this problem using intermittent imaging techniques. In addition, while subtle refinements to the Power Contrast Imaging™ method could conceivably have improved the accuracy of the technique, wall motion data could never be incorporated into it. Real-time myocardial perfusion imaging, recently developed as a natural progression from intermittent imaging techniques, offers an unique opportunity to avoid the problem of image plane loss while incorporating myocardial perfusion and wall motion information. The logical next phase of this research was therefore real-time low mechanical index myocardial contrast imaging using the Acuson system (Coherent Contrast Imaging™ package).

(ii) Technical Details of Real-Time Myocardial Contrast Echocardiography

The first reliable method available for echocardiographic perfusion assessment in real-time was Power Pulse Inversion imaging / Pulse Inversion Doppler (ATL, Phillips Medical Systems, Eindhoven, the Netherlands) which uses Pulse Inversion technology with additional Doppler processing to differentiate micro-bubble and tissue signal. These and other approaches have been outlined in Chapter 1. The Acuson Coherent Contrast Imaging System™ (CCI) was made available in prototype form in 2000 as a logical development from Intermittent Power Contrast Imaging™, using identical system hardware alongside substantial software alteration. CCI was designed to allow high frame rates while minimising wall motion artefact, and relies on specifically shaped ultrasound pulses generating separate returning micro-bubble and tissue signal, with subsequent single pulse cancellation of the latter.

(iii) Data Available Prior to this Study

The first demonstrations of non-destructive real-time myocardial contrast echocardiography using micro-bubble selective methods were in 1999 and early 2000. The progression of experiments from tissue-mimicking phantoms through animal experiments to human studies was rapid, such that by 2001 real-time myocardial contrast echocardiography had become the preferred method for ultrasound perfusion clinical research.

(a) Phantom models of the myocardial vascular bed:

Before animal experimentation could begin, the effects of real-time low mechanical index ultrasound on micro-bubbles in a variety of tissue phantom

models were examined. Initially, each imaging system was tested separately using this approach, but certain later studies add to our understanding of real-time low mechanical index imaging in general. While real-time perfusion imaging was being tested in animal and clinical settings, researchers continued to turn to specifically designed tissue phantom experiments to understand the interaction between contrast micro-bubbles and various types of real-time imaging.

The most important single aspect of the real-time imaging approach is micro-bubble preservation. Tiemann et al first demonstrated the imaging characteristics necessary for real-time myocardial perfusion using Power Pulse Inversion in an experimental design incorporating a flow phantom acting as a tissue model [265]. In this experiment, power pulse inversion at a low mechanical index of 0.1 resulted in non-destructive real-time imaging, while a mechanical index of 0.3 resulted in partial micro-bubble destruction, and a mechanical index of 0.8 resulted in near total micro-bubble destruction. Furthermore, it was shown that micro-bubble flow rate correlated highly with rate of contrast signal replenishment after high mechanical index destructive ultrasound pulses, implying that blood flow dynamics could be quantified using the technique. This series of experiments involved coupling the ATL Power Pulse Inversion system with infusions of Definity™ (DuPont Pharmaceutical Co., Wilmington DE, USA). The same authors went on to demonstrate that different ultrasound contrast agents had different durability under Power Pulse Imaging, showing Optison™ micro-bubbles to be destroyed in significant quantities compared to Definity™ and AFO 150 (Imavist ®, Alliance Pharmaceuticals, San Diego, CA,

USA) even at a mechanical index as low as 0.09 [266]. Higher mechanical index was again confirmed to be more destructive, whatever the micro-bubble type. Clearly, different contrast agents are capable of withstanding different ultrasound power before significant bubble destruction occurs. The question of whether variable micro-bubble destruction would occur if the same ultrasound contrast agent was used in conjunction with a variety of different real-time imaging systems was addressed by TR Porter and colleagues as recently as 2003 [267]. Their tissue phantom consisted of a set of vessels into which ultrasound was directed, connected to an input and output micro-bubble flow line. Pulse Inversion Doppler and then Power Modulation real-time imaging were commenced, with both contrast intensity and output micro-bubble concentration being measured during each phase. Contrast intensity was lower and micro-bubble destruction was higher during Pulse Inversion Doppler than Power Modulation, despite similar mechanical indices.

The lessons from these experiments were that low mechanical index real-time perfusion imaging was feasible, but that different systems and contrast agents were prone to different degrees of micro-bubble destruction. It therefore follows that it is important to use appropriate coupling of imaging system and contrast agent for clinical studies.

(b) Animal models of perfusion impairment and wall motion abnormality:

The ability of low mechanical index real-time imaging to detect both wall motion and perfusion was assessed in an animal model of acute ischaemia by Mor-Avi et al [268]. While coronary haemodynamics during acute ischaemia are not the same

as those occurring during non-flow-limiting coronary stenosis, their model is sufficient to allow clear demonstration of the system's capacity to display both perfusion and wall motion. In this set of experiments, anaesthetised pigs underwent trans-thoracic Power Modulation imaging during infusion of Definity™ contrast agent. Wall motion was analysed by semi-automated detection of endocardial borders and contrast signal was assessed by a combination of mean regional pixel intensity and contrast replenishment rate after high mechanical index destructive frames. Data was acquired at baseline, during, and after coronary occlusion. The pigs were then injected with fluorescent micro spheres to enable subsequent post mortem quantification of ischaemic area. Each ischaemic episode was evident by both wall motion abnormality and contrast parameters such as reduction in peak signal and contrast replenishment time delay. In addition, regional fluorescent microsphere defects matched regional contrast defects in those pigs that underwent post mortem examination.

The ability of real-time perfusion imaging to detect contrast deficit during Adenosine hyperaemia was assessed in a canine model of graded coronary stenosis by Masugata et al. [269], using Power Pulse Inversion and Sonovue™ (Bracco Diagnostics Inc., Princeton, NJ 08540, USA). Masugata's team used highly controlled conditions in that each dog had the heart surgically exposed and perfusion was assessed quantitatively for peak signal intensity as well as replenishment time after high power destructive ultrasound pulses. Calculated myocardial blood flow correlated highly with radiolabelled microsphere evidence of perfusion in both non flow-limiting stenosis (with Adenosine infusion) and

flow-limiting stenosis (without Adenosine). It was noted that simple visual assessment of contrast signal was possible during severe non-flow limiting stenosis as well as during vessel occlusion. Perfusion quantification has also been explored in the canine experimental model using Power Pulse Inversion and a facility to rapidly engage destructive high mechanical index ultrasound [270]. This work provided quantitative confirmation that high power ultrasound almost totally destroys micro-bubble signal, and also confirmed that Power Pulse Inversion allows quantification of micro-bubble replenishment rate, even after a bolus dose of Optison™.

Masugata's team went on to assess the comparability of Intermittent and Real-time low mechanical index perfusion imaging in a very similar experimental design to that outlined above [271]. In both techniques, correlation between contrast derived and fluorescent microsphere derived indices of perfusion was excellent. Furthermore, visual assessment was equally accurate for both intermittent and real-time imaging.

It should be noted that all of the above studies assessed perfusion in the Left Anterior Descending territory alone. Hence, the inference that other territories can be assessed with equal success by such techniques is not necessarily valid.

(c) Real-time perfusion and wall motion imaging in humans:

Early human work on myocardial perfusion and wall motion imaging tended to relate to healthy volunteers and to involve Power Pulse Inversion. For example, Tiemann and colleagues, from the University of Bonn, proceeded from tissue

phantom work to demonstrate the feasibility of simultaneous wall motion and perfusion assessment at a frame rate of 12 Hz in eighteen healthy humans at rest [272]. This was achieved using Optison™ infusions alongside the Power Pulse Inversion system. The findings were presented at the 49th Scientific Session of the American College of Cardiology in March 2000, although results of earlier stages in their research had been published in journal format shortly beforehand [203].

The issue of diagnosing coronary artery disease using low mechanical index real-time imaging was first investigated in 2000 and 2001. Porter et al published their findings in relation to Pulse Inversion Doppler with Optison™ and Definity during a Dobutamine Stress Echocardiography protocol in 117 patients in March 2001 [205]. This study demonstrated the feasibility of the method in a good sample size. However, the absence of a comparator for underlying disease in all but forty patients, and the fact that different contrast agents were used in the same series, limit the applicability of the results. Among the forty patients who underwent comparator imaging in the form of coronary angiography, agreement with myocardial contrast echocardiographic perfusion scoring was eighty-three percent, while agreement with wall motion was seventy-two percent. Analysis according to subgroups revealed eighty three percent agreement for the Left Anterior Descending territory, eighty percent for the Right Coronary territory, and eighty five percent for the Circumflex territory. It is difficult to calculate precise sensitivity and specificity values from the data made available in the published article, but the stated agreement levels with quantitative coronary angiography are high. A potential limitation, acknowledged as such by the

authors, was that micro-bubble contrast agents were injected as boluses. In fact, complete contrast opacification was often present at peak overall contrast intensity in regions that subsequently developed reduced contrast intensity.

The results discussed above using Power Pulse Inversion were similar to those obtained by the same group using Accelerated Intermittent Harmonic Imaging [202]. In this study, Thallium SPECT results were compared with real-time perfusion and wall motion assessment after bolus doses of Optison™ during exercise stress in one hundred consecutive patients. Myocardial contrast perfusion results matched SPECT data on a territorial basis in seventy six percent of cases, while perfusion and wall motion data matched in eighty eight percent of cases. Furthermore, among a subgroup of forty patients who also underwent coronary angiography, sensitivity of myocardial contrast perfusion assessment for significant coronary artery stenosis was equivalent to that of wall motion and SPECT, at seventy five percent. Specificity was above eighty percent for each imaging modality. When wall motion data was combined with perfusion data, sensitivity rose to 86%, specificity was 88%, and overall accuracy was 86%. Others have not demonstrated such a high accuracy using Accelerated Intermittent Harmonic Imaging, and the majority of recent attention to echocardiographic real-time perfusion assessment has focused on "micro-bubble selective" imaging techniques such as Power Pulse Inversion, Power Modulation, and Coherent Contrast Imaging™.

At the time this work was commenced (December 2000), there had been little published research relating to real-time perfusion and wall motion assessment

with the Acuson system. Indeed, there was no data available on diagnostic efficacy in patients with coronary artery stenosis undergoing Dobutamine Stress Echocardiography. The earliest results available in peer reviewed journal format demonstrated the potential of the technique in humans very convincingly [273]. In their study, researchers from the University of Michigan used the Acuson Sequoia™ system to compare real-time and triggered imaging in twenty-three normal adults without evidence of vascular disease. Real-time imaging differed from triggered imaging in that it did not show evidence of significant contrast signal intensity mismatch between different myocardial regions, despite careful digital quantification of grey scale signal. Furthermore, quantification of myocardial blood flow reserve using Dipyridamole infusion alongside contrast replenishment time and signal intensity data, which had been acquired after high power ultrasound destruction of micro-bubbles, demonstrated values entirely consistent with widely validated echocardiographic and invasive assessments of the same or equivalent parameters [274,275]. While it should be noted that the University of Michigan group used DMP-115 (Definity™), their results did set an important base from which investigation of Acuson's real-time perfusion imaging system could proceed, using Optison™ among a number micro-bubble agents.

2. HYPOTHESES

There are three sets of hypotheses relating to detection of coronary artery stenosis of > 50% luminal diameter. The first set refers to the comparability of wall motion assessment during Coherent Contrast Imaging™ and Standard

Harmonic Imaging, while the second and third sets refer to the sensitivity and specificity of combined wall motion and perfusion assessment.

Null Hypothesis 1 (Wall motion comparability): The agreement between wall motion assessment during Coherent Contrast Imaging™ and conventional harmonic imaging is MODERATE OR WEAK (matching in less than 70% of territories).

Alternative Hypothesis 1 (Wall motion comparability): The agreement between wall motion assessment during Coherent Contrast Imaging™ and conventional harmonic imaging is STRONG (matching in at least 85% of territories).

Null Hypothesis 2 (Sensitivity): The sensitivity of combined assessment of wall motion and micro-bubble signal during Coherent Contrast Imaging™ is NOT SUPERIOR to the sensitivity of conventional harmonic Dobutamine Stress Echocardiography.

Alternative Hypothesis 2 (Sensitivity): The sensitivity of combined assessment of wall motion and micro-bubble signal during Coherent Contrast Imaging™ is SUPERIOR to the sensitivity of conventional harmonic Dobutamine Stress Echocardiography.

Null Hypothesis 3 (Specificity): The specificity of combined assessment of wall motion and micro-bubble signal during Coherent Contrast Imaging™ is

INFERIOR to the specificity of conventional harmonic Dobutamine Stress Echocardiography.

Alternative Hypothesis 3 (Specificity): The specificity of combined assessment of wall motion and micro-bubble signal during Coherent Contrast Imaging™ is NOT INFERIOR to the specificity of conventional harmonic Dobutamine Stress Echocardiography.

3. AIMS

1. To assess the technical feasibility of Dobutamine Stress Coherent Contrast Imaging™.

2. To compare wall motion assessment during Coherent Contrast Imaging™ and standard Harmonic imaging.

3. To assess the ability of perfusion analysis by Coherent Contrast Imaging™ to detect underlying coronary artery stenosis in excess of 50% luminal diameter.

4. To compare the ability of standard harmonic wall motion analysis and combined wall motion and perfusion analysis during Coherent Contrast Imaging™ to detect underlying coronary artery stenosis in excess of 50% luminal diameter.

4. METHODS

(i) Ethical Approval

The study was approved and registered by the Royal Free Hospital medical ethics committee. (Reference: Royal Free Hampstead NHS Trust Ethics code 161-99,

protocol amendment number one, research and development reference number 3810). All subjects gave written informed consent.

(ii) Assumptions and Sample Size Calculations

The baseline accuracy of Dobutamine Stress Echocardiography, as discussed in Chapter 3, consists of a sensitivity of 70% and specificity of 80%.

To be clinically useful, Coherent Contrast Imaging™ would need to be no less specific but significantly more sensitive than current techniques. A clinically relevant improvement would probably require sensitivity of approximately 90%, while specificity would need to be maintained at 80%. No directly comparable studies were available for conjectured sensitivity and specificity values.

Thus, for sample size calculation, the threshold for superior sensitivity of Coherent Contrast Imaging™ was set at 90% compared to 70% for Dobutamine Stress Echocardiography, while the threshold for inferior specificity of Coherent Contrast Imaging™ was set at 75% compared to 80% for Dobutamine Stress Echocardiography. Conjectured sensitivity and specificity for Coherent Contrast Imaging™ under alternative hypotheses were both 90%.

Sample sizes were calculated using the principles and formulae of CA Beam [227] and WC Blackwelder [228]. The calculations were the same as those detailed in Chapter 3. Hence, as for the Power Contrast Imaging™ investigation, 33 patients with an equal balance of single and double vessel disease would satisfy this sample size requirement.

(iii) Subjects

Thirty-eight patients with >50% stenosis affecting one or two coronary arteries, but without occlusion or sub-total occlusion, were recruited. Inclusion criteria were diagnostic coronary angiography within one month and informed consent. Exclusion criteria were previous trans-mural myocardial infarction, acute coronary syndrome or symptomatic deterioration during the period between angiography and echocardiography, unstable angina, sensitivity to albumin products, valvular heart disease, and previous adverse reaction to Dobutamine. Each patient underwent Dobutamine Stress Echocardiography Myocardial Contrast Echocardiography.

(iv) Echocardiography Protocol

Echocardiography was performed with the patient in the left lateral decubitas position. Patients underwent baseline conventional imaging at the beginning of the investigation. Subsequently, baseline contrast imaging was undertaken. During this phase, imaging parameters were chosen according to the presets of the Acuson CCI system to optimise myocardial contrast effect. Image presets were as described in Table 4.1. Optison™ infusion was commenced at the beginning of baseline contrast imaging and interrupted for conventional imaging during Dobutamine stress. Immediately after acquisition of peak stress conventional images, Optison™ infusion was recommenced for acquisition of peak stage contrast images. A delay of one minute was set between recommencing Optison™ infusion and image acquisition, as a steady state was required. Dobutamine Stress Echocardiography was performed by adapting the standard protocol described in the previous chapter in order to accommodate

Optison™ infusion. Images were digitised on-line with an R–wave trigger to obtain a continuous loop using the Stress Echocardiography program of the Sequoia C256 echocardiography machine. Dobutamine was infused through a peripherally sited intravenous line using a mechanical pump as described previously, until an end-point was reached. If significant wall motion abnormalities were absent and the target heart rate had not been achieved (≥85% of maximum predicted for age and sex of the patient) the final stage was prolonged to a maximum of 5 minutes, and/or atropine was added in bolus doses of 300 mcg, up to a maximum of 1500 mcg.

Both the parasternal and apical echocardiographic windows were utilised for conventional harmonic imaging. As parasternal imaging during contrast infusion tends to result in significant shadowing of myocardial segments deep to the ventricular cavities, only the apical window was used for CCI. High power destructive ultrasound pulses were applied for one second during baseline and peak stages of CCI, allowing Contrast Replenishment Time (CRT) analysis.

(v) Optison™ Infusion

Optison™ was prepared and infused using the techniques described in Chapter 2, with a total infusion syringe volume of 30ml. Although it was evaluated with a view to Power Contrast Imaging™, it became clear that the same infusion technique provided high quality images during Coherent Contrast Imaging™. Infusions were started for baseline contrast imaging, discontinued for standard imaging during Dobutamine infusion, and recommenced for peak stage contrast imaging immediately after the last conventional imaging stage. An interval of

one minute was allowed to pass before peak contrast images were acquired, as steady state contrast concentration was necessary.

(vi) Clinical and Electrocardiographic Monitoring

Clinical and electrocardiographic monitoring was carried out continuously throughout the investigation exactly as described in Chapter 3.

(vii) Echocardiographic Image Analysis

Images were acquired digitally and stored in digital format on magneto-optical discs and in analogue format on VHS video.

Conventional wall motion images:

Conventional Dobutamine Stress Harmonic wall motion was analysed in the same way as described in Chapter 3.

Coherent Contrast Image analysis:

Contrast perfusion images were stored separately as baseline and peak stages. After review of all acquired images, the most representative and high quality baseline and peak stress images were selected and analysed for wall motion, contrast signal, and artefact. End-systolic frames were used for assessment of contrast image intensity. Wall motion was graded as normal, hypokinetic, akinetic, or dyskinetic in each of the myocardial regions depicted in figure 3.1. Contrast deficits were interpreted as genuine or artefact related based on specific signal characteristics and in relation to comparator segment signal as previously described [230] (Table 3.2). If a segment was not visualised at baseline, it was not

included in analysis. Reversible contrast deficits were categorised as genuine if contrast effect was visible in a myocardial region at baseline and either absent or diminished at peak stress. In regions not demonstrating peak stress contrast deficit, further assessment of perfusion capacity was undertaken by measurement of Contrast Replenishment Time (CRT). Perfusion was deemed to be impaired if the time interval between micro-bubble destruction and complete replenishment increased from baseline to peak stress. Contrast Replenishment Times were measured, to the nearest second in each myocardial region, from the end of each destructive pulse to the first point at which a systolic frame appeared to show full contrast signal.

(viii) Angiographic Image Interpretation

Coronary Angiographic Image interpretation was exactly as described in Chapter 3, section 4(vii).

(ix) Statistical Analysis

Parametric variables are expressed as mean plus standard deviation. Non-parametric variables are expressed as median with inter-quartile range. Statistical significance is set at a p value of ≤ 0.05 (two-sided).

Baseline to peak stress contrast replenishment changes were compared for stenotic and non-stenotic regions using the Mann-Whitney U test.

Sensitivity, specificity, negative and positive predictive values, and accuracy were calculated for:

a. Conventional wall motion.

b. CCI wall motion.

c. Reversible peak stress contrast deficit.

d. Combined reversible peak stress contrast deficit and impaired contrast replenishment.

e. Combined peak stress contrast deficit, contrast replenishment impairment, and CCI wall motion abnormality.

Coronary angiography was the reference standard. Sensitivities, specificities, and accuracies of each CCI modality were compared with conventional wall motion assessment using McNemar's test for dependent proportions. Fisher's Exact Test was used for comparison of categorical values for heterogeneous groups and when it was not feasible to calculate McNemar's Test due to sample size. Correlation of conventional imaging and CCI results with angiographic coronary stenosis territory were calculated using Chi square-based statistics (Phi and Kappa).

Alternate cases were selected for interobserver variability assessment, on an individual territory basis and for all territories combined. For this, two operators independently rated presence or absence of a peak stress wall motion abnormality in conventional and CCI™ modes, peak stress reversible contrast deficit, and contrast replenishment times. Comparison was made using the Kappa score.

5. RESULTS

Baseline characteristics of patients:

The group consisted of 28 males and 10 females, mean age 60.9 years, standard deviation 9.7 years. All patients had angina but none had a clinical history of Q wave myocardial infarction. For other baseline characteristics and distribution of coronary artery stenosis, see Tables 4.2 and 4.3.

Uninterpretable and inconclusive cases (Figure 4.1):

In one case, wall motion in conventional harmonic mode and CCI™ assessment were both impossible due to very poor image quality. In five cases, myocardial perfusion and contrast wall motion assessment were not possible despite successful conventional harmonic wall motion assessment. This was due to poor image quality in two cases, peak stress hypotension requiring the patient to lie flat with resulting image loss in two further cases (after conventional image acquisition and before CCI™ image acquisition), and uneven contrast infusion with a suboptimal heart rate in one case. The peak heart rate of the latter case was 79% of target, and there did not appear to be any wall motion defect, peak stress contrast defect or abnormality in contrast replenishment time. However, it was apparent that the contrast effect was much stronger at peak stress than at baseline in all regions. The case was therefore excluded from wall motion analysis on grounds of suboptimal heart rate and from contrast analysis on grounds of uneven contrast infusion (and suboptimal heart rate). Thus, conventional Dobutamine Stress Echocardiography yielded an interpretable positive or negative result in 36 cases, while Coherent Contrast Imaging yielded an interpretable positive or negative result in 32 cases.

Image artefact (Tables 4.4 and 4.5):

Artefact was a relatively frequent finding in contrast signal analysis, especially in the basal segment of the lateral wall. However, this did not usually affect the entirety of a coronary artery territory. Regions affected by artefact were excluded from contrast wall motion, signal intensity, and replenishment time analysis.

For territorial results according to each imaging modality, see Tables 4.6 and 4.7.

(i) Wall Motion Assessment: Conventional Harmonic Imaging

Interpretation of standard wall motion was possible in 37 out of 38 cases. One case was inconclusive on grounds of normal wall motion at sub-optimal heart rate, and was therefore excluded form analysis. Apical thinning and hypokinesia was evident in two cases due to previous unrecognised myocardial infarction, but both developed ischaemic wall motion abnormalities in other left anterior descending territory segments. For detection of >50% coronary artery stenosis among 108 coronary territories in these cases, sensitivity was 72.5% (95% confidence interval 58.0 to 83.7%), specificity was 94.7% (95% confidence interval 84.5 to 98.6%), positive predictive value was 92.5% (95% confidence interval 78.5 to 98.0%), and negative predictive value was 79.4% (95% confidence interval 63.2 to 90%). Overall accuracy was 84.3% (95% confidence interval 75.7 to 90.3%), while correlation with angiography was 0.70 (Chi square based Phi). For details, see Table 4.9.

Using standard wall motion assessment in the 32 patients for whom CCI based imaging was assessable resulted in a sensitivity of 71.7% (95% confidence

interval 56.3 to 83.5%%), specificity of 94% (95% confidence interval 82.5 to

98.4%), positive predictive value of 91.7% (95% confidence interval 76.4 to

97.8%), and negative predictive value of 78.3% (95% confidence interval 61 to

89.7%). Overall accuracy was 83.3% (95% confidence interval 74.0 to 89.9 %),

while correlation with angiographic result was 0.678 (Chi square based Phi). For

details, see Table 4.8.

(ii) Wall Motion Assessment: Conventional Harmonic Compared with Coherent Contrast Imaging™

Using CCI based wall motion assessment for identification of >50% coronary

artery stenosis among 96 coronary territories of 32 patients, sensitivity was

63.0% (95% confidence interval 47.5% to 76.4%), specificity was 100% (95%

confidence interval 91.1% to 100%), positive predictive value was 100% (95%

confidence interval 85.7% to 100%), and negative predictive value was 74.6%

(95% confidence interval 54.8% to 88.1%). Overall accuracy was 82.3% (95%

confidence interval 72.9% to 89.1%), while correlation with angiographic result

was 0.69 (Chi square based Phi). For details, see Tables 4.8 and 4.9.

When conventional and CCI wall motion were compared among these thirty-two

patients, there were no statistically significant differences for sensitivity,

specificity, predictive values, overall accuracy, or angiographic correlation

(Table 4.8). Furthermore, there were no statistically significant differences

between such parameters among the 108 territories assessable by conventional

wall motion and the 96 territories assessable by CCI wall motion (Table 4.9).

The agreement between conventional harmonic wall motion assessment and CCI wall motion assessment among cases for which both techniques were applicable is depicted in Table 4.10. Results matched in 86.5% of cases, with a Kappa score of 0.70, p<0.001. Tables 4.11, 4.12, and 4.13 denote agreement between the techniques for each coronary territory.

(iii) Conventional Harmonic Imaging Compared with Peak Stress Contrast Assessment

Two patients had apical peak stress contrast defects at rest associated with previous unnoticed myocardial infarction. These two segments were excluded from analysis. Using visually appreciable contrast defects at peak stress for identification of >50% coronary artery stenosis among 83 interpretable coronary territories of 32 patients, sensitivity was very low at 37.5% (95% confidence interval 23.2% to 54.2%), specificity was excellent at 97.7% (95% confidence interval 86.5% to 99.9%), positive predictive value was 93.8% (95% confidence interval 67.7% to 99.7%), and negative predictive value was 63.2% (95% confidence interval 36.5% to 84.2%). Overall accuracy was 68.7% (95% confidence interval 57.9% to 78.4%, while correlation with angiography was low at 0.45, (Chi square based Phi).

When the above results were compared with figures for conventional wall motion assessment among the same 32 cases, the differences between sensitivities and accuracies were statistically significant, whereas the differences between specificities and predictive values were not (Table 4.14).

(iv) Contrast Replenishment Time Analysis

There were one hundred and ninety two myocardial regions among the thirty-two patients included for analysis of CCI data, representing the six regions depicted in Figure 3.1. Artefact was present in seventeen myocardial regions at baseline, and a further six regions at peak stress. Reversible peak stress defects were present in thirty-three myocardial regions. Hence, there were one hundred and seventy five myocardial regions at baseline and one hundred and thirty six myocardial regions at peak stress that were suitable for Contrast Replenishment Time analysis (CRT) (Table 4.15).

At baseline, CRT was a median of 5 seconds (interquartile range 4 to 6) in both stenotic and non-stenotic coronary territories (Table 4.16). There were minor differences in CRT between regions, as depicted in Table 4.17. The lateral region in the apical 4-chamber view had the longest baseline CRT, with a median of 6 seconds and an inter-quartile range of 4 to 6 seconds, compared to medians of 5 seconds for the septal region and 4 seconds for other regions in the apical 2-chamber view. These differences were statistically significant, with a 2-sided p value of 0.015, based on the Kruskall-Wallis Test for comparison of multiple groups of non-parametric data.

Baseline to peak stress CRT changes were analysed according to presence or absence of stenosis in the supplying coronary artery (Table 4.18). There was a general trend of increase in CRT in regions with stenotic arterial supply and reduction in CRT in regions with non-stenotic arterial supply. In regions supplied by a stenotic coronary artery, there was a median increase in CRT of 33.3%

(interquartile range 0 to 60%), whereas in regions supplied by a non-stenotic coronary artery, there was a median decrease in CRT of 25% (interquartile range − 40 to 0%). The difference between these was statistically significant, with a 2-sided p value < 0.001, based on the Mann-Whitney U Test for comparison of two groups of non-parametric data.

Analysis of CRT changes in separate regions (Table 4.19) demonstrated similar trends for the apex in both 2-chamber and 4-chamber views and the inferior wall in the apical 2-chamber view. In septal and lateral walls supplied by a stenotic artery, there was no median percentage change in CRT, while there was a median decrease in CRT of 33.3% in septal and lateral walls supplied by a non-stenotic artery. In anterior wall regions supplied by a stenotic artery, the median CRT increased by 50%, while anterior wall regions supplied by a non-stenotic artery did not show any median change in CRT. With the exception of CRT changes in the lateral wall, the differences in CRT between regions supplied by stenotic and non-stenotic arteries were all statistically significant. For incorporation of CRT data into other aspects of CCI, an increase from baseline to peak stress was taken to imply significant stenosis in the supplying coronary artery, while either a reduction or no change in CRT was taken to imply a non-stenotic supplying artery.

Changes in CRT for combined and separate territories are depicted in Figures 4.2 through to 4.8. Delayed apical contrast replenishment in a case with left anterior descending coronary artery stenosis is shown in figure 4.9.

(v) Combined Peak Stress Contrast Assessment and Contrast Replenishment Time Analysis

By assuming peak stress contrast defects and increased baseline to peak contrast replenishment time to imply coronary artery stenosis, correlation with angiography among 85 assessable territories was high at 0.815 compared to 0.678 for conventional wall motion assessment (2-sided p value 0.036). While specificity, positive and negative predictive values, and overall accuracy were similar to the values obtained by conventional wall motion assessment, sensitivity appeared greater using the CCI technique than with conventional wall motion assessment, although the difference was not statistically significant (85.7% vs. 71.7%, 2-sided p value based on Fisher's Exact Probability = 0.128) (Table 4.20).

(vi) Combined Peak Stress Contrast Assessment, Contrast Replenishment Time Analysis, and Contrast Wall Motion Assessment

Combined assessment of peak stress contrast defects, contrast replenishment time, and contrast wall motion abnormalities was possible for 96 coronary artery territories in 32 patients. Assuming abnormalities in any of the three parameters to imply coronary stenosis resulted in a slightly higher sensitivity than that for conventional wall motion assessment (82.6% vs. 71.7%), although this did not reach statistical significance. Specificity, positive and negative predictive values, and overall accuracy were equivalent for each technique. Correlation with angiographic result appeared slightly better for combined peak stress contrast defect, CRT delay, and CCI wall motion than for conventional wall motion

assessment alone, although statistical significance was not reached (Chi square based Phi 0.80 vs. 0.68, 2-sided p value = 0.070). (Table 4.21).

When conventional imaging among all 108 assessable territories was compared with combined peak stress contrast defect, CRT delay, and CCI wall motion among 96 assessable territories, there were no significant differences for sensitivity, specificity, predictive values, or overall accuracy. Again, correlation between combined CCI parameters and angiographic result appeared slightly better than correlation between conventional wall motion assessment and angiographic result, but the difference did not reach statistical significance using a 2-sided p value (Chi square based Phi 0.797 vs. 0.696, p = 0.106). (Table 4.22).

(vii) Reproducibility

Interobserver variability testing was undertaken for sixteen cases, after selecting alternate cases from the group of thirty-two cases with satisfactory contrast images. Intraobserver variability was not assessed, as it was apparent that recall of previously studied images would bias the reproducibility assessment.

For combined territories, agreement between raters for conventional wall motion abnormality was 93.8%, with a Kappa score of 0.87 (p<0.001). For CCI™ based wall motion, agreement was 91.7%, with a Kappa score of 0.81 (p<0.001). For presence or absence of reversible peak stress contrast deficit, agreement was 95.1%, Kappa score 0.83 (p<0.001). For presence of either a reversible peak stress contrast deficit or abnormal contrast replenishment time, agreement was 93%, Kappa score 0.87 (p<0.001). For presence of either reversible contrast

abnormality or CCI™ wall motion abnormality, agreement was 95.8% with a Kappa score of 0.92 (p<0.001). These levels of agreement are very high, and it is noteworthy that although contrast replenishment timing was subject to minor variation between raters, this seldom resulted in discrepancy between the two raters when criteria for impaired or preserved perfusion were applied. For individual coronary territories, agreement levels were generally high, although statistical significance was not always reached because of the small numbers involved. For details, see Table 4.23.

6. DISCUSSION

These results relate to three core aspects of low mechanical index myocardial perfusion imaging, namely; CCI wall motion abnormality, peak stress contrast deficit, and peak stress contrast replenishment abnormality.

(i) Coherent Contrast Imaging™ Wall Motion

Despite the advantage of single pulse cancellation in CCI over the potential frame rate limiting disadvantage of multiple pulse cancellation techniques, CCI frame rates still cannot match those of conventional harmonic imaging, at approximately 20Hz compared to 40Hz. This might easily lead to CCI wall motion assessment being inferior to standard wall motion assessment, reducing the stated theoretical benefits of real-time over intermittent imaging. The finding that there is strong agreement between wall motion assessment in conventional harmonic and CCI modes is therefore important if wall motion and perfusion assessment are to be combined in a single stress test. Although the differences in sensitivity and specificity between these imaging techniques did not reach

statistical significance, it is noteworthy that it appears as if CCI wall motion is less sensitive but more specific than conventional wall motion assessment. The specificity of 100% for the former method is surprising and, in the context of moderate sensitivity, suggests that the threshold for identifying abnormal wall motion is simply too high. Despite this, it has been established that wall motion assessment in CCI mode during Dobutamine Stress Echocardiography is feasible and sufficiently accurate, especially if additional components of CCI imaging are to be incorporated to improve sensitivity of the technique as a whole.

It is possible to draw some conclusions from subgroup analysis according to separate coronary artery territories. The overall agreement between CCI and conventional imaging was excellent in all three territories, although the small number of stenotic Circumflex Coronary Arteries resulted in statistically non-significant results for this territory. It certainly seems appropriate to draw the conclusion that wall motion agreement between the two techniques is high for the Left Anterior Descending and Right Coronary Artery territories.

This was among the first studies of its kind to confirm the high level of wall motion agreement between CCI and conventional harmonic imaging during a Dobutamine Stress protocol. The results compare favourably with findings from other similar studies using different ultrasound systems. For example, agreement between angiography and wall motion was approximately ten percent inferior at seventy two percent in the series reported by Porter et al [205]. Results of a study comparing Optison™ enabled CCI wall motion assessment with SPECT based myocardial perfusion assessment on a territorial basis were published later, suggesting a similar level of agreement [261]. Although Dipyridamole was used as

the stressor and conventional wall motion was not assessed, level of agreement between SPECT and CCI wall motion in the study by MA Oraby et al and conventional wall motion and CCI wall motion in this study are similar, suggesting a real effect is present. Furthermore, extrapolation to slightly different protocols might be justified.

(ii) Peak Stress Contrast Deficit

Using intermittent imaging, Wei et al demonstrated that peak signal intensity fell more modestly than replenishment rate among mildly and severely stenotic regions under hyperaemic stress (to ninety-six and seventy-one percent of baseline respectively) [144]. There is also real-time imaging data to support the notion that Dobutamine and Adenosine induce a marked reduction in rate of contrast replenishment but only a modest reduction in peak stress contrast signal intensity [158]. This might support the notion that CCI peak stress contrast deficit should be relatively insensitive for coronary stenosis. However, as may have been the case with CCI wall motion, the threshold for identifying abnormal perfusion is likely to have been too high, as the coinciding specificity was very high at nearly ninety-eight percent. Notwithstanding this, the magnitude of inferiority for this method's overall accuracy compared to conventional wall motion assessment is both statistically significant and clinically relevant. It would appear that CCI peak stress deficit alone is insufficient for identifying regions likely to be supplied by a stenotic artery.

(iii) Contrast Replenishment Time

The landmark series of experiments conducted by Wei et al documented the relationship between signal intensity, rate of signal intensity rise, and replenishment time. This is expressed by the exponential function $y=A(1-exp^{-\beta t})$, where y is the signal intensity at time t, A is the plateau signal intensity, and ß is the rate constant determining the rate of rise of signal intensity [144]. In their series of experiments, contrast replenishment rate during hyperaemia reduced to fifty eight percent of baseline rate in territories of minor coronary stenosis and forty three percent of baseline rate in territories of severe stenosis. Such findings are in keeping with the results of CRT analysis in this study. Unlike Wei and colleagues' findings relating to intermittent imaging, the CCI results discussed here did not reveal contrast replenishment rate reduction (CRT increases) to be universal in stenotic regions. This relates in part to the fact that the University of Virginia group utilised open-chest dogs and artificial single coronary stenosis in otherwise entirely normal vessels, thereby removing most signal artefact and any confounding factors such as small vessel disease.

When myocardial regions in the present study were analysed separately, there was no significant difference between Dobutamine Stress CRT in lateral walls supplied by stenotic and non-stenotic coronary arteries. All other regions demonstrated significant differences. The reasons for the lateral wall results are unclear, although a relative deficiency of Circumflex artery stenosis compared to stenoses of the Right and Left Anterior Descending vessels may be partly responsible. Another important finding when regions were analysed separately is the fact that, while the general trend in CRT was a decrease in regions supplied

by a normal vessel and an increase in regions supplied by a stenotic vessel, septal regions supplied by a stenotic vessel and anterior regions supplied by a non-stenotic vessel both exhibited a median change of zero. Septal myocardium is well supplied by septal perforator vessels, which arise from the Left Anterior Descending coronary artery at various points along its course. In theory, a stenosis in the mid Left Anterior Descending coronary artery, prior to which several septal perforators have originated, might not be expected to cause a large stress induced septal wall contrast defect. Reasons for the absence of a median reduction in CRT in non-stenotic anterior regions are unclear.

Previous studies have generally utilised specifically designed hardware and processing software to quantify both myocardial contrast signal intensity and replenishment rate. This has not been particularly suitable for a clinical setting until very recently, with the advent of such facilities as an integral part of certain contrast perfusion packages. This CCI study utilised a semi-quantitative method based on visual estimation of contrast signal intensity and stopwatch estimation of contrast replenishment rate. While it was readily evident whether a reversible peak stress contrast deficit was present or absent, contrast replenishment time estimation was more difficult. It became clear that it was difficult to be certain of the exact point in time at which maximum contrast replenishment had occurred. To measure to fractions of a second would be to overestimate the accuracy of visual assessment. Furthermore, even precise signal intensity based quantification would have been an oversimplification, as replenishment in a "region of interest" is highly likely to differ from an adjacent region affected by the same arterial supply, and could therefore not be taken as representative of the

territory as a whole. It appears acceptable to use visual and stopwatch estimation as long as the above limitations are understood. However, these results may well have demonstrated true superiority over conventional wall motion assessment if precise quantification tools had been available.

Despite the obvious limitations of this in terms of subjectivity and therefore precision, the results do suggest that this form of CRT analysis, when combined with peak stress contrast deficit assessment, allows identification of stenotic territories with a sensitivity at least equivalent to that of conventional wall motion assessment.

(iv) Systolic and Diastolic Frames

Moving images are difficult to interpret for micro-bubble signal intensity. It seems apparent, even during visual assessment, that there are subtle differences in grey scale between systolic and diastolic phases. A plausible explanation for this might be that different diameter myocardial sections could result in the illusion of different signal intensity. However, there is data to support an alternative notion that signal intensity genuinely differs between systolic and diastolic frames. Bekeredjian et al demonstrated this phenomenon during real-time perfusion imaging in pigs (Sonovue™ infusion) and then in humans (Optison™ boluses) in 2002 [276]. The explanation for this is not clear, but the data does suggest higher signal intensity in systolic frames. The decision to choose systolic frames for comparisons in this series was based in part on the fact that they allow a greater section of myocardium to be visualized than diastolic frames. It was fortuitous that it was later recognized that systolic frames

displayed greater signal intensity. Comparison of systolic and diastolic signal intensity was not done in any systematic way in this study.

(v) Subendocardial and Transmural Micro-bubble Signal

As with Power Contrast Imaging™, perfusion may not always be evenly distributed across the entire myocardial wall. There is evidence that Power Pulse Inversion imaging can detect subendocardial perfusion impairment during Adenosine Stress in humans, but detection of this phenomenon tends to require dedicated imaging or processing [277]. There was no consistent pattern of transmural micro-bubble signal gradient in the series presented here, although this was not part of the protocol and was not specifically assessed.

(vi) Optison™ Infusion

As previously discussed, Optison™ has certain limitations when infusion is attempted instead of bolus injection. It is certainly conceivable that an ultrasound contrast agents designed specifically for infusion might have allowed more accurate perfusion data to be gained.

(vii) Single, Double, Triple, and Complex Coronary Artery Disease

As discussed in Chapter Three, the coronary artery disease patterns evaluated here were relatively simple. Extrapolation of these results to more complex situations should therefore be avoided. It remains to be seen whether CCI is capable of depicting such complex disease and perfusion patterns.

(viii) Choice of Stressor

Dobutamine is an excellent stressor in terms of increasing myocardial workload and it follows that perfusion defects should also be produced. Although there is a belief that Dobutamine is less effective than other stressors such as Adenosine at producing perfusion defects in stenotic coronary territories, there is data to suggest that it is very effective in precisely this role during real-time myocardial perfusion imaging [158]. In addition, simultaneous wall motion and perfusion assessment demand that effective induction of both be achieved.

(ix) Comparison with Dobutamine Stress Echocardiography and Coronary Angiography

As discussed previously, coronary angiography is not a physiological assessment of myocardial perfusion and ischaemia. Nevertheless, it remains necessary to evaluate the comparability of Coherent Contrast Imaging™ and Dobutamine Stress Echocardiography in diagnosis of coronary disease using coronary angiography as the gold standard, as the latter is still the main determinant of coronary artery disease treatment strategy and a strong indicator of prognosis.

7. CONCLUSIONS

Regarding detection of single or double vessel coronary artery stenosis of greater than 50% luminal diameter using visual assessment during CCI™ imaging:

1. Dobutamine Stress Coherent Contrast Imaging™ is feasible in a clinical setting.

2. Peak Stress Contrast Deficits have a very poor sensitivity for underlying coronary artery stenosis.

3. Increased Contrast Replenishment Time between baseline and peak stress may indicate underlying coronary artery stenosis, whereas a decrease in Contrast Replenishment Time may indicate a patent coronary artery.

4. There is strong agreement between wall motion assessment in the Conventional Harmonic and Coherent Contrast Imaging™ modes. There is evidence to reject Null Hypothesis 1. Alternative Hypothesis 1 is accepted.

5. Sensitivity of combined assessment of wall motion and micro-bubble signal characteristics during Coherent Contrast Imaging™ is not significantly greater than the sensitivity of wall motion assessment in Conventional Harmonic mode alone. There is insufficient evidence to accept Alternative Hypothesis 2. Null Hypothesis 2 is accepted.

6. Specificity of combined assessment of wall motion and micro-bubble signal characteristics during Coherent Contrast Imaging™ is equivalent to the specificity of wall motion assessment in Convention Harmonic mode alone. There is sufficient evidence to reject Null Hypothesis 3. Alternative Hypothesis 3 is accepted.

8. LIMITATIONS

1. As with the Power Contrast Imaging™ study, greater accuracy may have been achieved using quantitative measurement techniques rather than visual assessment.

2. The Optison™ infusion used in this CCI study was initially tested in a Power Contrast Imaging™ protocol. Imaging characteristics were good in CCI cases using the same infusion concentration and rate, but there was no formal reassessment of optimal infusion method for CCI purposes.

3. As discussed in relation to the Power Contrast Imaging™ work in Chapter Three, the following are acknowledged as limitations:

a. Coronary angiography was used as the reference test.

b. Small vessel coronary disease could have been present in some cases.

c. Sample size is relatively small.

CHAPTER FIVE

SUMMARY AND IMPLICATIONS FOR FUTURE RESEARCH AND CLINICAL PRACTICE

The first phase of this research established a reliable means of infusing Optison™ for purposes of a steady state contrast effect during Adenosine vasodilator stress. It is possible to utilise bolus doses during a stress protocol, but it was reasoned that, for these studies, a reliable steady state ultrasound contrast effect should be achieved. This success enabled progress with the second and third phases of the investigation into myocardial perfusion contrast echocardiography, namely Power Contrast Imaging™ and subsequently Coherent Contrast Imaging™. Although the Optison™ infusion method described in Chapter 1 was not specifically tested in conjunction with Coherent Contrast Imaging™, it became clear during early experience with this method that the infusion technique that had been developed with a view to Power Contrast Imaging™ also provided high quality myocardial contrast images during the real-time technique. While other solutions such as infusion of saline through a reservoir containing the contrast agent have been used with success, many investigators have turned to other infusible contrast agents, such as Levovist®. Further developments in ultrasound contrast design will completely resolve issues of micro-bubble buoyancy and separation from solution, enabling infusion for situations where a steady state contrast effect is required over long periods, especially if attempts at contrast quantification are to be made. Thus, the method for infusing Optison™ described in this thesis will become obsolete.

Nevertheless, the method allowed excellent quality contrast signal generation for the perfusion techniques investigated here.

Power Contrast Imaging™ might theoretically have been more sensitive than wall motion assessment for underlying ischaemia due to coronary artery stenosis. However, the results discussed in Chapter 3 certainly do not indicate such a high sensitivity. Indeed, sensitivity was at best moderate, while specificity was notably high. Such results suggest that the particular combination of imaging system, hardware, software, and vasodilator protocol used in this study is not appropriate for further investigation without modification, and is certainly unsuitable for clinical use. Reasons for the low sensitivity and overall accuracy have been discussed, including issues relating to thresholds for determining a contrast deficit, quantification, and trigger intervals. However, it is difficult to see how this and similar intermittent stimulated acoustic emission methods can play a role in clinical investigation now that real-time imaging systems are widely available and, at least according to a number of single institution studies, highly accurate. The only conceivable scenario in which intermittent stimulated acoustic emission methods might be subject to renewed interest would be failure to reproduce the early successes of real-time imaging techniques in clinical practice outside the handful of institutions that have thus far declared their impressive results. It is otherwise unlikely that intermittent imaging techniques will have a significant role in the future, and the results detailed in Chapter 3 will be of historical value only.

Real-time myocardial contrast echocardiography offers the possibility of simultaneous wall motion and perfusion assessment, and therefore has theoretical advantages over intermittent imaging techniques, which necessarily discard wall motion data. Coherent Contrast Imaging has been shown in the study detailed in Chapter 4 to allow accurate wall motion assessment and to allow an insight into myocardial perfusion dynamics during Dobutamine stress. It is noteworthy that the sensitivity of a reversible peak stress contrast deficit, in terms of a visually appreciable reduction in contrast signal intensity, was poor for underlying coronary artery stenosis. This was a similar finding to those discussed in Chapter Three, where a peak stress contrast deficit had a low and clinically unhelpful sensitivity for underlying coronary stenosis. It is unclear why the case remains the same for peak stress contrast deficit in real-time myocardial contrast echocardiography using Coherent Contrast Imaging™, but certain technical issues such as the reliability of visual quantification might have played a role. The fact that timing of contrast replenishment rates after destructive ultrasound pulses increased the sensitivity of the technique as a whole is a triumph for the real-time imaging technique over its' predecessor Power Contrast Imaging™ modality. This enabled the sensitivity and specificity of combined Coherent Contrast Imaging™ wall motion and perfusion assessment to reach that of conventional stress echocardiography. A caveat must be, however, that conventional wall motion imaging allowed a greater number of cases to be successfully investigated, owing in part to echocardiographic window problems in some Coherent Contrast Imaging™ cases. It would be incorrect to dismiss this fact, as the diagnostic effectiveness of the new method would be slightly lower on an "intention to diagnose" basis.

A question that should be addressed is the suitability of Coherent Contrast Imaging as a clinical tool to be used outside the research laboratory. This research suggest that the technique, at least in combination with other parts of the real-time imaging protocol detailed in Chapter Four, is currently not suitable as a clinical tool. Stress echocardiography, a well-established conventional method for which there is a wealth of supporting evidence, would appear to have a similar accuracy but greater applicability than Coherent Contrast Imaging ™.

Further research in other institutions is ongoing, with a number of variations in imaging system, ultrasound contrast agent, and stress protocol. Data is emerging to suggest real-time imaging techniques are very accurate for detecting coronary disease and ischaemia, and indeed of some prognostic value. However, even current large series cannot be taken as an indication to proceed with widespread perfusion based imaging instead of other well-established methods. Results need to be repeatable in a number of institutions, and there are certain to be issues of standardisation with respect to imaging system settings, contrast agent use, stress protocols, quantification, and interpretation of findings. If accuracy of real-time perfusion imaging is as high in widespread use as some investigators have shown in single centres, and the issues above are addressed, the future prospects for clinically applied real time myocardial contrast stress echocardiography are very good.

APPENDIX ONE

1. TABLES

<u>Key to Tables:</u>

M = Male

F = Female

Y = Yes

N = No

DSE = Dobutamine Stress Echocardiography

PCI = Power Contrast Imaging™

CCI = Coherent Contrast Imaging™

LAD = Left Anterior Descending Coronary Artery

CX = Circumflex Coronary Artery

RCA = Right Coronary Artery

WMA = Wall Motion Abnormality

PSCD = Peak Stress Contrast Deficit

CRT = Contrast Replenishment Time anomaly

95% CI = 95% Confidence Interval

IQR = Interquartile Range

Table 1.1

Examples of Transpulmonary Ultrasound Contrast Agents:

Agent	Gas	Shell or Stabiliser	Manufacturer
Albunex ®	Air	Albumin	Mallinckrodt pharmaceuticals (now part of Amersham Healthcare)
Levovist ®	Air	Palmitic acid	Schering AG, Berlin, Germany
Optison™	Octafluoro-propane	Albumin	Amersham Healthcare (GE Healthcare Bio-Sciences: United Kingdom)
Definity™	Perflouoro-propane	Liposome	DuPont Pharmaceutical Co., Wilmington DE, USA
Sonazoid™ (NC 100100)	Perfluoro-carbon	Phospholipid	Amersham Healthcare
SonoVue™ (BR1)	Sulphur-hexafluoride	Phospholipid	Bracco Diagnostics Inc., Princeton, NJ 08540, USA
Imavist ®	Perfluoro-hexane	Surfactant	Alliance Pharmaceuticals, San Diego, CA, USA
AI 700 ™	Perfluoro-carbon	Phospholipid and L-lactide co-glycolide	Accusphere Inc., Watertown, MA, USA

Table 2.1

Clinical characteristics among the twelve subjects:

Case	Age	Sex	Stenotic Territory (% of luminal diameter)	Resting Heart rate range (to nearest 5 beats /min)	Main Adenosine side effect	Completed Adenosine infusion
1	75	M	LAD 90%	70-80	Dyspnoea	N
2	64	M	CX 70%	60-65	Flushed	Y
3	63	M	LAD 50%	65-75	Dyspnoea	Y
4	69	F	CX 70%, LAD 50%	80-90	Dizziness	Y
5	54	M	LAD 90%	75-80	Chest pain	N
6	75	F	CX 90%	50-55	Dyspnoea	N
7	58	F	CX 50%	65-80	Dyspnoea	Y
8	70	M	CX 90%, LAD 50%	70-75	Dyspnoea	Y
9	73	F	LAD 70%	60-65	Dyspnoea	N
10	59	M	LAD 70%	55-60	Dizziness	Y
11	54	M	CX 70%	60-65	Nil	Y
12	63	M	LAD 70%	70-75	Nil	Y

Table 2.2

Summary of undiluted infusions (cases 1 to 4)

(Bold print highlights acceptable image quality)

Rate	Trigger settings	Acceptable quality at baseline (of 4)	Acceptable quality at peak (of 4)	Optison™ deposits in tubing (of 4)
72 ml/hr	1:1	0	NA	NA
	1:2	0	NA	NA
	1:4	0	NA	NA
	1:6	0	NA	NA
	1:8	0	NA	NA
36 ml/hr	1:1	0	NA	NA
	1:2	0	NA	NA
	1:4	0	NA	NA
	1:6	0	NA	NA
	1:8	0	NA	NA
24 ml/hr	1:1	0	NA	NA
	1:2	0	NA	NA
	1:4	**4**	**0**	**2**
	1:6	**3**	NA	NA
	1:8	0	NA	NA
18 ml/hr	1:1	0	NA	NA
	1:2	0	NA	NA
	1:4	**3**	**0**	**2**
	1:6	**4**	NA	NA
	1:8	**3**	NA	NA
14 (14.4) ml/hr	1:1	0	NA	NA
	1:2	0	NA	NA
	1:4	0	NA	NA
	1:6	0	NA	NA
	1:8	0	NA	NA

Table 2.3

Summary for diluted infusion A - 6ml Optison™ in 15 ml solution (cases 5 to 8)

(Bold print highlights acceptable image quality)

Rate	Trigger settings	Acceptable quality at baseline (of 4)	Acceptable quality at peak (of 4)	Optison™ deposits in tubing (of 4)
180 ml/hr	1:1	0	NA	NA
	1:2	0	NA	NA
	1:4	0	NA	NA
	1:6	0	NA	NA
	1:8	0	NA	NA
90 ml/hr	1:1	0	NA	NA
	1:2	0	NA	NA
	1:4	0	NA	NA
	1:6	**2**	**0**	**1**
	1:8	**2**	NA	NA
60 ml/hr	1:1	0	NA	NA
	1:2	0	NA	NA
	1:4	**2**	**2**	**0**
	1:6	**4**	**0**	**1**
	1:8	0	NA	NA
45 ml/hr	1:1	0	NA	NA
	1:2	0	NA	NA
	1:4	0	NA	NA
	1:6	**3**	NA	NA
	1:8	0	NA	NA
36 ml/hr	1:1	0	NA	NA
	1:2	0	NA	NA
	1:4	0	NA	NA
	1:6	0	NA	NA
	1:8	0	NA	NA

Table 2.4

Summary for diluted infusion B - 6ml Optison™ in 30 ml solution (cases 9 to

12)

(Bold print highlights acceptable image quality)

Rate	Trigger settings	Acceptable quality at baseline (of 4)	Acceptable quality at peak (of 4)	Optison™ deposits in tubing (of 4)
360 ml/hr	1:1	0	NA	NA
	1:2	0	NA	NA
	1:4	0	NA	NA
	1:6	0	NA	NA
	1:8	0	NA	NA
180 ml/hr	1:1	0	NA	NA
	1:2	0	NA	NA
	1:4	0	NA	NA
	1:6	**4**	NA	NA
	1:8	**4**	NA	NA
120 ml/hr	1:1	0	NA	NA
	1:2	0	NA	NA
	1:4	**4**	**4**	**0**
	1:6	**4**	NA	NA
	1:8	**3**	NA	NA
90 ml/hr	1:1	0	NA	NA
	1:2	0	NA	NA
	1:4	0	NA	NA
	1:6	**1**	NA	NA
	1:8	**4**	NA	NA
72 ml/hr	1:1	0	NA	NA
	1:2	0	NA	NA
	1:4	0	NA	NA
	1:6	0	NA	NA
	1:8	0	NA	NA

Table 2.5

Power Contrast Imaging™ Results: Summaries of all cases using most suitable

trigger interval

Case	Optison ™ Dilution	Best Baseline Infusion rate	Best Baseline Trigger Interval	Contrast effect at Peak stage	Optison ™ deposits in tubing	Revers -ible deficit	ECG
1	Not diluted	24 ml/hr	1:4	Poor	Yes	NA	Pos
2	Not diluted	24 ml/hr	1:4	Poor	Yes	NA	Neg
3	Not diluted	18 ml/hr	1:4	Poor	Yes	NA	Neg
4	Not diluted	18 ml/hr	1:4	Poor	Yes	NA	Inc
5	6ml in 15ml	60 ml/hr	1:4	Good	No	No	Inc
6	6ml in 15ml	60 ml/hr	1:4	Good	No	No	Inc
7	6ml in 15ml	90 ml/hr	1:6	Poor	Yes	NA	Inc
8	6ml in 15ml	60 ml/hr	1:6	Poor	Yes	NA	Pos
9	6 ml in 30 ml	120 ml/hr	1:4	Good	No	No	Inc
10	6 ml in 30 ml	120 ml/hr	1:4	Good	No	No	Neg
11	6 ml in 30 ml	120 ml/hr	1:4	Good	No	No	Neg
12	6 ml in 30 ml	120 ml/hr	1:4	Good	No	No	Neg

NA   = Not Assessable due to poor image quality
Neg   = Negative (No electrocardiographic changes)
Pos   = Positive (Significant ST segment depression)
Inc   = Inconclusive (Non-specific T wave changes or Adenosine terminated
       early)

Table 3.1

Standard Power Contrast Imaging™ Settings on Acuson Sequoia C256

Transmit Power	Full, 0 dB
Filter	2
Gate	2
Post Processing map	E3 +1
Depth	Level of Mitral Valve
Dynamic Range	55
Persistence	0
Doppler Gain	65
Space Time	T3
Edge	-3
Frequency	Harmonic
R-wave Trigger	N=4

Table 3.2

Interpretation of perfusion defects:

ANALYSED SEGMENT	COMPARATOR SEGMENT(S)
Basal Septum (A4c)	Basal Lateral (A4c)
Mid Septum (A4c)	Basal Septum, Mid Lateral (A4c)
Basal Lateral (A4c)	**
Mid Lateral (A4c)	Basal Lateral (A4c)
Apex (A4c)	Mid Septum and Mid Lateral (A4c)
Basal Inferior (A2c)	Basal Anterior (A2c)
Mid Inferior (A2c)	Mid Anterior, Basal Inferior (A2c)
Basal Anterior (A2c)	**
Mid Anterior (A2c)	Basal Anterior, Mid Inferior (A2c)
Apex (A2c)	Mid Inferior and Mid Anterior (A2c)

** The basal anterior and basal lateral walls are often poorly visualised. A perfusion defect was only deemed present in these if there was evidence of perfusion impairment in the adjacent proximal segments of the anterior and lateral walls respectively, and if the image quality for the entire myocardium was very good at baseline.

A4c = Apical four chamber view

A2c = Apical two chamber view

Table 3.3

Baseline characteristics

RISK FACTOR	NUMBER (of 28 cases interpretable by both DSE and PCI)
Diabetes	9
Hypertension	9
Hypercholesterolaemia (total cholesterol >5.2 mmol/l)	14
Family history of premature Coronary Artery Disease	10
Peripheral arterial disease	4
Obesity	10
Smoking	5
Male	23
Female	5

Table 3.4

Coronary angiographic stenoses > 50%

TERRITORY	NUMBER (of 28 cases interpretable by both DSE and PCI)
LAD alone	10
RCA alone	5
CIRCUMFLEX alone	0
LAD + RCA	4
LAD + CIRCUMFLEX	6
RCA + CIRCUMFLEX	3
TOTAL NUMBER OF STENOSES	41

Table 3.5

Comparative ability of PCI and DSE to detect coronary artery stenosis (28 cases interpretable by both DSE and PCI)

	Among cases for which both DSE and PCI were interpretable (84 territories)			
	DSE	PCI	Test	P Value (2 sided)
Sensitivity (%) (95% CI)	85.4 (70.1 – 93.9)	58.5 (42.2 – 73.3)	McNemar	0.003
Specificity (%) (95% CI)	95.4 (82.9 – 99.2)	88.4 (74.1 – 95.6)	McNemar	0.453
Positive Predictive Value (%) (95%CI)	94.6 (80.5 – 99.1)	82.8 (63.5 – 93.5)	Fisher's Exact	0.226
Negative Predictive Value (%) (95% CI)	87.2 (71.3 – 95.4)	69.1 (49.2 – 84.1)	Fisher's Exact	0.034
Accuracy (%) (95% CI)	90.0 (81.6 – 95.5)	73.8 (62.9 – 82.5)	McNemar	0.003
Angio. correlation (Phi)	0.81 (p<0.001)	0.49 (p<0.001)	Z 3.79	<0.001

Table 3.6

Comparative ability of PCI and DSE to detect coronary artery stenosis (30 interpretable DSE cases and 28 interpretable PCI cases)

	Among 30 interpretable DSE cases and 28 interpretable PCI cases			
	DSE cases (90 territories)	PCI cases (84 territories)	Test Statistic	P Value (2-sided)
Sensitivity (%) (95% CI)	86.1 (71.4 – 94.2)	58.5 (42.2 – 73.3)	Fisher's Exact	0.007
Specificity (%) (95% CI)	95.7 (84.3 – 99.3)	88.4 (74.1 – 95.6)	Fisher's Exact	0.252
Positive Predictive Value (%) (95% CI)	94.9 (81.4 – 99.1)	82.8 (63.5 – 93.5)	Fisher's Exact	0.127
Negative Predictive Value (%) (95% CI)	88.2 (73.0 – 95.8)	69.1 (49.2 – 84.1)	Fisher's Exact	0.020
Accuracy (%) (95% CI)	91.1 (82.7 – 95.8)	73.8 (62.9 – 82.5)	Fisher's Exact	0.004
Angio. correlation (Phi)	0.82 (p < 0.001)	0.49 (p<0.001)	Z 4.02	< 0.001

Table 3.7

Comparative ability of PCI and DSE to detect coronary artery stenosis (after exclusion of cases with poor image quality)

	After exclusion of all cases of poor image quality (78 coronary territories)			
	DSE	PCI	Test Statistic	P Value (2-sided)
Sensitivity (%) (95% CI)	84.6 (68.8 – 93.6)	61.5 (44.7 – 76.2)	McNemar	0.012
Specificity (%) (95% CI)	94.9 (81.4 – 99.1)	92.3 (78.0 – 98.0)	McNemar	1.0
Positive Predictive Value (%) (95% CI)	94.3 (79.5 – 99.0)	88.9 (69.7 – 97.1)	Fisher's Exact	0.645
Negative Predictive Value (%) (95% CI)	86.0 (69.3 – 94.8)	70.6 (49.9 – 85.7)	Fisher's Exact	0.086
Accuracy (%) (95% CI)	90.4 (80.3 – 95.2)	76.9 (65.8 – 85.4)	McNemar	0.021
Angio. correlation (Phi)	0.80 (p < 0.001)	0.57 (p < 0.001)	Z 2.762	0.006

Table 3.8 (continued on next page)

Comparative ability of PCI and DSE to detect coronary stenosis subdivided

according to coronary territory (28 cases interpretable by both DSE and PCI)

		Among 28 cases for which both DSE and PCI were interpretable			
	Terr-itory	DSE cases	PCI cases	Test Statistic	P value (2-sided)
Sensitivity (%) (95% CI)	LAD	90.0 (66.0 – 98.2)	70.0 (45.7 – 87.2)	McNemar	0.219
	RCA	91.7 (59.8 – 99.6)	50.0 (22.3 – 77.7)	McNemar	0.063
	CX	66.7 (30.9 – 91.0)	44.4 (15.3 – 77.3)	McNemar	0.5
Specificity (%) (95% CI)	LAD	100 (59.8 – 100)	87.5 (46.7 – 99.3)	McNemar	1.0
	RCA	87.5 (60.4 – 97.8)	100 (75.9 – 100)	McNemar	0.5
	CX	100 (79.1 – 95.5)	78.9 (53.9 – 93.0)	McNemar	0.125
Positive Predictive Value (%) (95% CI)	LAD	100 (78.1 – 100)	93.3 (66.7 – 99.7)	Fisher's Exact	0.455
	RCA	84.6 (53.7 – 97.3)	100 (51.7 – 100)	Fisher's Exact	0.544
	CX	100 (51.7 – 100)	50.0 (17.4 – 82.6)	Fisher's Exact	0.085
Negative Predictive Value (%) (95% CI)	LAD	80.0 (54.2 – 93.9)	53.8 (27.8 – 78.1)	Fisher's Exact	0.379
	RCA	93.3 (63.3 – 99.8)	72.7 (28.3 – 96.3)	Fisher's Exact	0.204
	CX	86.4 (39.0 – 99.6)	75.0 (35.6 – 95.5)	Fisher's Exact	0.445

		Table 3.8 continued			
Accuracy (%) (95% CI)	LAD	92.9 (75 – 98.8)	75.0 (54.8 – 88.6)	McNemar	0.125
	RCA	89.3 (70.6 – 97.2)	78.6 (58.5 – 91.0)	McNemar	0.453
	CX	89.3 (70.6 – 97.2)	67.9 (47.6 – 83.4)	McNemar	0.031
Angio correlation (Phi)	LAD	0.849 (p< 0.001)	0.521 (p = 0.009)	Z 2.386	0.017
	RCA	0.786 (p< 0.001)	0.603 (p = 0.001)	Z 1.284	0.200
	CX	0.759 (p< 0.001)	0.242 (p = 0.201)	Z 2.641	0.004*

* Although the p value is below 0.05, it does not take account of the fact that the Phi value for Angiography and PCI in the Circumflex territory could be a chance finding (Phi 0.242, p=0.201). It therefore cannot be concluded that the difference in Angiographic correlation between DSE and PCI is statistically significant.

Table 3.9 (continued on next page)

Comparative ability of PCI and DSE to detect coronary stenosis, according to coronary territory (30 interpretable DSE cases and 28 interpretable PCI cases)

	Territory	Among 30 interpretable DSE cases and 28 interpretable PCI cases			
		DSE cases (90 territories)	PCI cases (84 territories)	Test Statistic	P value (2-sided)
Sensitivity (%) (95% CI)	LAD	90.9 (69.4 – 98.4)	70.0 (45.7 – 87.2)	Fisher's Exact	0.123
	RCA	91.7 (59.8 – 99.6)	50.0 (22.3 – 77.7)	Fisher's Exact	0.069
	CX	66.7 (30.9 – 91.0)	44.4 (15.3 – 77.3)	Fisher's Exact	0.637
Specificity (%) (95% CI)	LAD	100 (58.9 – 100)	87.5 (46.7 – 99.3)	Fisher's Exact	1.0
	RCA	88.9 (63.9 – 98.1)	100 (75.9 – 100)	Fisher's Exact	0.487
	CX	100 (80.8 – 100)	78.9 (53.9 – 93.0)	Fisher's Exact	0.042
Positive Predictive Value (%) (95% CI)	LAD	100 (80.0 – 100)	93.3 (66.7 – 99.7)	Fisher's Exact	0.429
	RCA	84.6 (53.7 – 97.3)	100 (51.7 – 100)	Fisher's Exact	0.544
	CX	100 (51.7 – 100)	50.0 (17.4 – 82.6)	Fisher's Exact	0.085
Negative Predictive Value (%) (95% CI)	LAD	80.0 (55.7 – 93.4)	53.8 (27.8 – 78.1)	Fisher's Exact	0.379
	RCA	94.1 (64.2 – 99.9)	72.7 (28.3 – 96.3)	Fisher's Exact	0.113
	CX	87.5 (40.0 – 99.8)	75.0 (35.6 – 95.5)	Fisher's Exact	0.436

		Table 3.9 continued			
Accuracy (%) (95% CI)	LAD	93.0 (76.5 – 98.8)	75.0 (54.8 – 88.6)	Fisher's Exact	0.075
	RCA	90.0 (72.3 – 97.4)	78.6 (58.5 – 91.0)	Fisher's Exact	0.290
	CX	90.0 (72.3 – 97.4)	67.9 (47.6 – 83.4)	Fisher's Exact	0.053
Angio correlation (Phi)	LAD	0.853 (p< 0.001)	0.521 (p = 0.009)	Z 2.484	0.013
	RCA	0.80 (p< 0.001)	0.603 (p = 0.001)	Z 1.444	0.148
	CX	0.76 (p<0.001)	0.242 (p = 0.201)	Z 2.700	0.008*

* Although the p value is below 0.05, it does not take account of the fact that the Phi value for Angiography and PCI in the Circumflex territory could be a chance finding (Phi 0.242, p=0.201). It therefore cannot be concluded that the difference in Angiographic correlation between DSE and PCI is statistically significant.

Table 3.10

Comparison of DSE and PCI in 28 cases for which both imaging methods were

interpretable and conclusive

Territory	Angiographic stenosis		DSE WMA		PCI contrast defect	
			N	Y	N	Y
LAD	N	8	8	0	7	1
	Y	20	2	18	6	14
RCA	N	16	14	2	16	0
	Y	12	1	11	6	6
CX	N	19	19	0	15	4
	Y	9	3	6	5	4
All	N	43	41	2	38	5
	Y	41	6	35	17	24

Table 3.11

Comparison of DSE and PCI in 26 cases after exclusion of inconclusive, non-interpretable, and poor image quality cases

Territory	Angiographic stenosis		DSE WMA (26 cases)		PCI contrast defect (26 cases)	
			N	Y	N	Y
LAD	N	6	6	0	6	0
	Y	20	2	18	6	14
RCA	N	16	14	2	16	0
	Y	10	1	9	4	6
CX	N	17	17	0	14	3
	Y	9	3	6	5	4
All	N	39	37	2	36	3
	Y	39	6	33	15	24

Table 3.12

Comparison of DSE and Coronary Angiography results for all cases interpretable

/ conclusive according to DSE

| Territory | Angiographic stenosis | DSE WMA | | Total |
		N	Y	
LAD	N	8	0	8
	Y	2	20	22
RCA	N	16	2	18
	Y	1	11	12
CX	N	21	0	21
	Y	3	6	9
All	N	45	2	47
	Y	6	37	43

Table 4.1

Coherent Contrast Imaging™ Presets

CCI PARAMETER	EASY All wall visible with clear myocardial texture	AVERAGE All walls visible but myocardial texture unclear	DIFFICULT Poor endocardial and myocardial definition.
Space Time	T1	S1	S2
Mechanical Index	0.1	0.1 / 0.2	0.2 / 0.3
Depth	140 mm	140 mm	140 mm
Dynamic Range	50 – 55 dB	50 dB	45 – 50 dB
Trigger Interval	50 ms	50 ms	50 to 75 ms
Focus level	Mid Left Ventricle	Mid Left Ventricle	Mid Left Ventricle
Time Gain Control	Slight Diagonal	Slight Diagonal	Slight Diagonal

Table 4.2

Baseline characteristics

RISK FACTOR	Original group of 38	Final group of 32
Diabetes	13	12
Hypertension	11	10
Hypercholesterolaemia (total cholesterol >5.2 mmol/l)	23	19
Family history of premature Coronary Artery Disease	17	15
Peripheral arterial disease	4	4
Obesity	14	12
Smoking	7	7
Male	28	23
Female	10	9

Table 4.3

Coronary angiographic stenoses > 50%

TERRITORY	NUMBER (of total 38 cases recruited)	NUMBER (of 32 cases interpretable in CCI mode)
LAD alone	13	10
RCA alone	6	5
CIRCUMFLEX alone	3	3
LAD + RCA	8	8
LAD + CIRCUMFLEX	5	4
RCA + CIRCUMFLEX	3	2
TOTAL NUMBER OF STENOSES	54	46

Table 4.4

Distribution of artefacts and fixed contrast defects.

WALL SEGMENT	NUMBER (Total = 320)
Artefact in basal lateral wall alone	21
Artefact in basal and mid lateral wall	5
Artefact in basal septal wall alone	4
Artefact in basal and mid septal wall	1
Artefact in basal and mid inferior wall	6
Artefact in basal anterior wall alone	9
Artefact in basal and mid anterior wall	3
Artefact in apical wall in 2 Chamber view	3
Fixed defect in apical wall in 4 Chamber view	2
Fixed defect apical wall alone in 2 Chamber view	1
Fixed defects in apical and mid anterior walls	1
Total number of regions affected by artefact (10 segment model)	**67**
Total number of regions affected by fixed defects (unrecognised infarction, 10 segment model)	**5**

Fixed defects were due to previous unrecognised apical myocardial infarction in one case and limited antero-apical myocardial infarction in one further case.

Table 4.5

Regions interpretable by Contrast Imaging

	WALL REGION	ARTE-FACT	OTHER DEFECT	INTER-PRETED
LAD (32)	CCI wall motion	0	0	32
	PSCD	0	2	30
	PSCD / CRT	0	0	32
	PSCD / CRT / Wall motion	0	0	32
RCA (32)	CCI wall motion	0	0	32
	PSCD	6	0	26
	PSCD / CRT	6	0	26
	PSCD / CRT / Wall motion	0	0	32
CX (32)	CCI wall motion	0	0	32
	PSCD	5	0	27
	PSCD / CRT	5	0	27
	PSCD / CRT / Wall motion	0	0	32
Total	CCI wall motion	0	0	96
	PSCD	11	2	83
	PSCD / CRT	11	0	85
	PSCD / CRT / Wall motion	0	0	96

Table 4.6

Contrast imaging parameters divided according to presence or absence of coronary artery stenosis (32 patients for whom a contrast imaging parameter and conventional DSE wall motion were interpretable and conclusive)

Territory		Angio	DSE wma (96)		CCI wma (96)		PSCD (83)		PSCD / CRTI (85)		PSCD / CRTI / CCI wma (96)	
			N	Y	N	Y	N	Y	N	Y	N	Y
LAD	N	10	9	1	10	0	10	0	10	0	10	0
	Y	22	5	17	6	16	10	10	1	21	1	21
RCA	N	17	16	1	17	0	13	1	12	2	15	2
	Y	15	4	11	5	10	10	2	2	10	4	11
CX	N	23	22	1	23	0	19	0	19	0	23	0
	Y	9	4	5	6	3	5	3	3	5	3	6
All	N	50	47	3	50	0	42	1	41	2	48	2
	Y	46	13	33	17	29	25	15	6	36	8	38

Table 4.7

Conventional wall motion results divided according to presence or absence of coronary artery stenosis (36 patients for whom conventional DSE wall motion was interpretable and conclusive)

Territory	Angiographic stenosis		DSE wma (of 108 territories)	
			N	Y
LAD	N	12	11	1
	Y	24	5	19
RCA	N	19	18	1
	Y	17	4	13
CX	N	26	25	1
	Y	10	5	5
All	N	57	54	3
	Y	51	14	37

Table 4.8

Comparison of Standard wall motion and CCI based wall motion assessment for detection of > 50% coronary artery stenosis (32 cases interpretable / conclusive according to both tests)

	Among cases of successful DSE + CCI (32 subjects, 96 territories)			
	DSE wma	CCI wma	Test statistic	P value (2-sided)
Sensitivity (%) (95% CI)	71.7 (56.3 – 83.5)	63.0 (47.5 – 76.4)	McNemar	0.344
Specificity (%) (95% CI)	94.0 (82.5 – 98.4)	100 (91.1 - 100)	Fisher's Exact	0.242
Positive Predictive Value (%) (95% CI)	91.7 (76.4 – 97.8)	100 (85.7 – 100)	Fisher's Exact	0.247
Negative Predictive Value (%) (95% CI)	78.3 (61.0 – 89.7)	74.6 (54.8 – 88.1)	Fisher's Exact	0.679
Accuracy (%) (95% CI)	83.3 (74.0 – 89.9)	82.3 (72.9 – 89.1)	McNemar	1.0
Angio correlation (Phi)	0.678 (p<0.001)	0.690 (p<0.001)	Z 0.102	0.918

Table 4.9

Comparison of Standard wall motion and CCI based wall motion assessment for detection of > 50% coronary artery stenosis (all interpretable / conclusive DSE cases and 32 interpretable / conclusive CCI cases)

	DSE wma (108 territories)	CCI wma (96 territories)	Test statistic	P value (2-sided)
Sensitivity (%) (95% CI)	72.5 (58.0 – 83.7)	63.0 (47.5 – 76.4)	Fisher's Exact	0.385
Specificity (%) (95% CI)	94.7 (84.5 – 98.6)	100 (91.1 - 100)	Fisher's Exact	0.246
Positive Predictive Value (%) (95% CI)	92.5 (78.5 – 98.0)	100 (85.7 – 100)	Fisher's Exact	0.258
Negative Predictive Value (%) (95% CI)	79.4 (63.2 – 90.0)	74.6 (54.8 – 88.1)	Fisher's Exact	0.545
Accuracy (%) (95% CI)	84.3 (75.7 – 90.3)	82.3 (72.9 – 89.1)	Yates Chi sq. 0.035	0.851
Angio correlation (Phi)	0.696 (p<0.001)	0.690 (p<0.001)	Z 0.134	0.849

Table 4.10

Agreement between DSE and CCI regional wall motion abnormality (32 conclusive cases interpretable by both methods)

	CCI wma absent	CCI wma present	TOTAL
DSE wma absent	57	3	60
DSE wma present	10	26	36
TOTAL	67	29	96

Chi-Square = 48.2, degrees of freedom = 1, Phi correlation = 0.71 (p<0.001)

Kappa score = 0.70 (p<0.001), Agreement 86.5%.

Table 4.11

Agreement between DSE and CCI regional wall motion abnormality for the Left Anterior Descending Territory (32 conclusive cases interpretable by both methods)

	CCI wma absent	CCI wma present	TOTAL
DSE wma absent	13	1	14
DSE wma present	3	15	18
TOTAL	16	16	32

Chi-Square = 18.3, degrees of freedom = 1, Phi correlation = 0.76 (p<0.001)

Kappa score = 0.75 (p<0.001), Agreement 87.5%.

Table 4.12

Agreement between DSE and CCI regional wall motion abnormality for the

Right Coronary Artery Territory (32 conclusive cases interpretable by both

methods)

	CCI wma absent	CCI wma present	TOTAL
DSE wma absent	19	1	20
DSE wma present	3	9	12
TOTAL	22	10	32

Chi-Square = 17.1, degrees of freedom = 1, Phi correlation = 0.73 (p<0.001)

Kappa score = 0.72 (p<0.001), Agreement 87.5%.

Table 4.13

Agreement between DSE and CCI regional wall motion abnormality for the

Circumflex Coronary Artery Territory (32 conclusive cases interpretable by both

methods)

	CCI wma absent	CCI wma present	TOTAL
DSE wma absent	25	1	26
DSE wma present	4	2	6
TOTAL	29	3	32

Chi-Square = 5.0, degrees of freedom = 1, Phi correlation = 0.40 (p=0.026)

Kappa score = 0.37 (p=0.083), Agreement 84.4%.

Table 4.14

Comparison of Standard Wall Motion assessment and Peak Stress Contrast Deficit for detection of > 50% coronary artery stenosis (32 cases interpretable by both tests)

	DSE wall motion assessment (96 territories)	Peak Stress Contrast Deficit (83 territories)	Test statistic	P value (2-sided)
Sensitivity (%) (95% CI)	71.7 (56.3 – 83.5)	37.5 (23.2 – 54.2)	Fisher's Exact	0.002
Specificity (%) (95% CI)	94.0 (82.5 – 98.4)	97.7 (86.5 – 99.9)	Fisher's Exact	0.620
Positive Predictive Value (%) (95% CI)	91.7 (76.4 – 97.8)	93.8 (67.7 – 99.7)	Fisher's Exact	1.000
Negative Predictive Value (%) (95% CI)	78.3 (61.0 – 89.7)	63.2 (36.5 – 84.2)	Fisher's Exact	0.080
Accuracy (%) (95% CI)	83.3 (74.0 – 89.9)	68.7 (57.9 – 78.4)	Yates Chi sq. 4.541	0.033
Angio correlation (Phi)	0.678 (p<0.001)	0.446 (p<0.001)	Z 2.27	0.024

Table 4.15

Contrast replenishment – regions eligible for assessment

REGIONS	NUMBER
Total	192
Baseline Artefact	17
Assessable by CRT at Baseline	175
Peak Stress Artefact	23
Reversible Peak Stress Contrast Deficit	33
Assessable by CRT at Peak	136

Table 4.16

Baseline contrast replenishment – all regions combined

	CRT (seconds) (Median plus Interquartile range)	
	STENOSIS N = 103	NO STENOSIS N = 72
All Regions	5 (iqr 4 to 6)	5 (iqr 4 to 6)

Table 4.17

Baseline contrast replenishment – according to territory

REGION	CRT (seconds) (Median plus Interquartile range)	P value (2-sided, based on Kruskall-Wallis Test)
Inferior	4 (iqr 4 to 5)	
Anterior	4 (iqr 4 to 5)	
Apex 2-chamber	4 (iqr 4 to 5)	0.015
Septal	5 (iqr 4 to 6)	
Lateral	6 (iqr 4 to 6)	
Apex 4-chamber	5 (iqr 4 to 6)	

Table 4.18

Peak contrast replenishment – all regions combined

	% CHANGE IN CRT (Median plus Interquartile range)		P value (2-sided, based on Mann-Whitney U)
	STENOSIS, N=66	NO STENOSIS, N=70	
All Regions	+ 33.3 (iqr 0 to 60)	– 25 (iqr – 40 to 0)	<0.001

Table 4.19

Peak contrast replenishment – according to territory

Territory	% CHANGE IN CRT (Median plus Interquartile range)		P value (2-sided, based on Mann-Whitney U)
	STENOSIS	NO STENOSIS	
Inferior	+ 55 (iqr 30 to 70)	– 25 (iqr – 40 to 0)	0.002
Anterior	+ 50 (iqr 10 to 67.5)	0.0 (iqr – 43.8 to 0)	0.002
Apex 2-chamber	+ 50 (iqr 25 to 71.3)	– 10 (iqr – 27.1 to 0)	0.001
Septal	0.0 (iqr – 40 to 33.3)	– 33.3 (iqr – 44.6 to – 25)	0.017
Lateral	0.0 (iqr –31.4 to 41.7)	– 33.3 (iqr – 42.9 to 0)	0.091
Apex 4-chamber	+ 33.3 (iqr 0 to 60)	– 29.2 (iqr –33.7 to – 15)	<0.001

Table 4.20

Comparison of Standard Wall Motion assessment with combined assessment of

Peak Stress Contrast Deficit and Contrast Replenishment Abnormality for

detection of > 50% coronary artery stenosis (32 cases interpretable by both tests)

	DSE wall motion assessment (96 territories)	Combined peak stress contrast defect and contrast replenishment abnormality (85 territories)	Test statistic	P value (2-sided)
Sensitivity (%) (95% CI)	71.7 (56.3 – 83.5)	85.7 (70.8 – 94.1)	Fisher's Exact	0.128
Specificity (%) (95% CI)	94.0 (82.5 – 98.4)	95.3 (83.3 – 99.2)	Fisher's Exact	1.0
Positive Predictive Value (%) (95% CI)	91.7 (76.4 – 97.8)	94.7 (80.9 – 99.1)	Fisher's Exact	0.670
Negative Predictive Value (%) (95% CI)	78.3 (61.0 – 89.7)	87.2 (71.9 – 95.4)	Fisher's Exact	0.309
Accuracy (%) (95% CI)	83.3 (74.0 – 89.9)	90.6 (82.0 – 95.6)	Yates Chi sq. 1.55	0.213
Angio correlation (Phi)	0.678 (p<0.001)	0.815 (p<0.001)	Z 2.088	0.036

Table 4.21

Comparison of Standard Wall Motion assessment with combined assessment of
Peak Stress Contrast Deficit, Contrast Replenishment Abnormality, and CCI
based Wall Motion assessment for detection of > 50% coronary artery stenosis
(32 cases interpretable by both tests)

	DSE wall motion assessment (96 territories)	Combined CCI wall motion, peak stress contrast defect, and contrast replenishment abnormality (96 territories)	Test statistic	P value (2-sided)
Sensitivity (%) (95% CI)	71.7 (56.3 – 83.5)	82.6 (68.0 – 91.7)	McNemar	0.267
Specificity (%) (95% CI)	94.0 (82.5 – 98.4)	96.0 (85.1 – 99.3)	McNemar	1.0
Positive Predictive Value (%) (95% CI)	91.7 (76.4 – 97.8)	95.0 (81.8 – 99.1)	Fisher's Exact	0.663
Negative Predictive Value (%) (95% CI)	78.3 (61.0 – 89.7)	85.7 (70.3 – 94.2)	Fisher's Exact	0.342
Accuracy (%) (95% CI)	83.3 (74.0 – 89.9)	89.6 (81.3 – 94.6)	McNemar	0.238
Angio correlation (Phi)	0.678 (p<0.001)	0.797 (p<0.001)	Z 1.807	0.070 (2-sided) 0.035 (1-sided)

Table 4.22

Comparison of Standard Wall Motion assessment with combined assessment of Peak Stress Contrast Deficit, Contrast Replenishment Abnormality, and CCI based Wall Motion assessment for detection of > 50% coronary artery stenosis (All 36 interpretable DSE cases and 32 cases interpretable by CCI)

	DSE wall motion assessment (108 territories)	Combined CCI wall motion, peak stress contrast defect, and contrast replenishment abnormality (96 territories)	Test statistic	P value (2-sided)
Sensitivity (%) (95% CI)	72.5 (58.0 – 83.7)	82.6 (68.0 – 91.7)	Fisher's Exact	0.332
Specificity (%) (95% CI)	94.7 (84.5 – 98.6)	96.0 (85.1 – 99.3)	Fisher's Exact	1.0
Positive Predictive Value (%) (95% CI)	92.5 (78.5 – 98.0)	95.0 (81.8 – 99.1)	Fisher's Exact	1.0
Negative Predictive Value (%) (95% CI)	79.4 (63.2 – 90.0)	85.7 (70.3 – 94.2)	Fisher's Exact	0.480
Accuracy (%) (95% CI)	84.3 (75.7 – 90.3)	89.6 (81.3 – 94.6)	Yates Chi sq. 0.830	0.362
Angio correlation (Phi)	0.696 (p<0.001)	0.797 (p<0.001)	Z 1.621	0.106 (2-sided) 0.053 (1-sided)

Table 4.23

Interobserver variability for CCI™ cases

Parameter	Territory	Agreement (%)	Kappa
Conventional WMA	LAD (n=16)	93.8	0.86 (p=0.001)
	RCA (n=16)	87.5	0.733 ((p=0.008)
	CX (n=16)	100	1 (p=0.002)
CCI™ WMA	LAD (n=16)	100	1 (p=0.001)
	RCA (n=16)	87.5	0.71 (0.013)
	CX (n=16)	87.5	0.45 (p=0.187)
PSCD	LAD (n=14)	92.9	0.84 (p=0.005)
	RCA (n=14)	100	1 (p=0.071)
	CX (n=13)	92.3	0.63 (p=0.154)
PSCD / CRT	LAD (n=16)	93.8	0.85 (p=0.003)
	RCA (n=14)	92.9	0.86 (p=0.005)
	CX (n=13)	92.3	0.81 (p=0.014)
PSCD / CRT / CCI™ WMA	LAD (n=16)	93.8	0.846 (p=0.003)
	RCA (n=16)	100	1 (p=0.001)
	CX (n=16)	93.8	0.82 (p=0.007)

2. FIGURES

Figure 1.1

The ischaemic cascade

PEAK STRESS

Ischaemic
symptoms

Electrocardio-
graphic
changes

Systolic
wall
motion
abnormalities

Diastolic
wall
motion
abnormalities

Perfusion
defect

REST
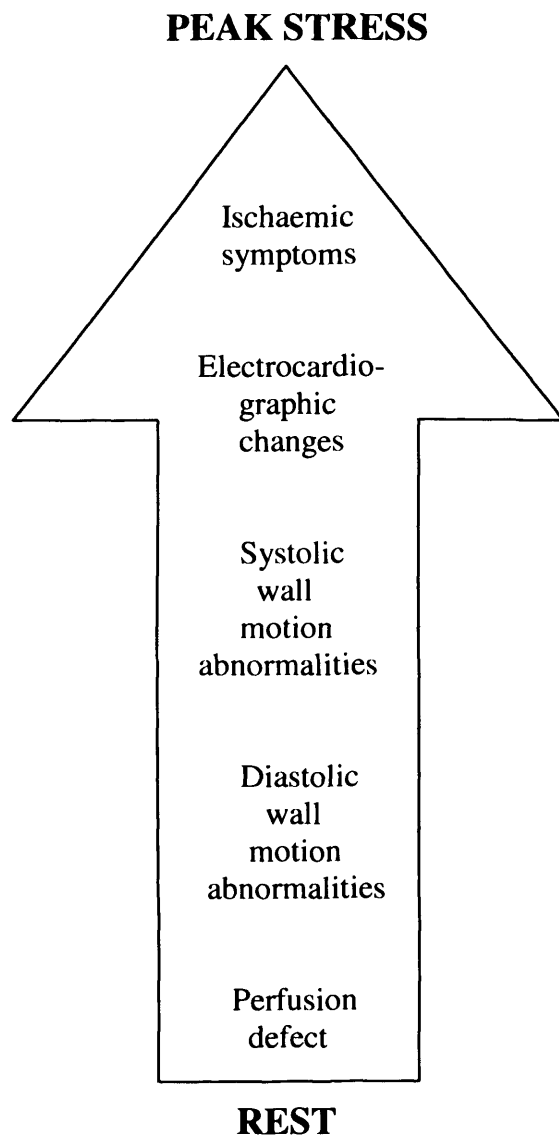
Figure 1.2

Components of Coronary Blood Volume

TOTAL CORONARY BLOOD VOLUME

Arteries	Arterioles	Capillaries	Venules	Veins

INTRAMYOCARDIAL BLOOD

(Myocardial blood volume)
(90% capillary blood volume, 10%
arteriolar and venular)
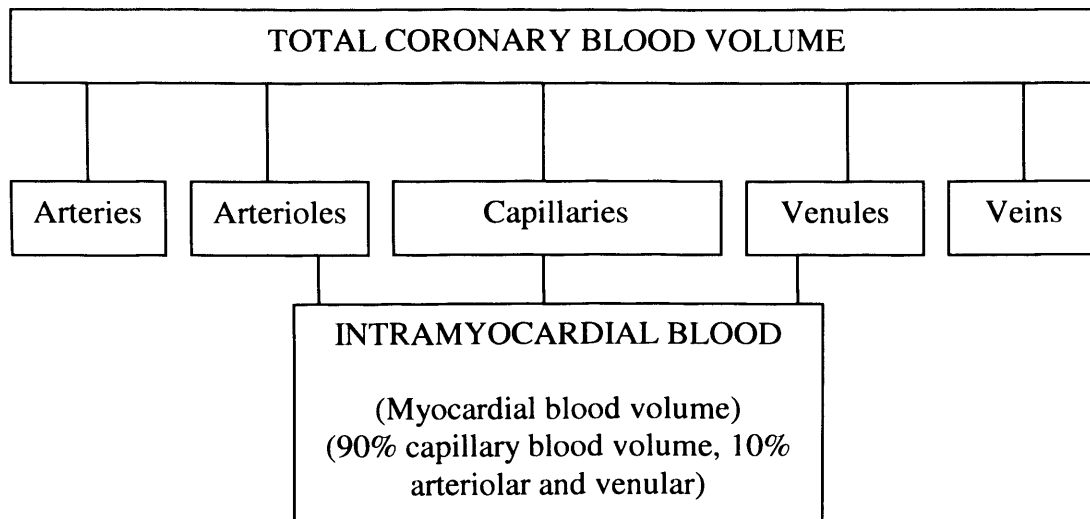
Figure 1.3

Graphical representation of bolus dose micro-bubble signal

SIGNAL INTENSITY

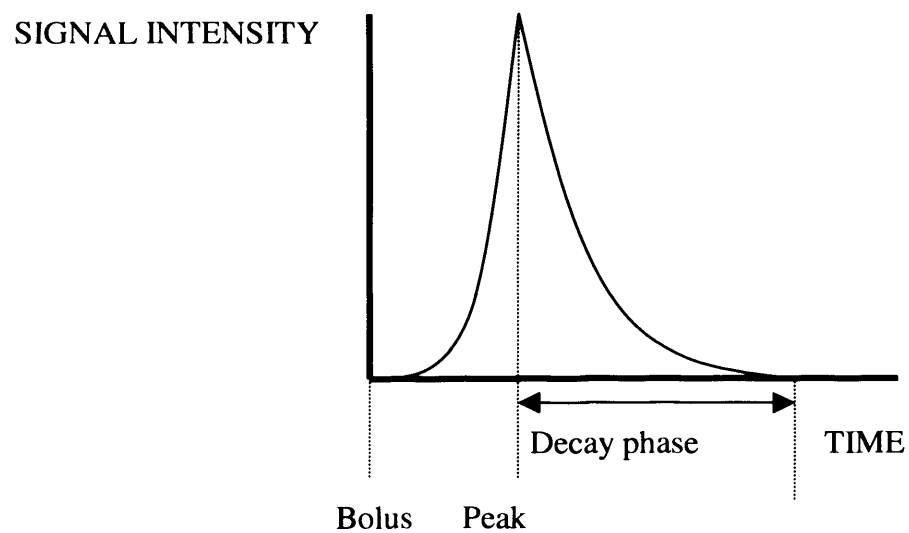Decay phase   TIME

Bolus   Peak

Figure 1.4

Graphical representation of in vivo association between signal intensity and time
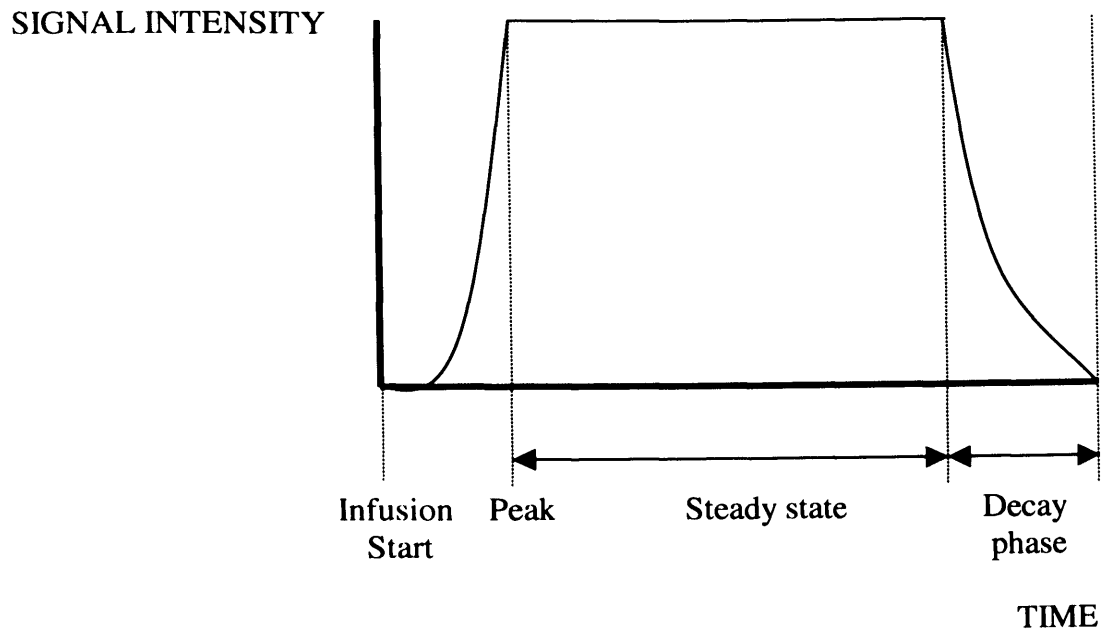
with micro-bubble infusion

Figure 2.1

Power Contrast Imaging™ Apical 4 chamber view with image acquisition once

every four cardiac cycles
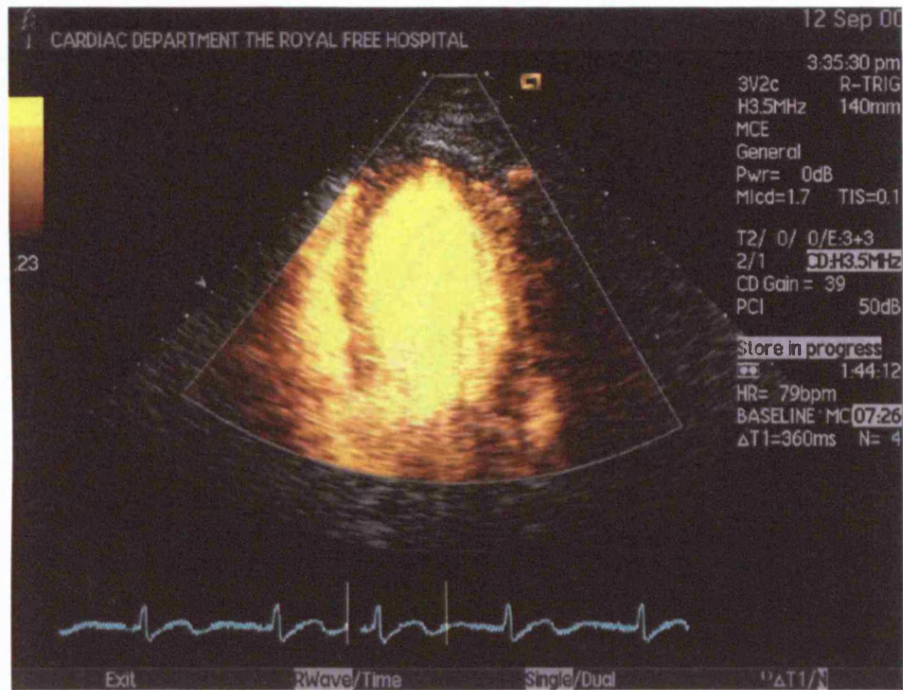
Figure 3.1

Division of myocardial regions by territory for assessment of perfusion using the 3-territory, 10-segment model. All cases had dominant Right Coronary circulation, hence RCA equates to Posterior Descending Artery territory

APICAL 2 CHAMBER VIEW   APICAL 4 CHAMBER VIEW

Left Anterior Descending coronary artery

Right coronary artery

Circumflex coronary artery

Figure 3.2

Example Power Contrast Imaging™ case

A. Baseline image showing strong septal contrast signal

B. Stress image showing diminished septal contrast signal

Figure 4.1
Cases for which each imaging modality was successful / conclusive

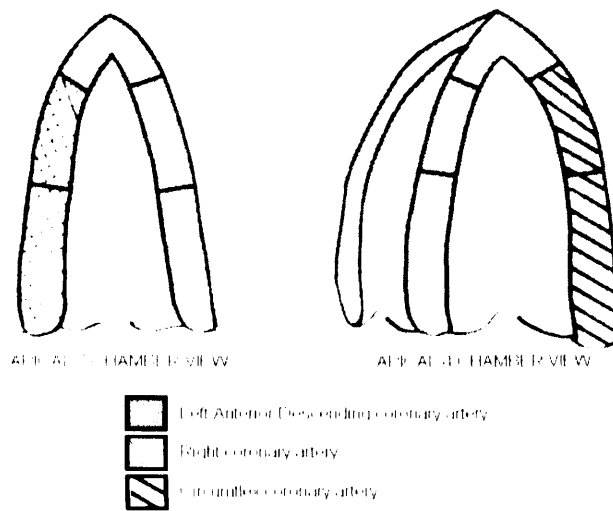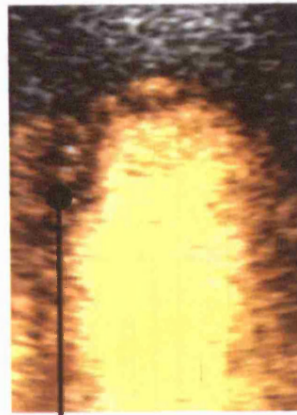SWM = Standard wall motion
CCI = Coherent contrast imaging
CWM = Contrast wall motion
PSCD = Peak stress contrast deficit
PSCD / = Combined peak stress
CRT contrast deficit and contrast
replenishment time
PSCD / = Combined
CRT / peak stress contrast deficit /
CWM contrast replenishment time /
contrast wall motion

38 angiographic cases

1 case excluded
(image quality)

37 cases interpretable
by SWM

2 cases excluded
(image quality)

2 cases excluded
(peak stage
image quality)

1 case excluded
(sub-optimal
HR)

36 conclusive
SWM cases

32 conclusive
CCI cases

1 case excluded
(uneven contrast
infusion and sub-
optimal HR)

108 territories
SWM

96 territories
CWM

83 territories
PSCD

85 territories
PSCD / CRT

96 territories
PSCD / CRT / CWM

Figure 4.2

Contrast Replenishment Time for all Regions Combined

Angiogram result

Figure 4.3

Contrast Replenishment Time for the Anterior Wall in the Apical 2 Chamber View

Angiogram Result
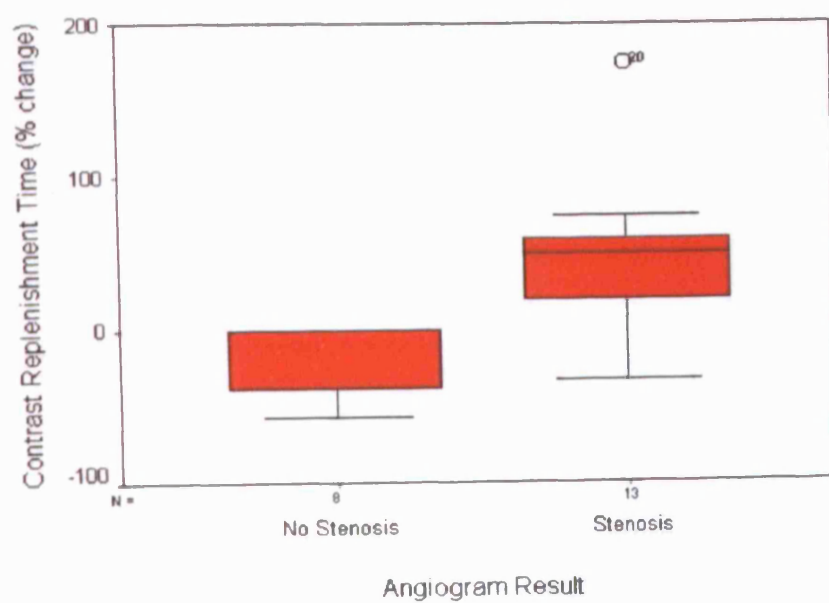
Figure 4.4

Contrast Replenishment Time for the Apical Wall in the Apical 2 Chamber View
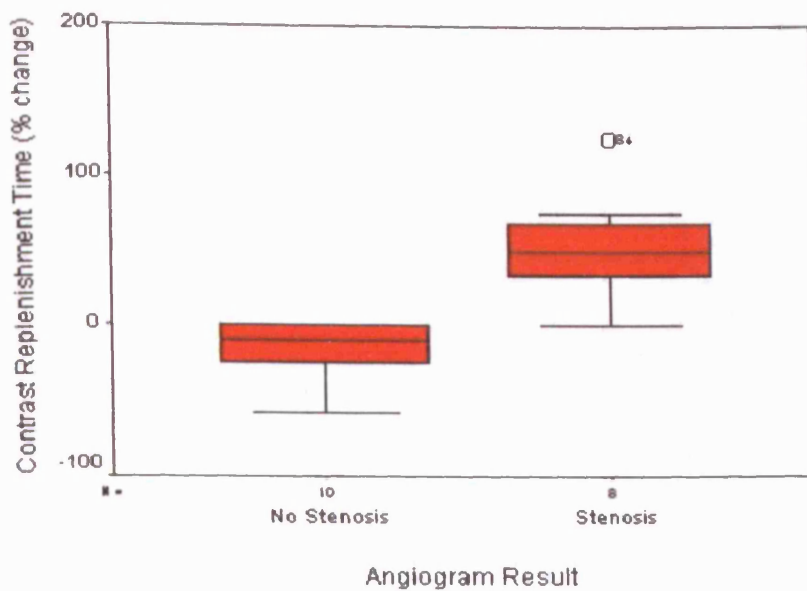
Figure 4.5

Contrast Replenishment Time for the Inferior Wall in the Apical 2 Chamber View
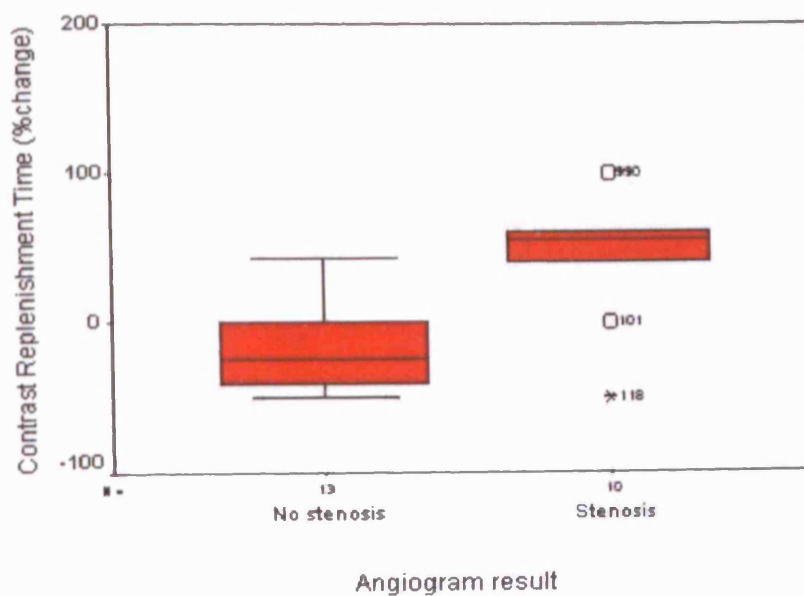
Figure 4.6

Contrast Replenishment Time for the Septal Wall in the Apical 4 Chamber View
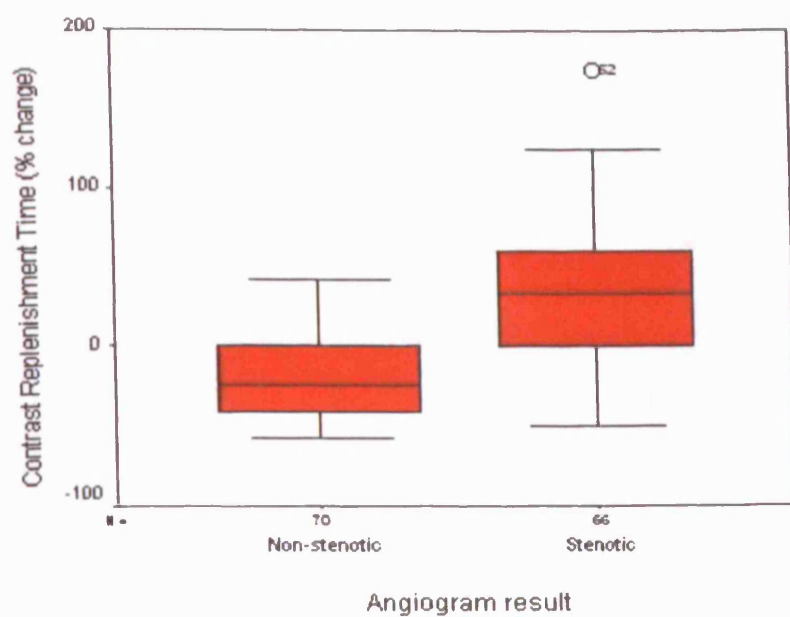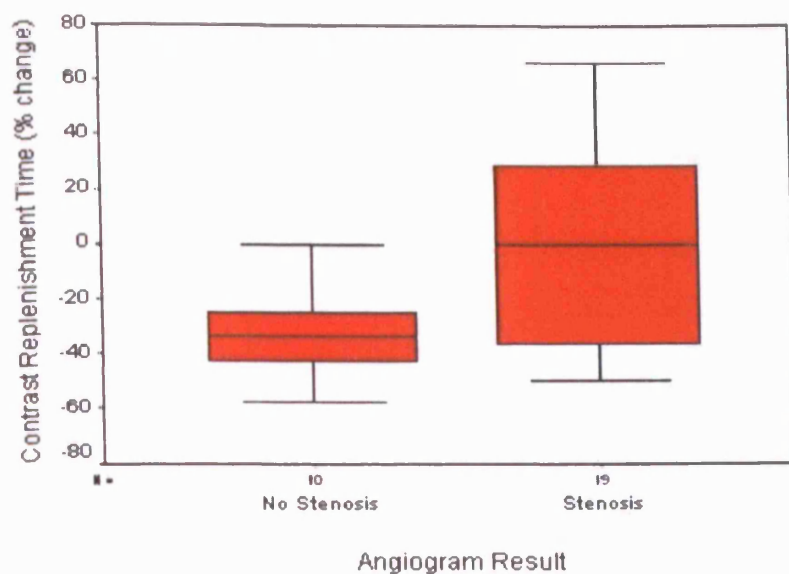

Figure 4.7

Contrast Replenishment Time for the Apical Wall in the Apical 4 Chamber View
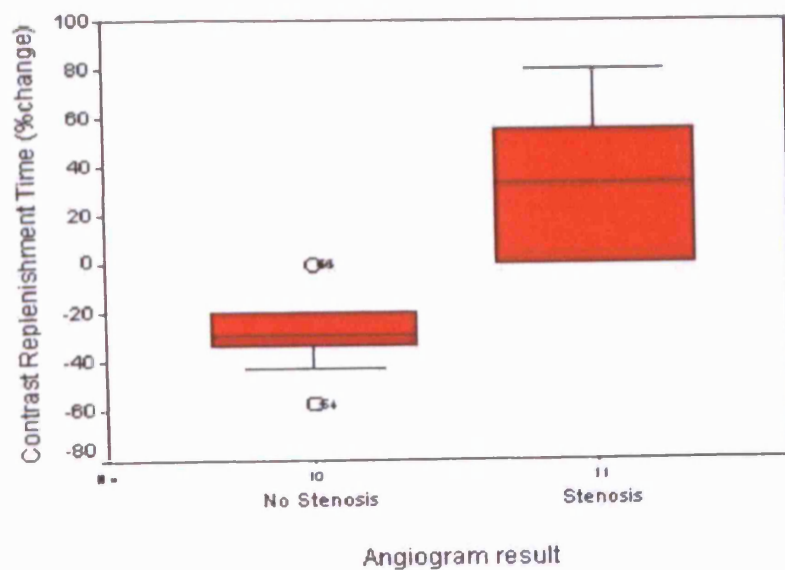
Figure 4.8

Contrast Replenishment Time for the Lateral Wall in the Apical 4 Chamber View
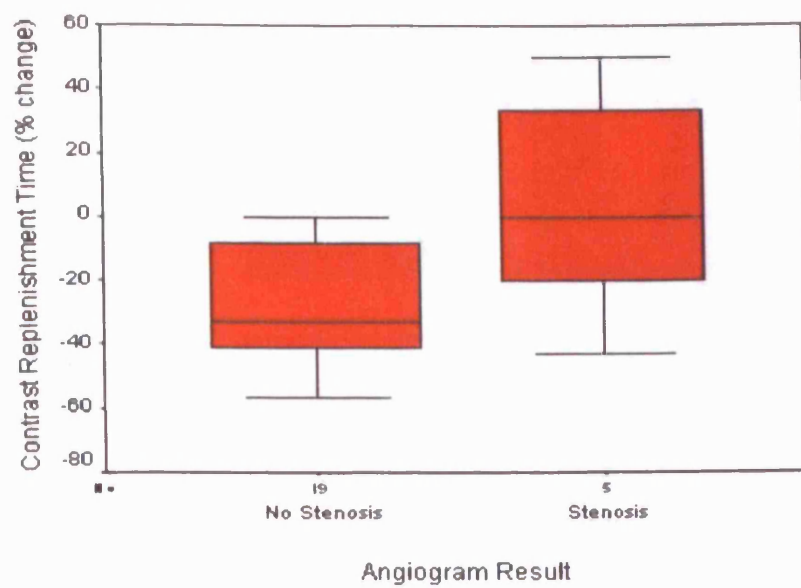
Figure 4.9

Example of Coherent Contrast Imaging™ case
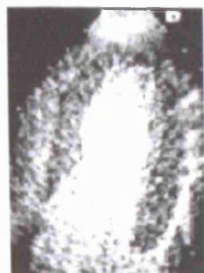
| A. Baseline
Good contrast signal throughout myocardial regions(4 chamber view) | B. Stress
Minimal contrast signal immediately after destruction pulse | C. Stress
Diminished contrast signal in apical region 5 seconds after destruction pulse |

APPENDIX TWO

1. ETHICAL APPROVAL

This research was approved by the Royal Free Hampstead NHS Trust Local Research Ethics Committee, under the Title "Myocardial Perfusion as Assessed by Myocardial Contrast Echocardiography".

Reference number: 161-99.

Date of approval: September 1999. Chairman Dr Michael S Pegg.

This research was registered with and approved by the Royal Free Hampstead NHS Trust Research and Development Committee, under the title above.

Reference number: R&D 3810.

Date of Approval: September 1999.

....

Elved Roberts, MBChB, MRCP.

2. PATIENT INFORMATION SHEETS

a. Sample patient information sheet 1 (Adenosine Power Contrast Imaging™).

MYOCARDIAL CONTRAST ECHOCARDIOGRAPHY (MCE) AND STRESS ECHOCARDIOGRAPHY

We would like to invite you to take part in this study. It is entirely voluntary.

What is myocardial contrast echocardiography (MCE)?
MCE is a technique for studying blood supply to heart muscle. It involves having an echocardiogram (ultrasound picture of the heart) at the same time as injection of a contrast agent (Optison) and a drug called Adenosine. These substances are injected through small needles in an arm vein. You may already have been referred for a Dobutamine Stress Echocardiogram (DSE) test by your consultant. A DSE test will be incorporated into our study.

Why are we undertaking this research?
We believe that MCE could provide an important insight into the nature of coronary artery disease. We would like to compare the accuracy of information gained by MCE with other tests for coronary artery disease such as Dobutamine Stress Echocardiography and Coronary Angiography.

How could you be affected by the test?
The echocardiogram is painless and requires the patient to lie on a couch for about 30 minutes. Minor discomfort may occur on the chest wall where the probe is placed. Two needles will be inserted into a vein in the arm (like having a blood test – it can hurt but only for a few seconds). The contrast agent (Optison) is a safe substance that is widely used for similar purposes and usually has no noticeable effects. Adenosine and Dobutamine are also widely used drugs with which we have extensive experience. Adenosine can cause brief feelings of flushing, faintness, wheeziness, or shortness of breath and can slow the heart rate temporarily but has no lasting effects. It cannot be given to Asthmatics or patients with certain types of heart rate problems – so we will check with you first that you can be given the drug. Dobutamine can cause brief sensations of tingling or flushing in the skin, dizziness, palpitations (feeling of the heart racing), and can cause the blood pressure to fluctuate during the test, but these effects are completely gone within a few minutes of stopping the test. It is possible but very unusual for people to have an allergic reaction to Adenosine, Dobutamine, or the contrast agent. It is also possible, although extremely unlikely, that the insertion of a needle into a vein could introduce infection.

IT IS ESSENTIAL FOR YOU TO UNDERSTAND THAT ANY TREATMENTS YOU NEED WILL BE GIVEN AS USUAL. THIS STUDY DOES NOT PREVENT YOUR DOCTORS FROM DECIDING WHAT IS BEST FOR YOU AND THEN GOING AHEAD WITH THE TREATMENT.

What does being a subject involve?

If you take part in our study, you will undergo the following:

1. Brief interview about your symptoms and a physical examination
2. Insertion of two small needles into your arm followed by MCE (echocardiogram, plus injection of Adenosine and Optison through the needles)
3. Insertion of a needle into your arm followed by DSE (echocardiogram, plus injection of Dobutamine through the needle).

The interview and examination will take approximately 10 minutes. The MCE and DSE tests will take approximately 60 minutes each and will be done on separate days. It is anticipated that these tests could be started within 2 weeks of you agreeing to take part in the study.

b. Sample patient information sheet 2 (Real time Coherent Contrast Imaging™).

MYOCARDIAL CONTRAST ECHOCARDIOGRAPHY (MCE) AND STRESS ECHOCARDIOGRAPHY

We would like to invite you to take part in this study. It is entirely voluntary.

What is myocardial contrast echocardiography (MCE)?
MCE is a technique for studying blood supply to heart muscle. It involves having an echocardiogram (ultrasound picture of the heart) at the same time as injection of a contrast agent (Optison) and a drug called Dobutamine. These substances are injected through small needles in an arm vein. You may already have been referred for a Dobutamine Stress Echocardiogram (DSE) test by your consultant. A DSE test will be incorporated into our study.

Why are we undertaking this research?
We believe that MCE could provide an important insight into the nature of coronary artery disease. We would like to compare the accuracy of information gained by MCE with other tests for coronary artery disease such as Dobutamine Stress Echocardiography and Coronary Angiography.

How could you be affected by the test?
The echocardiogram is painless and requires the patient to lie on a couch for about 30 minutes. Minor discomfort may occur on the chest wall where the probe is placed. Two needles will be inserted into a vein in the arm (like having a blood test – it can hurt but only for a few seconds). The contrast agent (Optison) is a safe substance that is widely used for similar purposes and usually has no noticeable effects. Dobutamine is also a widely used drug with which we have extensive experience. It can cause brief sensations of tingling or flushing in the skin, dizziness, palpitations (feeling of the heart racing), and can cause the blood pressure to fluctuate during the test, but these effects are completely gone within a few minutes of stopping the test. It is possible but very unusual for people to have an allergic reaction to Dobutamine or the contrast agent. It is also possible, although extremely unlikely, that the insertion of a needle into a vein could introduce infection.

IT IS ESSENTIAL FOR YOU TO UNDERSTAND THAT ANY TREATMENTS YOU NEED WILL BE GIVEN AS USUAL. THIS STUDY DOES NOT PREVENT YOUR DOCTORS FROM DECIDING WHAT IS BEST FOR YOU AND THEN GOING AHEAD WITH THE TREATMENT.

What does being a subject involve?
If you take part in our study, you will undergo the following:

1. Brief interview about your symptoms and a physical examination
2. Insertion of two small needles into your arm followed by combined MCE and DSE (echocardiogram, plus injection of Dobutamine and Optison through the needles)

The interview and examination will take approximately 10 minutes. The MCE and DSE test will take approximately 60 minutes. It is anticipated that this tests could be started within 2 weeks of you agreeing to take part in the study.

3. CONSENT FORMS

CONSENT FORM FOR MYOCARDIAL CONTRAST ECHOCARDIOGRAPHY STUDIES AT THE ROYAL FREE HOSPITAL

PATIENT ....
DATE OF BIRTH ....
RESEARCH NUMBER...................HOSPITAL NUMBER...................
SEX.....M.../...F ....

DOCTOR:

MYOCARDIAL CONTRAST ECHO AND DOBUTAMINE STRESS ECHO

I confirm that I have explained the above examination and any likely risks associated with it in terms which, in my judgement, are understandable by the patient. I have explained that this examination is part of clinical research and will not hinder any necessary treatments or investigations.

SIGNATURE...DATE ....
NAME...

SUBJECT:

Please read this form and the attached information sheet carefully.
1. If you do not understand anything or if you would like more information please ask the Doctor.
2. Please check that all the information on the form is correct.
3. If you are happy with the information given and are willing to take part in this study, please sign the form below.

I am the above named individual.

I understand the procedure above and consent to being recruited as a subject for the study specified above.

I understand that I can withdraw from the study at any time.

I understand that my usual treatments will continue regardless of the study.

SIGNATURE .... DATE ....
NAME ....
ADDRESS ....

APPENDIX THREE

PUBLICATIONS AND PRESENTATIONS

PEER REVIEWED JOURNAL ARTICLE

EB Roberts, F Schafer, W Akhtar, D Patel, TR Evans, JG Coghlan, DP Lipkin, JI Davar. Real-time myocardial contrast dobutamine stress echocardiography in coronary stenosis. Original research article, accepted for publication in the International Journal of Cardiology, 19th August 2005. Available online 9th December 2005.

PUBLISHED ABSTRACTS

1. EB Roberts, F Schafer, W Akhtar, D Patel, TR Evans, JG Coghlan, DP Lipkin, JI Davar. Regional dynamics of myocardial vascular bed contrast replenishment after destructive ultrasound pulses: lessons for quantitative myocardial perfusion assessment. European Journal of Echocardiography 2002;3(Supplement 1): No 349.

2. EB Roberts, W Akhtar, F Schafer, TR Evans, JG Coghlan, DP Lipkin, JI Davar. Assessment of single or double vessel coronary artery disease with real time myocardial perfusion imaging. European Journal of Echocardiography 2001;2(Supplement A): No. 113.

3. EB Roberts, DP Lipkin, JG Coghlan, TR Evans, JI Davar. Adenosine Myocardial Contrast versus Dobutamine Stress Echocardiography for Assessment of Coronary Artery Disease. Heart 2001;85(Supplement 1):No. 87 pp.27.

PRESENTATIONS

1. Regional dynamics of myocardial vascular bed contrast replenishment after destructive ultrasound pulses: lessons for quantitative myocardial perfusion assessment. EB Roberts, F Schafer, W Akhtar, D Patel, TR Evans, JG Coghlan, DP Lipkin, JI Davar. Oral presentation, Euroecho VI, Munich, Germany, December 2002 (publication details 1. above).

2. Assessment of single or double vessel coronary artery disease with real time myocardial perfusion imaging. EB Roberts, W Akhtar, F Schafer, TR Evans, JG Coghlan, DP Lipkin, JI Davar. Poster presentation, Euroecho V, Nice, France, December 2001 (publication details 2. above).

3. Wall motion and perfusion assessment using real-time myocardial contrast dobutamine stress echocardiography. EB Roberts, W Akhtar, F Schafer, TR Evans, JG Coghlan, DP Lipkin, JI Davar. Oral presentation, 10th Annual Scientific and Clinical Meeting of the British Society of Echocardiography, Birmingham, UK, October 2001.

4. Adenosine Myocardial Contrast versus Dobutamine Stress Echocardiography for Assessment of Coronary Artery Disease. EB Roberts, DP Lipkin, JG Coghlan, TR Evans, JI Davar. Oral presentation, Annual Scientific Conference of the British Cardiac Society, Manchester, UK, April 2001 (publication details 3. above).

APPENDIX FOUR

REFERENCES

1. Peterson S, Peto V, Scarborough P, Rayner M. CHD 2005: Mortality. In: *Coronary Heart Disease Statistics*. 13 ed. London: British Heart Foundation; 2005.

2. Peterson S, Peto V, Scarborough P, Rayner M. CHD 2005: Morbidity. In: *Coronary Heart Disease Statistics*. 13 ed. London: British Heart Foundation; 2005.

3. Department of Heath. Winning the war on heart disease. In: *National Service Framework for Coronary Heart Disease: Progress report 2004*. London: Department of Health, Her Majesty's Government, United Kingdom; 2004.

4. Heberden W. Some account of a disorder of the breast. In: *Royal College of Physicians of London. Medical transactions*. London; 1772:59-67.

5. Tresch DD, Alla HR. Diagnosis and management of myocardial ischemia (angina) in the elderly patient. *Am J Geriatr Cardiol*. 2001;10:337-44.

6. Ting HH, Lee TH, Soukup JR, Cook EF, Tosteson AN, Brand DA, Rouan GW, Goldman L. Impact of physician experience on triage of emergency room patients with acute chest pain at three teaching hospitals. *Am J Med*. 1991;91:401-8.

7. Berger JP, Buclin T, Haller E, Van Melle G, Yersin B. Right arm involvement and pain extension can help to differentiate coronary diseases from chest pain of other origin: a prospective emergency ward study of 278 consecutive patients admitted for chest pain. *J Intern Med*. 1990;227:165-72.

8.   Gregoire J, Theroux P. Detection and assessment of unstable angina using

        myocardial perfusion imaging: comparison between technetium-99m

        sestamibi SPECT and 12-lead electrocardiogram. *Am J Cardiol.*

        1990;66:42E-46E.

9.   Mirvis DM, el-Zeky F, Vander Zwaag R, Ramanathan KB, Crenshaw JH,

        Kroetz FW, Sullivan JM. Clinical and pathophysiologic correlates of ST-T-

        wave abnormalities in coronary artery disease. *Am J Cardiol.* 1990;66:699-

        704.

10.   Norell M, Lythall D, Coghlan G, Cheng A, Kushwaha S, Swan J, Ilsley C,

        Mitchell A. Limited value of the resting electrocardiogram in assessing

        patients with recent onset chest pain: lessons from a chest pain clinic. *Br

        Heart J.* 1992;67:53-6.

11.   Department of Health. Appendix A: Examples of models of care. In: *National

        Service Frameworks. Coronary Heart Disease - Chapter Three: Heart

        attacks & other acute coronary syndromes.*: Department of Health, Her

        Majesty's Government, United Kingdom; 2000.

12.   Bruce RA, Hornsten TR. Exercise stress testing in evaluation of patients with

        ischemic heart disease. *Prog Cardiovasc Dis.* 1969;11:371-90.

13.   Froelicher VF, Lehmann KG, Thomas R, Goldman S, Morrison D, Edson R,

        Lavori P, Myers J, Dennis C, Shabetai R, Do D, Froning J. The

        electrocardiographic exercise test in a population with reduced workup bias:

        diagnostic performance, computerized interpretation, and multivariable

        prediction. Veterans Affairs Cooperative Study in Health Services #016

        (QUEXTA) Study Group. Quantitative Exercise Testing and Angiography.

        Ann Intern Med. 1998;128:965-74.

14. Tavel ME, Shaar C. Relation between the electrocardiographic stress test and degree and location of myocardial ischemia. *Am J Cardiol.* 1999;84:119-24.

15. Bartel AG, Behar VS, Peter RH, Orgain ES, Kong Y. Graded exercise stress tests in angiographically documented coronary artery disease. *Circulation.* 1974;49:348-56.

16. McHenry PL, Phillips JF, Knoebel SB. Correlation of computer-quantitated treadmill exercise electrocardiogram with arteriographic location of coronary artery disease. *Am J Cardiol.* 1972;30:747-52.

17. Gianrossi R, Detrano R, Mulvihill D, Lehmann K, Dubach P, Colombo A, McArthur D, Froelicher V. Exercise-induced ST depression in the diagnosis of coronary artery disease. A meta-analysis. *Circulation.* 1989;80:87-98.

18. Riley CP, Oberman A, Lampton TD, Hurst DC. Submaximal exercise testing in a random sample of an elderly population. *Circulation.* 1970;42:43-52.

19. Duprez DA. Angina in the elderly. *Eur Heart J.* 1996;17 Suppl G:8-13.

20. Fleg JL. Angina pectoris in the elderly. *Cardiol Clin.* 1991;9:177-87.

21. Kwok Y, Kim C, Grady D, Segal M, Redberg R. Meta-analysis of exercise testing to detect coronary artery disease in women. *Am J Cardiol.* 1999;83:660-6.

22. Dunn RF, Freedman B, Bailey IK, Uren RF, Kelly DT. Localization of coronary artery disease with exercise electrocardiography: correlation wit thallium-201 myocardial perfusion scanning. *Am J Cardiol.* 1981;48:837-43.

23. Fox RM, Hakki AH, Iskandrian AS. Relation between electrocardiographic and scintigraphic location of myocardial ischemia during exercise in one-vessel coronary artery disease. *Am J Cardiol.* 1984;53:1529-31.

24.   Mark DB, Hlatky MA, Lee KL, Harrell FE, Jr., Califf RM, Pryor DB.

        Localizing coronary artery obstructions with the exercise treadmill test. *Ann*

        Intern Med. 1987;106:53-5.

25.   Michaelides AP, Psomadaki ZD, Dilaveris PE, Richter DJ, Andrikopoulos

        GK, Aggeli KD, Stefanadis CI, Toutouzas PK. Improved detection of

        coronary artery disease by exercise electrocardiography with the use of right

        precordial leads. *N Engl J Med.* 1999;340:340-5.

26.   Michaelides AP, Psomadaki ZD, Richter DJ, Dilaveris PE, Andrikopoulos

        GK, Kakaidis S, Stefanadis C, Gialafos JE, Toutouzas PK. Exercise-induced

        ST-segment changes in lead V1 identify the significantly narrowed coronary

        artery in patients with single-vessel disease: correlation with thallium-201

        scintigraphy and coronary arteriography data. *J Electrocardiol.* 1999;32:7-14.

27.   Nordstrom-Ohrberg G. Effect of digitalis glycosides on electrocardiogram

        and exercise test in healthy subjects. *Acta Med Scand.* 1964;24:1-75.

28.   Sketch MH, Mooss AN, Butler ML, Nair CK, Mohiuddin SM. Digoxin-

        induced positive exercise tests: their clinical and prognostic significance. *Am*

        J Cardiol. 1981;48:655-9.

29.   Georgeopoulos AJ, Proudfit WL, Page IH. Effect of exercise on the

        elctrocardiograms of patients with low serum potassium. *Circulation.*

        1961;23:567-572.

30.   Soloff LA, Fewell JW. Abnormal electrocardiographic responses in exercise

        in subjects with hypokalemia. *American Journal of Medical Science.*

        1961;242:724-728.

31. Mattingly TW. The postexercise electrocardiogram: its value in the diagnosis and prognosis of coronary arterial disease. *American Journal of Cardiology.* 1962;9:395-409.

32. Roitman D, Jones WB, Sheffield LT. Comparison of submaximal exercise ECG test with coronary cineangiocardiogram. *Ann Intern Med.* 1970;72:641-7.

33. Smith RH, LePetri B, Moisa RB, Studzinski M, Flaster E, Steingart RM. Association of increased left ventricular mass in the absence of electrocardiographic left ventricular hypertrophy with ST depression during exercise. *Am J Cardiol.* 1995;76:973-4.

34. Engel PJ, Alpert BL, Hickman JR, Jr. The nature and prevalence of the abnormal exercise electrocardiogram in mitral valve prolapse. *Am Heart J.* 1979;98:716-24.

35. Gardin JM, Isner JM, Ronan JA, Jr., Fox SM, 3rd. Pseudoischemic "false positive" S-T segment changes induced by hyperventilation in patients with mitral valve prolapse. *Am J Cardiol.* 1980;45:952-8.

36. Feil H, Brofman BL. The effects of exercise on the electrocardiogram of bundle branch block. *American Heart Journal.* 1953;45:665-669.

37. Kattus AA. Exercise electrocardiography: recognition of the ischemic response, false positive and negative patterns. *Am J Cardiol.* 1974;33:721-31.

38. Bruce RA, DeRouen TA, Hossack KF. Value of maximal exercise tests in risk assessment of primary coronary heart disease events in healthy men. Five years' experience of the Seattle heart watch study. *Am J Cardiol.* 1980;46:371-8.

39.   Froelicher VF, Jr., Thomas MM, Pillow C, Lancaster MC. Epidemiologic

         study of asymptomatic men screened by maximal treadmill testing for latent

         coronary artery disease. *Am J Cardiol.* 1974;34:770-6.

40.   Giagnoni E, Secchi MB, Wu SC, Morabito A, Oltrona L, Mancarella S,

         Volpin N, Fossa L, Bettazzi L, Arangio G, et al. Prognostic value of exercise

         EKG testing in asymptomatic normotensive subjects. A prospective matched

         study. *N Engl J Med.* 1983;309:1085-9.

41.   McHenry PL, O'Donnell J, Morris SN, Jordan JJ. The abnormal exercise

         electrocardiogram in apparently healthy men: a predictor of angina pectoris

         as an initial coronary event during long-term follow-up. *Circulation.*

         1984;70:547-51.

42.   Doyle JT, Kinch SH. The prognosis of an abnormal electrocardiographic

         stress test. *Circulation.* 1970;41:545-53.

43.   Ellestad MH, Wan MK. Predictive implications of stress testing. Follow-up

         of 2700 subjects after maximum treadmill stress testing. *Circulation.*

         1975;51:363-9.

44.   Rautaharju PM, Prineas RJ, Eifler WJ, Furberg CD, Neaton JD, Crow RS,

         Stamler J, Cutler JA. Prognostic value of exercise electrocardiogram in men

         at high risk of future coronary heart disease: Multiple Risk Factor

         Intervention Trial experience. *J Am Coll Cardiol.* 1986;8:1-10.

45.   Mark DB, Shaw L, Harrell FE, Jr., Hlatky MA, Lee KL, Bengtson JR,

         McCants CB, Califf RM, Pryor DB. Prognostic value of a treadmill exercise

         score in outpatients with suspected coronary artery disease. *N Engl J Med.*

         1991;325:849-53.

46. Chatziioannou SN, Moore WH, Ford PV, Fisher RE, Lee VV, Alfaro-Franco C, Dhekne RD. Prognostic value of myocardial perfusion imaging in patients with high exercise tolerance. *Circulation.* 1999;99:867-72.

47. Roger VL, Jacobsen SJ, Pellikka PA, Miller TD, Bailey KR, Gersh BJ. Prognostic value of treadmill exercise testing: a population-based study in Olmsted County, Minnesota. *Circulation.* 1998;98:2836-41.

48. Froelicher V, Morrow K, Brown M, Atwood E, Morris C. Prediction of atherosclerotic cardiovascular death in men using a prognostic score. *Am J Cardiol.* 1994;73:133-8.

49. Mahmarian JJ, Boyce TM, Goldberg RK, Cocanougher MK, Roberts R, Verani MS. Quantitative exercise thallium-201 single photon emission computed tomography for the enhanced diagnosis of ischemic heart disease. *J Am Coll Cardiol.* 1990;15:318-29.

50. Van Train KF, Maddahi J, Berman DS, Kiat H, Areeda J, Prigent F, Friedman J. Quantitative analysis of tomographic stress thallium-201 myocardial scintigrams: a multicenter trial. *J Nucl Med.* 1990;31:1168-79.

51. Kiat H, Maddahi J, Roy LT, Van Train K, Friedman J, Resser K, Berman DS. Comparison of technetium 99m methoxy isobutyl isonitrile and thallium 201 for evaluation of coronary artery disease by planar and tomographic methods. *Am Heart J.* 1989;117:1-11.

52. Hendel RC, McSherry B, Karimeddini M, Leppo JA. Diagnostic value of a new myocardial perfusion agent, teboroxime (SO 30,217), utilizing a rapid planar imaging protocol: preliminary results. *J Am Coll Cardiol.* 1990;16:855-61.

53. Fleming RM, Kirkeeide RL, Taegtmeyer H, Adyanthaya A, Cassidy DB, Goldstein RA. Comparison of technetium-99m teboroxime tomography with automated quantitative coronary arteriography and thallium-201 tomographic imaging. *J Am Coll Cardiol*. 1991;17:1297-302.

54. Tamaki N, Yonekura Y, Senda M, Yamashita K, Koide H, Saji H, Hashimoto T, Fudo T, Kambara H, Kawai C, et al. Value and limitation of stress thallium-201 single photon emission computed tomography: comparison with nitrogen-13 ammonia positron tomography. *J Nucl Med*. 1988;29:1181-8.

55. Demer LL, Gould KL, Goldstein RA, Kirkeeide RL. Noninvasive assessment of coronary collaterals in man by PET perfusion imaging. *J Nucl Med*. 1990;31:259-70.

56. Maisey MN, Mistry R, Sowton E. Planar imaging techniques used with technetium-99m sestamibi to evaluate chronic myocardial ischemia. *Am J Cardiol*. 1990;66:47E-54E.

57. Maddahi J, Garcia EV, Berman DS, Waxman A, Swan HJ, Forrester J. Improved noninvasive assessment of coronary artery disease by quantitative analysis of regional stress myocardial distribution and washout of thallium-201. *Circulation*. 1981;64:924-35.

58. Gerson MC, Thomas SR, Van Heertum RL. Tomographic myocardial perfusion imaging. In: Gerson MC, ed. *Cardiac Nuclear Medicine*. New York, NY: McGraw-Hill Inc; 1991:25-52.

59. Mahmarian JJ, Verani MS. Exercise thallium-201 perfusion scintigraphy in the assessment of coronary artery disease. *Am J Cardiol*. 1991;67:2D-11D.

60. Caldwell JH, Williams DL, Hamilton GW, Ritchie JL, Harp GD, Eisner RL, Gullberg GT, Nowak DJ. Regional distribution of myocardial blood flow

measured by single-photon emission tomography: comparison with in vitro counting. *J Nucl Med.* 1982;23:490-5.

61. Tamaki N, Yonekura Y, Mukai T, Kodama S, Kadota K, Kambara H, Kawai C, Torizuka K. Stress thallium-201 transaxial emission computed tomography: quantitative versus qualitative analysis for evaluation of coronary artery disease. *J Am Coll Cardiol.* 1984;4:1213-21.

62. DePasquale EE, Nody AC, DePuey EG, Garcia EV, Pilcher G, Bredlau C, Roubin G, Gober A, Gruentzig A, D'Amato P, et al. Quantitative rotational thallium-201 tomography for identifying and localizing coronary artery disease. *Circulation.* 1988;77:316-27.

63. Iskandrian AS, Heo J, Kong B, Lyons E. Effect of exercise level on the ability of thallium-201 tomographic imaging in detecting coronary artery disease: analysis of 461 patients. *J Am Coll Cardiol.* 1989;14:1477-86.

64. Zaret BL, Wackers FJT, Soufer R. Nuclear cardiology. In: Braunwald E, ed. *Heart Disease.* Philadelphia, Pa: WB Saunders; 1992:276-311.

65. Garcia E, Maddahi J, Berman D, Waxman A. Space/time quantitation of thallium-201 myocardial scintigraphy. *J Nucl Med.* 1981;22:309-17.

66. Kaul S, Boucher CA, Newell JB, Chesler DA, Greenberg JM, Okada RD, Strauss HW, Dinsmore RE, Pohost GM. Determination of the quantitative thallium imaging variables that optimize detection of coronary artery disease. *J Am Coll Cardiol.* 1986;7:527-37.

67. Nishimura S, Mahmarian JJ, Verani MS. Significance of increased lung thallium uptake during adenosine thallium-201 scintigraphy. *J Nucl Med.* 1992;33:1600-7.

68. Weiss AT, Berman DS, Lew AS, Nielsen J, Potkin B, Swan HJ, Waxman A, Maddahi J. Transient ischemic dilation of the left ventricle on stress thallium-201 scintigraphy: a marker of severe and extensive coronary artery disease. *J Am Coll Cardiol.* 1987;9:752-9.

69. Fintel DJ, Links JM, Brinker JA, Frank TL, Parker M, Becker LC. Improved diagnostic performance of exercise thallium-201 single photon emission computed tomography over planar imaging in the diagnosis of coronary artery disease: a receiver operating characteristic analysis. *J Am Coll Cardiol.* 1989;13:600-12.

70. Kiat H, Berman DS, Maddahi J. Comparison of planar and tomographic exercise thallium-201 imaging methods for the evaluation of coronary artery disease. *J Am Coll Cardiol.* 1989;13:613-6.

71. Maddahi J, Abdulla A, Garcia EV, Swan HJ, Berman DS. Noninvasive identification of left main and triple vessel coronary artery disease: improved accuracy using quantitative analysis of regional myocardial stress distribution and washout of thallium-201. *J Am Coll Cardiol.* 1986;7:53-60.

72. Rehn T, Griffith LS, Achuff SC, Bailey IK, Bulkley BH, Burow R, Pitt B, Becker LC. Exercise thallium-201 myocardial imaging in left main coronary artery disease: sensitive but not specific. *Am J Cardiol.* 1981;48:217-23.

73. Nygaard TW, Gibson RS, Ryan JM, Gascho JA, Watson DD, Beller GA. Prevalence of high-risk thallium-201 scintigraphic findings in left main coronary artery stenosis: comparison with patients with multiple- and single-vessel coronary artery disease. *Am J Cardiol.* 1984;53:462-9.

74. Christian TF, Miller TD, Bailey KR, Gibbons RJ. Noninvasive identification of severe coronary artery disease using exercise tomographic thallium-201 imaging. *Am J Cardiol.* 1992;70:14-20.

75. Hadjimiltiades S, Watson R, Hakki AH, Heo J, Iskandrian AS. Relation between myocardial thallium-201 kinetics during exercise and quantitative coronary angiography in patients with one vessel coronary artery disease. *J Am Coll Cardiol.* 1989;13:1301-8.

76. Mahmarian JJ, Pratt CM, Boyce TM, Verani MS. The variable extent of jeopardized myocardium in patients with single vessel coronary artery disease: quantification by thallium-201 single photon emission computed tomography. *J Am Coll Cardiol.* 1991;17:355-62.

77. Matzer L, Kiat H, Van Train K, Germano G, Papanicolaou M, Silagan G, Eigler N, Maddahi J, Berman DS. Quantitative severity of stress thallium-201 myocardial perfusion single-photon emission computed tomography defects in one-vessel coronary artery disease. *Am J Cardiol.* 1993;72:273-9.

78. White CW, Wright CB, Doty DB, Hiratza LF, Eastham CL, Harrison DG, Marcus ML. Does visual interpretation of the coronary arteriogram predict the physiologic importance of a coronary stenosis? *N Engl J Med.* 1984;310:819-24.

79. Marcus ML, Skorton DJ, Johnson MR, Collins SM, Harrison DG, Kerber RE. Visual estimates of percent diameter coronary stenosis: "a battered gold standard". *J Am Coll Cardiol.* 1988;11:882-5.

80. Brown KA, Boucher CA, Okada RD, Guiney TE, Newell JB, Strauss HW, Pohost GM. Prognostic value of exercise thallium-201 imaging in patients presenting for evaluation of chest pain. *J Am Coll Cardiol.* 1983;1:994-1001.

81. Ladenheim ML, Pollock BH, Rozanski A, Berman DS, Staniloff HM, Forrester JS, Diamond GA. Extent and severity of myocardial hypoperfusion as predictors of prognosis in patients with suspected coronary artery disease. *J Am Coll Cardiol*. 1986;7:464-71.

82. Hendel RC, Layden JJ, Leppo JA. Prognostic value of dipyridamole thallium scintigraphy for evaluation of ischemic heart disease. *J Am Coll Cardiol*. 1990;15:109-16.

83. Verani MS, Marcus ML, Razzak MA, Ehrhardt JC. Sensitivity and specificity of thallium-201 perfusion scintigrams under exercise in the diagnosis of coronary artery disease. *J Nucl Med*. 1978;19:773-82.

84. Osbakken MD, Okada RD, Boucher CA, Strauss HW, Pohost GM. Comparison of exercise perfusion and ventricular function imaging: an analysis of factors affecting the diagnostic accuracy of each technique. *J Am Coll Cardiol*. 1984;3:272-83.

85. Braat SH, Brugada P, Bar FW, Gorgels AP, Wellens HJ. Thallium-201 exercise scintigraphy and left bundle branch block. *Am J Cardiol*. 1985;55:224-6.

86. Hirzel HO, Senn M, Nuesch K, Buettner C, Pfeiffer A, Hess OM, Krayenbuehl HP. Thallium-201 scintigraphy in complete left bundle branch block. *Am J Cardiol*. 1984;53:764-9.

87. DePuey EG, Guertler-Krawczynska E, Robbins WL. Thallium-201 SPECT in coronary artery disease patients with left bundle branch block. *J Nucl Med*. 1988;29:1479-85.

88. Burns RJ, Galligan L, Wright LM, Lawand S, Burke RJ, Gladstone PJ. Improved specificity of myocardial thallium-201 single-photon emission

computed tomography in patients with left bundle branch block by

dipyridamole. *Am J Cardiol.* 1991;68:504-8.

89.   O'Keefe JH, Jr., Bateman TM, Silvestri R, Barnhart C. Safety and diagnostic

accuracy of adenosine thallium-201 scintigraphy in patients unable to

exercise and those with left bundle branch block. *Am Heart J.* 1992;124:614-

21.

90.   Stary HC. The development of calcium deposits in atherosclerotic lesions and

their persistence after lipid regression. *Am J Cardiol.* 2001;88:16E-19E.

91.   Schmermund A, Erbel R. Unstable coronary plaque and its relation to

coronary calcium. *Circulation.* 2001;104:1682-7.

92.   Agatston AS, Janowitz WR, Hildner FJ, Zusmer NR, Viamonte M, Jr.,

Detrano R. Quantification of coronary artery calcium using ultrafast

computed tomography. *J Am Coll Cardiol.* 1990;15:827-32.

93.   Callister TQ, Cooil B, Raya SP, Lippolis NJ, Russo DJ, Raggi P. Coronary

artery disease: improved reproducibility of calcium scoring with an electron-

beam CT volumetric method. *Radiology.* 1998;208:807-14.

94.   O'Rourke RA, Brundage BH, Froelicher VF, Greenland P, Grundy SM,

Hachamovitch R, Pohost GM, Shaw LJ, Weintraub WS, Winters WL, Jr.,

Forrester JS, Douglas PS, Faxon DP, Fisher JD, Gregoratos G, Hochman JS,

Hutter AM, Jr., Kaul S, Wolk MJ. American College of Cardiology/American

Heart Association Expert Consensus document on electron-beam computed

tomography for the diagnosis and prognosis of coronary artery disease.

Circulation. 2000;102:126-40.

95.   Wayhs R, Zelinger A, Raggi P. High coronary artery calcium scores pose an

extremely elevated risk for hard events. *J Am Coll Cardiol.* 2002;39:225-30.

96.   Schroeder S, Kopp AF, Baumbach A, Meisner C, Kuettner A, Georg C,

       Ohnesorge B, Herdeg C, Claussen CD, Karsch KR. Noninvasive detection

       and evaluation of atherosclerotic coronary plaques with multislice computed

       tomography. *J Am Coll Cardiol.* 2001;37:1430-5.

97.   Becker CR, Ohnesorge BM, Schoepf UJ, Reiser MF. Current development of

       cardiac imaging with multidetector-row CT. *Eur J Radiol.* 2000;36:97-103.

98.   Achenbach S, Moshage W, Ropers D, Nossen J, Daniel WG. Value of

       electron-beam computed tomography for the noninvasive detection of high-

       grade coronary-artery stenoses and occlusions. *N Engl J Med.*

       1998;339:1964-71.

99.   Budoff MJ, Oudiz RJ, Zalace CP, Bakhsheshi H, Goldberg SL, French WJ,

       Rami TG, Brundage BH. Intravenous three-dimensional coronary

       angiography using contrast enhanced electron beam computed tomography.

       Am J Cardiol. 1999;83:840-5.

100.   Achenbach S, Giesler T, Ropers D, Ulzheimer S, Derlien H, Schulte C,

       Wenkel E, Moshage W, Bautz W, Daniel WG, Kalender WA, Baum U.

       Detection of coronary artery stenoses by contrast-enhanced, retrospectively

       electrocardiographically-gated, multislice spiral computed tomography.

       Circulation. 2001;103:2535-8.

101.   Knez A, Becker CR, Leber A, Ohnesorge B, Becker A, White C, Haberl R,

       Reiser MF, Steinbeck G. Usefulness of multislice spiral computed

       tomography angiography for determination of coronary artery stenoses. *Am J

       Cardiol.* 2001;88:1191-4.

102. Manning WJ, Li W, Edelman RR. A preliminary report comparing magnetic resonance coronary angiography with conventional angiography. *N Engl J Med*. 1993;328:828-32.

103. Post JC, van Rossum AC, Hofman MB, de Cock CC, Valk J, Visser CA. Clinical utility of two-dimensional magnetic resonance angiography in detecting coronary artery disease. *Eur Heart J*. 1997;18:426-33.

104. Pennell DJ, Bogren HG, Keegan J, Firmin DN, Underwood SR. Assessment of coronary artery stenosis by magnetic resonance imaging. *Heart*. 1996;75:127-33.

105. Post JC, van Rossum AC, Hofman MB, Valk J, Visser CA. Three-dimensional respiratory-gated MR angiography of coronary arteries: comparison with conventional coronary angiography. *AJR Am J Roentgenol*. 1996;166:1399-404.

106. Muller MF, Fleisch M, Kroeker R, Chatterjee T, Meier B, Vock P. Proximal coronary artery stenosis: three-dimensional MRI with fat saturation and navigator echo. *J Magn Reson Imaging*. 1997;7:644-51.

107. van Geuns RJ, de Bruin HG, Rensing BJ, Wielopolski PA, Hulshoff MD, van Ooijen PM, Oudkerk M, de Feyter PJ. Magnetic resonance imaging of the coronary arteries: clinical results from three dimensional evaluation of a respiratory gated technique. *Heart*. 1999;82:515-9.

108. Kessler W, Achenbach S, Moshage W, Zink D, Kroeker R, Nitz W, Laub G, Bachmann K. Usefulness of respiratory gated magnetic resonance coronary angiography in assessing narrowings > or = 50% in diameter in native coronary arteries and in aortocoronary bypass conduits. *Am J Cardiol*. 1997;80:989-93.

109.   Sandstede JJ, Pabst T, Beer M, Geis N, Kenn W, Neubauer S, Hahn D.

Three-dimensional MR coronary angiography using the navigator technique

compared with conventional coronary angiography. *AJR Am J Roentgenol.*

1999;172:135-9.

110.   Sardanelli F, Molinari G, Zandrino F, Balbi M. Three-dimensional,

navigator-echo MR coronary angiography in detecting stenoses of the major

epicardial vessels, with conventional coronary angiography as the standard of

reference. *Radiology.* 2000;214:808-14.

111.   Nikolaou K, Huber A, Knez A, Scheidler J, Petsch R, Reiser M. Navigator

echo-based respiratory gating for three-dimensional MR coronary

angiography: reduction of scan time using a slice interpolation technique. *J

Comput Assist Tomogr.* 2001;25:378-87.

112.   Huber A, Nikolaou K, Gonschior P, Knez A, Stehling M, Reiser M.

Navigator echo-based respiratory gating for three-dimensional MR coronary

angiography: results from healthy volunteers and patients with proximal

coronary artery stenoses. *AJR Am J Roentgenol.* 1999;173:95-101.

113.   Gonschior P, Pragst I, Valassis G, Vogel-Wiens C, Huber A. High-resolution

MR angiography: results in diseased arteries. *J Invasive Cardiol.*

2001;13:151-7; discussion 158-70.

114.   Kim WY, Danias PG, Stuber M, Flamm SD, Plein S, Nagel E, Langerak SE,

Weber OM, Pedersen EM, Schmidt M, Botnar RM, Manning WJ. Coronary

magnetic resonance angiography for the detection of coronary stenoses. *N

Engl J Med.* 2001;345:1863-9.

115.   Regenfus M, Ropers D, Achenbach S, Kessler W, Laub G, Daniel WG,

Moshage W. Noninvasive detection of coronary artery stenosis using

contrast-enhanced three-dimensional breath-hold magnetic resonance coronary angiography. *J Am Coll Cardiol.* 2000;36:44-50.

116. van Geuns RJ, Wielopolski PA, de Bruin HG, Rensing BJ, Hulshoff M, van Ooijen PM, de Feyter PJ, Oudkerk M. MR coronary angiography with breath-hold targeted volumes: preliminary clinical results. *Radiology.* 2000;217:270-7.

117. Giorgi B, Dymarkowski S, Maes F, Kouwenhoven M, Bogaert J. Improved visualization of coronary arteries using a new three-dimensional submillimeter MR coronary angiography sequence with balanced gradients. *AJR Am J Roentgenol.* 2002;179:901-10.

118. Nesto RW, Kowalchuk GJ. The ischemic cascade: temporal sequence of hemodynamic, electrocardiographic and symptomatic expressions of ischemia. *Am J Cardiol.* 1987;59:23C-30C.

119. Alam M, Khaja F, Brymer J, Marzelli M, Goldstein S. Echocardiographic evaluation of left ventricular function during coronary artery angioplasty. *Am J Cardiol.* 1986;57:20-5.

120. Tennant R, Wiggers C, J. The effect of coronary occlusion on myocardial contraction. *American Journal of Physiology.* 1935:351-361.

121. Marwick TH, Nemec JJ, Pashkow FJ, Stewart WJ, Salcedo EE. Accuracy and limitations of exercise echocardiography in a routine clinical setting. *J Am Coll Cardiol.* 1992;19:74-81.

122. Maurer G, Nanda NC. Two dimensional echocardiographic evaluation of exercise-induced left and right ventricular asynergy: correlation with thallium scanning. *Am J Cardiol.* 1981;48:720-7.

123. Limacher MC, Quinones MA, Poliner LR, Nelson JG, Winters WL, Jr.,
      Waggoner AD. Detection of coronary artery disease with exercise two-
      dimensional echocardiography. Description of a clinically applicable method
      and comparison with radionuclide ventriculography. *Circulation.*
      1983;67:1211-8.

124. Sawada SG, Ryan T, Fineberg NS, Armstrong WF, Judson WE, McHenry
      PL, Feigenbaum H. Exercise echocardiographic detection of coronary artery
      disease in women. *J Am Coll Cardiol.* 1989;14:1440-7.

125. Mertes H, Erbel R, Nixdorff U, Mohr-Kahaly S, Wolfinger D, Meyer J.
      [Stress echocardiography: a sensitive method in diagnosis of coronary heart
      disease]. *Herz.* 1991;16:355-66.

126. Quinones MA, Verani MS, Haichin RM, Mahmarian JJ, Suarez J, Zoghbi
      WA. Exercise echocardiography versus 201Tl single-photon emission
      computed tomography in evaluation of coronary artery disease. Analysis of
      292 patients. *Circulation.* 1992;85:1026-31.

127. Hecht HS, DeBord L, Shaw R, Dunlap R, Ryan C, Stertzer SH, Myler RK.
      Digital supine bicycle stress echocardiography: a new technique for
      evaluating coronary artery disease. *J Am Coll Cardiol.* 1993;21:950-6.

128. Ryan T, Segar DS, Sawada SG, Berkovitz KE, Whang D, Dohan AM,
      Duchak J, White TE, Foltz J, O'Donnell JA, et al. Detection of coronary
      artery disease with upright bicycle exercise echocardiography. *J Am Soc
      Echocardiogr.* 1993;6:186-97.

129. Marwick TH, Anderson T, Williams MJ, Haluska B, Melin JA, Pashkow F,
      Thomas JD. Exercise echocardiography is an accurate and cost-efficient

technique for detection of coronary artery disease in women. *J Am Coll Cardiol.* 1995;26:335-41.

130. Geleijnse ML, Fioretti PM, Roelandt JR. Methodology, feasibility, safety and diagnostic accuracy of dobutamine stress echocardiography. *J Am Coll Cardiol.* 1997;30:595-606.

131. Verani MS. Myocardial perfusion imaging versus two-dimensional echocardiography: comparative value in the diagnosis of coronary artery disease. *J Nucl Cardiol.* 1994;1:399-414.

132. Verani MS. Stress myocardial perfusion imaging versus echocardiography for the diagnosis and risk stratification of patients with known or suspected coronary artery disease. *Semin Nucl Med.* 1999;29:319-29.

133. O'Keefe JH, Jr., Barnhart CS, Bateman TM. Comparison of stress echocardiography and stress myocardial perfusion scintigraphy for diagnosing coronary artery disease and assessing its severity. *Am J Cardiol.* 1995;75:25D-34D.

134. Poldermans D, Fioretti PM, Boersma E, Bax JJ, Thomson IR, Roelandt JR, Simoons ML. Long-term prognostic value of dobutamine-atropine stress echocardiography in 1737 patients with known or suspected coronary artery disease: A single-center experience. *Circulation.* 1999;99:757-62.

135. Krivokapich J, Child JS, Walter DO, Garfinkel A. Prognostic value of dobutamine stress echocardiography in predicting cardiac events in patients with known or suspected coronary artery disease. *J Am Coll Cardiol.* 1999;33:708-16.

136. Steinberg EH, Madmon L, Patel CP, Sedlis SP, Kronzon I, Cohen JL. Long-term prognostic significance of dobutamine echocardiography in patients

with suspected coronary artery disease: results of a 5-year follow-up study. *J Am Coll Cardiol.* 1997;29:969-73.

137. Davar JI, Brull DJ, Bulugahipitiya S, Coghlan JG, Lipkin DP, Evans TR. Prognostic value of negative dobutamine stress echo in women with intermediate probability of coronary artery disease. *Am J Cardiol.* 1999;83:100-2, A8.

138. Popp R, Agatston A, Armstrong W, Nanda N, Pearlman A, Rakowski H, Seward J, Silverman N, Smith M, Stewart W, Taylor R, Thys D, Davis C. Recommendations for training in performance and interpretation of stress echocardiography. Committee on Physician Training and Education of the American Society of Echocardiography. *J Am Soc Echocardiogr.* 1998;11:95-6.

139. Guyton AC, Hall JE. *Textbook of Medical Physiology.* 10 ed: W B Saunders; 2000.

140. Skyba DM, Jayaweera AR, Goodman NC, Ismail S, Camarano G, Kaul S. Quantification of myocardial perfusion with myocardial contrast echocardiography during left atrial injection of contrast. Implications for venous injection. *Circulation.* 1994;90:1513-21.

141. Kaul S, Jayaweera AR. Coronary and myocardial blood volumes: noninvasive tools to assess the coronary microcirculation? *Circulation.* 1997;96:719-24.

142. Linka AZ, Sklenar J, Wei K, Jayaweera AR, Skyba DM, Kaul S. Assessment of transmural distribution of myocardial perfusion with contrast echocardiography. *Circulation.* 1998;98:1912-20.

143. Wei K, Jayaweera AR, Firoozan S, Linka A, Skyba DM, Kaul S. Basis for detection of stenosis using venous administration of microbubbles during myocardial contrast echocardiography: bolus or continuous infusion? *J Am Coll Cardiol.* 1998;32:252-60.

144. Wei K, Jayaweera AR, Firoozan S, Linka A, Skyba DM, Kaul S. Quantification of myocardial blood flow with ultrasound-induced destruction of microbubbles administered as a constant venous infusion. *Circulation.* 1998;97:473-83.

145. Chilian WM, Layne SM. Coronary microvascular responses to reductions in perfusion pressure. Evidence for persistent arteriolar vasomotor tone during coronary hypoperfusion. *Circ Res.* 1990;66:1227-38.

146. Kanatsuka H, Lamping KG, Eastham CL, Marcus ML. Heterogeneous changes in epimyocardial microvascular size during graded coronary stenosis. Evidence of the microvascular site for autoregulation. *Circ Res.* 1990;66:389-96.

147. Henquell L, Honig CR. Intercapillary distances and capillary reserve in right and left ventricles: significance for control of tissue po2. *Microvasc Res.* 1976;12:35-41.

148. Crystal GJ, Downey HF, Bashour FA. Small vessel and total coronary blood volume during intracoronary adenosine. *Am J Physiol.* 1981;241:H194-201.

149. Weiss HR, Conway RS. Morphometric study of the total and perfused arteriolar and capillary network of the rabbit left ventricle. *Cardiovasc Res.* 1985;19:343-54.

150. Acad B, Weiss HR. Chemical sympathectomy and utilisation of coronary capillary reserve in rabbits. *Microvascular Research.* 1988;36:250-261.

151.   Rose CP, Goresky CA. Vasomotor control of capillary transit time

heterogeneity in the canine coronary circulation. *Circ Res.* 1976;39:541-54.

152.   Wu CC, Feldman MD, Mills JD, Manaugh CA, Fischer D, Jafar MZ,

Villanueva FS. Myocardial contrast echocardiography can be used to quantify

intramyocardial blood volume: new insights into structural mechanisms of

coronary autoregulation. *Circulation.* 1997;96:1004-11.

153.   Gould DK, Lipscomb K. Effects of coronary stenosis on coronary flow

reserve and resistance. *Am.J.Cardiol.* 1974;34:48-55.

154.   Eliasen P, Amtorp O. Effect of intracoronary adenosine upon regional blood

flow, microvascular blood volume and hematocrit in canine myocardium. *Int

J Microcirc Clin Exp.* 1984;3:3-12.

155.   Canty JM, Jr., Judd RM, Brody AS, Klocke FJ. First-pass entry of nonionic

contrast agent into the myocardial extravascular space. Effects on

radiographic estimates of transit time and blood volume. *Circulation.*

1991;84:2071-8.

156.   Ismail S, Jayaweera AR, Goodman NC, Camarano GP, Skyba DM, Kaul S.

Detection of coronary stenoses and quantification of the degree and spatial

extent of blood flow mismatch during coronary hyperemia with myocardial

contrast echocardiography. *Circulation.* 1995;91:821-30.

157.   Jayaweera AR, Wei K, Coggins M, Bin JP, Goodman C, Kaul S. Role of

capillaries in determining CBF reserve: new insights using myocardial

contrast echocardiography. *Am J Physiol.* 1999;277:H2363-72.

158.   Lafitte S, Matsugata H, Peters B, Togni M, Strachan M, Kwan OL, DeMaria

AN. Comparative value of dobutamine and adenosine stress in the detection

of coronary stenosis with myocardial contrast echocardiography. *Circulation.* 2001;103:2724-30.

159. Iskandrian AS, Verani MS, Heo J. Pharmacologic stress testing: mechanism of action, hemodynamic responses, and results in detection of coronary artery disease. *J Nucl Cardiol.* 1994;1:94-111.

160. Gramiak R, Shah PM. Echocardiography of the aortic root. *Invest Radiol.* 1968;3:356-66.

161. Feigenbaum H, Stone JM, Lee DA, Nasser WK, Chang S. Identification of ultrasound echoes from the left ventricle by use of intracardiac injections of indocyanine green. *Circulation.* 1970;41:615-21.

162. Jiang L, Pu SY, Yang MZ, et al. Left heart contrast echocardiography using a carbon dioxide producing agent (Abstract). *Circulation.* 1984;70:5.

163. Armstrong WF, Mueller TM, Kinney EL, Tickner EG, Dillon JC, Feigenbaum H. Assessment of myocardial perfusion abnormalities with contrast-enhanced two-dimensional echocardiography. *Circulation.* 1982;66:166-73.

164. Kemper AJ, O'Boyle JE, Cohen CA, Taylor A, Parisi AF. Hydrogen peroxide contrast echocardiography: quantification in vivo of myocardial risk area during coronary occlusion and of the necrotic area remaining after myocardial reperfusion. *Circulation.* 1984;70:309-17.

165. Tei C, Sakamaki T, Shah PM, Meerbaum S, Shimoura K, Kondo S, Corday E. Myocardial contrast echocardiography: a reproducible technique of myocardial opacification for identifying regional perfusion deficits. *Circulation.* 1983;67:585-93.

166. Feinstein SB, Ten Cate FJ, Zwehl W, Ong K, Maurer G, Tei C, Shah PM, Meerbaum S, Corday E. Two-dimensional contrast echocardiography. I. In vitro development and quantitative analysis of echo contrast agents. *J Am Coll Cardiol*. 1984;3:14-20.

167. Feinstein SB, Shah PM, Bing RJ, Meerbaum S, Corday E, Chang BL, Santillan G, Fujibayashi Y. Microbubble dynamics visualized in the intact capillary circulation. *J Am Coll Cardiol*. 1984;4:595-600.

168. de Jong N, Ten Cate FJ, Lancee CT, Roelandt JR, Bom N. Principles and recent developments in ultrasound contrast agents. *Ultrasonics*. 1991;29:324-30.

169. Dick CD, Feinstein SB, Peterson EM, et al. Biodistribution of a transpulmonary echocardiographic contrast agent (Abstract). *Circulation*. 1987;76:IV-506.

170. Plesset MS. The dynamics of cavitation bubbles. *Journal of Applied Mechanics*. 1949;16:272-282.

171. Miller MW, Miller DL, Brayman AA. A review of in vitro bioeffects of inertial ultrasonic cavitation from a mechanistic perspective. *Ultrasound Med Biol*. 1996;22:1131-54.

172. Miller DL, Thomas RM. Ultrasound contrast agents nucleate inertial cavitation in vitro. *Ultrasound Med Biol*. 1995;21:1059-65.

173. Everbach EC, Makin IR, Francis CW, Meltzer RS. Effect of acoustic cavitation on platelets in the presence of an echo-contrast agent. *Ultrasound Med Biol*. 1998;24:129-36.

174. Williams AR, Kubowicz G, Cramer E, Schlief R. The effects of the microbubble suspension SH U 454 (Echovist) on ultrasound-induced cell lysis in a rotating tube exposure system. *Echocardiography*. 1991;8:423-33.

175. Skyba DM, Camarano G, Goodman NC, Price RJ, Skalak TC, Kaul S. Hemodynamic characteristics, myocardial kinetics and microvascular rheology of FS-069, a second-generation echocardiographic contrast agent capable of producing myocardial opacification from a venous injection. *J Am Coll Cardiol*. 1996;28:1292-300.

176. Cohen JL, Cheirif J, Segar DS, Gillam LD, Gottdiener JS, Hausnerova E, Bruns DE. Improved left ventricular endocardial border delineation and opacification with OPTISON (FS069), a new echocardiographic contrast agent. Results of a phase III Multicenter Trial. *J Am Coll Cardiol*. 1998;32:746-52.

177. Crouse LJ, Cheirif J, Hanly DE, Kisslo JA, Labovitz AJ, Raichlen JS, Schutz RW, Shah PM, Smith MD. Opacification and border delineation improvement in patients with suboptimal endocardial border definition in routine echocardiography: results of the Phase III Albunex Multicenter Trial. *J Am Coll Cardiol*. 1993;22:1494-500.

178. Feinstein SB, Cheirif J, Ten Cate FJ, Silverman PR, Heidenreich PA, Dick C, Desir RM, Armstrong WF, Quinones MA, Shah PM. Safety and efficacy of a new transpulmonary ultrasound contrast agent: initial multicenter clinical results. *J Am Coll Cardiol*. 1990;16:316-24.

179. Grayburn PA, Weiss JL, Hack TC, Klodas E, Raichlen JS, Vannan MA, Klein AL, Kitzman DW, Chrysant SG, Cohen JL, Abrahamson D, Foster E, Perez JE, Aurigemma GP, Panza JA, Picard MH, Byrd BF, 3rd, Segar DS,

Jacobson SA, Sahn DJ, DeMaria AN. Phase III multicenter trial comparing the efficacy of 2% dodecafluoropentane emulsion (EchoGen) and sonicated 5% human albumin (Albunex) as ultrasound contrast agents in patients with suboptimal echocardiograms. *J Am Coll Cardiol.* 1998;32:230-6.

180. Mulvagh SL, Foley DA, Aeschbacher BC, Klarich KK, Seward JB. Second harmonic imaging of an intravenously administered echocardiographic contrast agent: Visualization of coronary arteries and measurement of coronary blood flow. *J Am Coll Cardiol.* 1996;27:1519-25.

181. von Bibra H, Sutherland G, Becher H, Neudert J, Nihoyannopoulos P. Clinical evaluation of left heart Doppler contrast enhancement by a saccharide-based transpulmonary contrast agent. The Levovist Cardiac Working Group. *J Am Coll Cardiol.* 1995;25:500-8.

182. Lambertz H, Schuhmacher U, Tries HP, Stein T. Improvement of pulmonary venous flow Doppler signal after intravenous injection of Levovist. *J Am Soc Echocardiogr.* 1997;10:891-8.

183. Caiati C, Montaldo C, Zedda N, Bina A, Iliceto S. New noninvasive method for coronary flow reserve assessment: contrast-enhanced transthoracic second harmonic echo Doppler. *Circulation.* 1999;99:771-8.

184. Rajagopalan B, Greenleaf J, Chevalier P, Bahn R. Myocardial blood flow: visualization with ultrasonic contrast agents. In: Metherell A, ed. *Acoustical Imaging.* New York: Plenum Publishing; 1980:719-729.

185. Kemper AJ, Force T, Kloner R, Gilfoil M, Perkins L, Hale S, Alker K, Parisi AF. Contrast echocardiographic estimation of regional myocardial blood flow after acute coronary occlusion. *Circulation.* 1985;72:1115-24.

186. Ten Cate FJ, Drury JK, Meerbaum S, Noordsy J, Feinstein S, Shah PM, Corday E. Myocardial contrast two-dimensional echocardiography: experimental examination at different coronary flow levels. *J Am Coll Cardiol.* 1984;3:1219-26.

187. Kondo S, Tei C, Meerbaum S, Corday E, Shah PM. Hyperemic response of intracoronary contrast agents during two-dimensional echographic delineation of regional myocardium. *J Am Coll Cardiol.* 1984;4:149-56.

188. Gage S, Vasey CG, Dillon JC, et al. Reactive hyperaemia: Evaluation with myocardial contrast echocardiography. (Abstract). *Journal of the American College of Cardiology.* 1986;7:189A.

189. Grayburn PA, Erickson JM, Escobar J, Womack L, Velasco CE. Peripheral intravenous myocardial contrast echocardiography using a 2% dodecafluoropentane emulsion: identification of myocardial risk area and infarct size in the canine model of ischemia. *J Am Coll Cardiol.* 1995;26:1340-7.

190. Eatock BC, Nishi RY, Johnston GW. Numerical studies of the spectrum of low-intensity ultrasound scattered by bubbles. *Journal of the Acoustical Society of America.* 1985;77:1692-1701.

191. de Jong N, Cornet R, Lancée CT. Higher harmonics of vibrating gas-filled microspheres. Part one: simulations. *Ultrasonics.* 1994;32:447-453.

192. de Jong N, Cornet R, Lancée CT. Higher harmonics of vibrating gas-filled microspheres. Part two: measurements. *Ultrasonics.* 1994;32:455-459.

193. Porter TR, Li S, Kricsfeld D, Armbruster RW. Detection of myocardial perfusion in multiple echocardiographic windows with one intravenous

injection of microbubbles using transient response second harmonic imaging. *J Am Coll Cardiol.* 1997;29:791-9.

194. Kaul S, Senior R, Dittrich H, Raval U, Khattar R, Lahiri A. Detection of coronary artery disease with myocardial contrast echocardiography: comparison with 99mTc-sestamibi single-photon emission computed tomography. *Circulation.* 1997;96:785-92.

195. Agrawal DI, Malhotra S, Nanda NC, Carvalho Truffa C, Agrawal G, Thakur AC, Jamil F, Taylor GW, Becher H. Harmonic Power Doppler Contrast Echocardiography: Preliminary Experimental Results. *Echocardiography.* 1997;14:631-636.

196. Becher H, Tiemann K, Schlief R, Luderitz B, Nanda NC. Harmonic Power Doppler Contrast Echocardiography: Preliminary Clinical Results. *Echocardiography.* 1997;14:637.

197. Tiemann K, Becher H, Bimmel D, Schlief R, Nanda NC. Stimulated Acoustic Emission Nonbackscatter Contrast Effect of Microbubbles Seen with Harmonic Power Doppler Imaging. *Echocardiography.* 1997;14:65-70.

198. Marwick TH, Brunken R, Meland N, Brochet E, Baer FM, Binder T, Flachskampf F, Kamp O, Nienaber C, Nihoyannopoulos P, Pierard L, Vanoverschelde JL, van der Wouw P, Lindvall K. Accuracy and feasibility of contrast echocardiography for detection of perfusion defects in routine practice: comparison with wall motion and technetium-99m sestamibi single-photon emission computed tomography. The Nycomed NC100100 Investigators. *J Am Coll Cardiol.* 1998;32:1260-9.

199. Porter TR, Xie F. Transient myocardial contrast after initial exposure to diagnostic ultrasound pressures with minute doses of intravenously injected

microbubbles. Demonstration and potential mechanisms. *Circulation.*
1995;92:2391-5.

200.   Wei K, Skyba DM, Firschke C, Jayaweera AR, Lindner JR, Kaul S.
       Interactions between microbubbles and ultrasound: in vitro and in vivo
       observations. *J Am Coll Cardiol.* 1997;29:1081-8.

201.   Porter TR, Li S, Jiang L, Grayburn P, Deligonul U. Real-time visualization of
       myocardial perfusion and wall thickening in human beings with intravenous
       ultrasonographic contrast and accelerated intermittent harmonic imaging. *J
       Am Soc Echocardiogr.* 1999;12:266-71.

202.   Shimoni S, Zoghbi WA, Xie F, Kricsfeld D, Iskander S, Gobar L, Mikati IA,
       Abukhalil J, Verani MS, O'Leary EL, Porter TR. Real-time assessment of
       myocardial perfusion and wall motion during bicycle and treadmill exercise
       echocardiography: comparison with single photon emission computed
       tomography. *J Am Coll Cardiol.* 2001;37:741-7.

203.   Tiemann K, Lohmeier S, Kuntz S, Koster J, Pohl C, Burns P, R T, Nanda NC,
       Luderitz B, Becher H. Real-Time Contrast Echo Assessment of Myocardial
       Perfusion at Low Emission Power: First Experimental and Clinical Results
       Using Power Pulse Inversion Imaging. *Echocardiography.* 1999;16:799-809.

204.   Hope Simpson D, Chin CT, Burns PN. Pulse Inversion Doppler: A New
       Method for Detecting Nonlinear Echoes from Microbubble Contrast Agents.
       IEEE Transactions on Ultrasonics, Ferroelectrics, and Frequency Control.
       1999;46:372-382.

205.   Porter TR, Xie F, Silver M, Kricsfeld D, Oleary E. Real-time perfusion
       imaging with low mechanical index pulse inversion Doppler imaging. *J Am
       Coll Cardiol.* 2001;37:748-53.

206. Armstrong WF, O'Donnell J, Ryan T, Feigenbaum H. Effect of prior myocardial infarction and extent and location of coronary disease on accuracy of exercise echocardiography. *J Am Coll Cardiol*. 1987;10:531-8.

207. Becher H, Burns P. Contrast Agents for Echocardiography: Principles and Instrumentation. In: *Handbook of Contrast Echocardiography. Left Ventricular Function and Myocardial Perfusion*. Frankfurt and New York: Springer Verlag; 2000:pp 15. Figures 17 and 18.

208. Goldberg BB, Liu JB, Burns PN, Merton DA, Forsberg F. Galactose-based intravenous sonographic contrast agent: experimental studies. *J Ultrasound Med*. 1993;12:463-470.

209. Albrecht T, Urbank A, Mahler M, Bauer A, Dore C, Blomley M, Cosgrove D, Schlief R. Prolongation and optimization of Doppler enhancement with a microbubble US contrast agent by using continuous infusion: preliminary experience. *Radiology*. 1998;207:339-347.

210. Weissman NJ, Cohen MC, Hack TC, Gillam LD, Cohen JL, Kitzman DW. Infusion versus bolus contrast echocardiography: a multicenter, open-label, crossover trial. *Am Heart J*. 2000;139:399-404.

211. Correas JM, Burns PN, Lai X, Qi X. Infusion versus bolus of an ultrasound contrast agent: in vivo dose-response measurements of BR1. *Invest Radiol*. 2000;35:72-9.

212. Albrecht T, Urbank A, Mahler M, Bauer A, Dore CJ, Blomley MJ, Cosgrove DO, Schlief R. Prolongation and optimization of Doppler enhancement with a microbubble US contrast agent by using continuous infusion: preliminary experience. *Radiology*. 1998;207:339-47.

213. Miller JJ, Tiemann K, Podell S, Doerr Stevens JK, Kuvelas T, Greener Y, Killam AL, Goenechea J, Dittrich HC, Becher H. In vitro, animal, and human characterization of OPTISON infusions for myocardial contrast echocardiography. *J Am Soc Echocardiogr.* 1999;12:1027-34.

214. Kolias TJ, Avelar E, Bradsher K, Cermak L, Armstrong WF, Vannan MA. Power Doppler dual-frame triggering of myocardial contrast echocardiography: a quantitative video intensity analysis. *Echocardiography.* 2001;18:497-501.

215. Heinle SK, Noblin J, Goree-Best P, Mello A, Ravad G, Mull S, Mammen P, Grayburn PA. Assessment of myocardial perfusion by harmonic power Doppler imaging at rest and during adenosine stress: comparison with (99m)Tc-sestamibi SPECT imaging. *Circulation.* 2000;102:55-60.

216. Bransford TL, Pyatt L, McKinney L, Dolan M, Habermehl K, St. Vrain J, Totta C, Labovitz AJ. Continuous Echo Contrast Infusion is Superior to Bolus Injection During Dobutamine Stress Echocardiography for Simultaneous Wall Motion Myocardial Perfusion Analysis. *Journal of the American College of Cardiology.* 2000;35:425.

217. Ugolini P, Delouche A, Herment A, Diebold B. In vitro quantification of flow using continuous infusion of Levovist and pairs of harmonic power Doppler images. *Ultrasound Med Biol.* 2001;27:637-42.

218. Koster J, Schlosser T, Pohl C, Lentz C, Lohmaier S, Veltmann C, Kuntz-Hehner S, Omran H, Luderitz B, Becher H, Tiemann K. Blood flow assessment by ultrasound-induced destruction of echocontrast agents using harmonic power Doppler imaging: which parameters determine contrast replenishment curves? *Echocardiography.* 2001;18:1-8.

219. Ugolini P, Delouche A, Herment A, Diebold B. In vitro flow quantification with contrast power Doppler imaging. *Ultrasound Med Biol.* 2000;26:113-20.

220. Broillet A, Puginier J, Ventrone R, Schneider M. Assessment of myocardial perfusion by intermittent harmonic power Doppler using SonoVue, a new ultrasound contrast agent. *Invest Radiol.* 1998;33:209-15.

221. Masugata H, Cotter B, Peters B, Ohmori K, Mizushige K, DeMaria AN. Assessment of coronary stenosis severity and transmural perfusion gradient by myocardial contrast echocardiography: comparison of gray-scale B-mode with power Doppler imaging. *Circulation.* 2000;102:1427-33.

222. Hirooka K, Miyatake K, Hanatani A, Komamura K, Nakatani S, Yasumura Y, Yamagishi M. Enhanced methods for visualizing myocardial perfusion with peripheral venous injection of levovist: application of triggered harmonic imaging and triggered harmonic power Doppler imaging techniques. *Int J Card Imaging.* 2000;16:233-46.

223. Yao J, Takeuchi M, Teupe C, Sheahan M, Connolly R, Walovitch RC, Fetterman RC, Church CC, Udelson JE, Pandian NG. Evaluation of a new ultrasound contrast agent (AI-700) using two-dimensional and three-dimensional imaging during acute ischemia. *J Am Soc Echocardiogr.* 2002;15:686-94.

224. Nanda NC, Miller A, Puri VK, Fan PH, Tiemann K, Becher H, Main J, Batra S. Assessment of myocardial perfusion by power contrast imaging using a new echo contrast agent. *Echocardiography.* 2000;17:457-61.

225. Senior R, Kaul S, Soman P, Lahiri A. Power doppler harmonic imaging: a feasibility study of a new technique for the assessment of myocardial perfusion. *Am Heart J.* 2000;139:245-51.

226. Moraes A, Morcerf F, Carrinho M, Salek F, Nogueira A, Palheiro F, Dohmann H. Accuracy of Intravenous Myocardial Contrast Echocardiography to Detect Single-vessel Coronary Artery Disease. *Journal of the American Society of Echocardiography*. 1999;12:(ABSTRACT)364.

227. Beam C. Strategies for improving power in diagnostic radiology research. *Am J Roentgenol*. 1992;159:631-637.

228. Blackwelder W. Proving the null hypothesis in clinical trials. *Control. Clin. Trials*. 1982;3:345-353.

229. Schiller NB, Shah PM, Crawford M, DeMaria A, Devereux R, Feigenbaum H, Gutgesell H, Reichek N, Sahn D, Schnittger I, et al. Recommendations for quantitation of the left ventricle by two-dimensional echocardiography. American Society of Echocardiography Committee on Standards, Subcommittee on Quantitation of Two-Dimensional Echocardiograms. *J Am Soc Echocardiogr*. 1989;2:358-67.

230. Becher H, Burns P. Assessment of Myocardial Perfusion by Contrast Echocardiography. In: *Handbook of Contrast Echocardiography. Left Ventricular Function and Myocardial Perfusion*. Frankfurt and New York: Springer Verlag; 2000.

231. Baim D, Grossman W. *Grossman's Cardiac Catheterization, Angiography, and Intervention*. 5 ed. Philadelphia: Lippincott Williams & Wilkins; 1996.

232. Wilson RF, Wyche K, Christensen BV, Zimmer S, Laxson DD. Effects of adenosine on human coronary arterial circulation. *Circulation*. 1990;82:1595-606.

233. Ogilby JD, Iskandrian AS, Untereker WJ, Heo J, Nguyen TN, Mercuro J. Effect of intravenous adenosine infusion on myocardial perfusion and

function. Hemodynamic/angiographic and scintigraphic study. *Circulation.* 1992;86:887-95.

234.   Ogilby JD, Heo J, Iskandrian AS. Effect of adenosine on coronary blood flow and its use as a diagnostic test for coronary artery disease. *Cardiovasc Res.* 1993;27:48-53.

235.   Bartunek J, Wijns W, Heyndrickx GR, de Bruyne B. Effects of dobutamine on coronary stenosis physiology and morphology: comparison with intracoronary adenosine. *Circulation.* 1999;100:243-9.

236.   Krahwinkel W, Ketteler T, Godke J, Wolfertz J, Ulbricht LJ, Krakau I, Gulker H. Dobutamine stress echocardiography. *Eur Heart J.* 1997;18 Suppl D:D9-15.

237.   Picano E, Marini C, Pirelli S, Maffei S, Bolognese L, Chiriatti G, Chiarella F, Orlandini A, Seveso G, Colosso MQ, et al. Safety of intravenous high-dose dipyridamole echocardiography. The Echo-Persantine International Cooperative Study Group. *Am J Cardiol.* 1992;70:252-8.

238.   Pirelli S, Danzi GB, Alberti A, Massa D, Piccalo G, Faletra F, Picano E, Campolo L, De Vita C. Comparison of usefulness of high-dose dipyridamole echocardiography and exercise electrocardiography for detection of asymptomatic restenosis after coronary angioplasty. *Am J Cardiol.* 1991;67:1335-8.

239.   Previtali M, Lanzarini L, Fetiveau R, Poli A, Ferrario M, Falcone C, Mussini A. Comparison of dobutamine stress echocardiography, dipyridamole stress echocardiography and exercise stress testing for diagnosis of coronary artery disease. *Am J Cardiol.* 1993;72:865-70.

240. Cortigiani L, Lombardi M, Michelassi C, Paolini EA, Nannini E. Significance of myocardial ischemic electrocardiographic changes during dipyridamole stress echocardiography. *Am J Cardiol*. 1998;82:1008-12.

241. Nagarajan R, Abou-Mohamed G, Myers T, Caldwell RW. A novel catecholamine, arbutamine, for a pharmacological cardiac stress agent. *Cardiovasc Drugs Ther*. 1996;10:31-8.

242. Dennis CA, Pool PE, Perrins EJ, Mohiuddin SM, Sklar J, Kostuk WJ, Muller DW, Starling MR. Stress testing with closed-loop arbutamine as an alternative to exercise. The International Arbutamine Study Group. *J Am Coll Cardiol*. 1995;26:1151-8.

243. Bach DS, Cohen JL, Fioretti PM, Ginzton LE, Sklar J, Zabalgoitia M, Crouse L. Safety and efficacy of closed-loop arbutamine stress echocardiography for detection of coronary artery disease. International Arbutamine Study Group. *Am J Cardiol*. 1998;81:32-5.

244. Djordjevic-Dikic AD, Ostojic MC, Beleslin BD, Stepanovic J, Petrasinovic Z, Babic R, Stojkovic SM, Stankovic G, Nedeljkovic M, Nedeljkovic I, Kanjuh V. High dose adenosine stress echocardiography for noninvasive detection of coronary artery disease. *J Am Coll Cardiol*. 1996;28:1689-95.

245. Salustri A, Fioretti PM, McNeill AJ, Pozzoli MM, Roelandt JR. Pharmacological stress echocardiography in the diagnosis of coronary artery disease and myocardial ischaemia: a comparison between dobutamine and dipyridamole. *Eur Heart J*. 1992;13:1356-62.

246. Kugiyama K, Inobe Y, Ohgushi M, Morita E, Motoyama T, Ogawa H, Yasue H. Comparison of coronary hemodynamics during infusions of dobutamine and adenosine in patients with angina pectoris. *Jpn Circ J*. 1998;62:1-6.

247. Verani MS, Mahmarian JJ, Hixson JB, Boyce TM, Staudacher RA. Diagnosis of coronary artery disease by controlled coronary vasodilation with adenosine and thallium-201 scintigraphy in patients unable to exercise. *Circulation.* 1990;82:80-7.

248. Nguyen T, Heo J, Ogilby JD, Iskandrian AS. Single photon emission computed tomography with thallium-201 during adenosine-induced coronary hyperemia: correlation with coronary arteriography, exercise thallium imaging and two-dimensional echocardiography. *J Am Coll Cardiol.* 1990;16:1375-83.

249. Gupta NC, Esterbrooks DJ, Hilleman DE, Mohiuddin SM. Comparison of adenosine and exercise thallium-201 single-photon emission computed tomography (SPECT) myocardial perfusion imaging. The GE SPECT Multicenter Adenosine Study Group. *J Am Coll Cardiol.* 1992;19:248-57.

250. Parodi O, Marcassa C, Casucci R, Sambuceti G, Verna E, Galli M, Inglese E, Marzullo P, Pirelli S, Bisi G, et al. Accuracy and safety of technetium-99m hexakis 2-methoxy-2-isobutyl isonitrile (Sestamibi) myocardial scintigraphy with high dose dipyridamole test in patients with effort angina pectoris: a multicenter study. Italian Group of Nuclear Cardiology. *J Am Coll Cardiol.* 1991;18:1439-44.

251. Leppo JA. Dipyridamole myocardial perfusion imaging. *J Nucl Med.* 1994;35:730-3.

252. Pennell DJ, Underwood SR, Swanton RH, Walker JM, Ell PJ. Dobutamine thallium myocardial perfusion tomography. *J Am Coll Cardiol.* 1991;18:1471-9.

253. Pennell DJ, Underwood SR, Ell PJ. Safety of dobutamine stress for thallium-201 myocardial perfusion tomography in patients with asthma. *Am J Cardiol.* 1993;71:1346-50.

254. Hays JT, Mahmarian JJ, Cochran AJ, Verani MS. Dobutamine thallium-201 tomography for evaluating patients with suspected coronary artery disease unable to undergo exercise or vasodilator pharmacologic stress testing. *J Am Coll Cardiol.* 1993;21:1583-90.

255. Levine MG, Ahlberg AW, Mann A, White MP, McGill CC, Mendes de Leon C, Piriz JM, Waters D, Heller GV. Comparison of exercise, dipyridamole, adenosine, and dobutamine stress with the use of Tc-99m tetrofosmin tomographic imaging. *J Nucl Cardiol.* 1999;6:389-96.

256. Morcerf F, Moraes A, Nogueira A, Castier M, Salek F, Pereira W, Palheiro F, Dohmann H. Myocardial contrast echocardiography with intravenous microbubbles and adenosine bolus injection: a new method to identify myocardial perfusion defects in humans. *J Am Coll Cardiol.* 1998;31(suppl C):273C.

257. Morcerf F, Moraes A, Carrinho M, Salek F, Nogueira A, Palheiro F, Dohmann H. Adenosine contrast echocardiography in 936 consecutive patients with suspected coronary artery disease: experience of a single center. *J Am Coll Cardiol.* 2000;35 (suppl A):413A.

258. Nesser H, Yao J, Tkalec W, et al. Comparison of Adenosine infusion and Adenosine bolus in myocardial contrast echocardiography (Optison) for detection of coronary artery disease using nuclear imaging as the independent standard. *Journal of the American College of Cardiology.* 2000;35(2, Suppl. A):414.

259. Tani T, Tanabe K, Ono M, Katayama M, Ibuki M, Mizoguchi S, Takagi T, Yamamuro A, Tamita K, Yamabe K, Yagi T, Nagai K, Shiratori K, Morioka S. Quantitative assessment of harmonic power Doppler myocardial perfusion imaging with intravenous Levovist in patients with myocardial infarction: comparison with myocardial viability evaluated by thallium-201 single-photon emission computed tomography and coronary flow reserve. *Eur J Echocardiogr.* 2002;3:287-97.

260. Branco L. Accuracy and feasibility of contrast echocardiography for detection of perfusion defects in routine practice. Comparison with wall motion and technetium--99m sestamibi single--photon emission computed tomography. *Rev Port Cardiol.* 1999;18:415-6.

261. Oraby MA, Hays J, Maklady FA, El-Hawary AA, Yaneza LO, Zabalgoitia M. Comparison of real-time coherent contrast imaging to dipyridamole thallium-201 single-photon emission computed tomography for assessment of myocardial perfusion and left ventricular wall motion. *Am J Cardiol.* 2002;90:449-54.

262. Verna E, Ceriani L, Giovanella L, Binaghi G, Garancini S. "False-positive" myocardial perfusion scintigraphy findings in patients with angiographically normal coronary arteries: insights from intravascular sonography studies. *J Nucl Med.* 2000;41:1935-40.

263. Cheirif J, Zoghbi WA, Bolli R, O'Neill PG, Hoyt BD, Quinones MA. Assessment of regional myocardial perfusion by contrast echocardiography. II. Detection of changes in transmural and subendocardial perfusion during dipyridamole-induced hyperemia in a model of critical coronary stenosis. *J Am Coll Cardiol.* 1989;14:1555-65.

264. Hyodo E, Muro T, Hozumi T, Fukuda S, Watanebe H, Yoshiyama M, Takeuchi K, Iwao H, Yoshikawa J. Observation of the ischemic cascade in humans using contrast echocardiography during dobutamine stress. *Circ J.* 2003;67:406-10.

265. Tiemann K, Becher H, Lohmeier S, et al. Real-time assessment of tissue perfusion following bubble destruction at low emission power. First experimental results using power pulse inversion imaging. In: *49th Scientific Session of the American College of Cardiology.* Anaheim, California, USA: Journal of The American College of Cardiology; 2000.

266. Tiemann K, Veltmann C, Ghanem A, Lohmaier S, Bruce M, Kuntz-Hehner S, Pohl C, Ehlgen A, Schlosser T, Omran H, Becher H. The impact of emission power on the destruction of echo contrast agents and on the origin of tissue harmonic signals using power pulse-inversion imaging. *Ultrasound Med Biol.* 2001;27:1525-33.

267. Porter TR, Oberdorfer J, Rafter P, Lof J, Xie F. Microbubble responses to a similar mechanical index with different real-time perfusion imaging techniques. *Ultrasound Med Biol.* 2003;29:1187-92.

268. Mor-Avi V, Caiani EG, Collins KA, Korcarz CE, Bednarz JE, Lang RM. Combined assessment of myocardial perfusion and regional left ventricular function by analysis of contrast-enhanced power modulation images. *Circulation.* 2001;104:352-7.

269. Masugata H, Peters B, Lafitte S, Strachan GM, Ohmori K, DeMaria AN. Quantitative assessment of myocardial perfusion during graded coronary stenosis by real-time myocardial contrast echo refilling curves. *J Am Coll Cardiol.* 2001;37:262-9.

270. Skyba D, Averkiou M, Loflin C, et.al. Imaging myocardial perfusion in real time: a feasibility study using rapid mechanical index switching during power pulse inversion imaging. *Journal of the American College of Cardiology.* 2000;35:488.

271. Masugata H, Lafitte S, Peters B, Strachan GM, DeMaria AN. Comparison of real-time and intermittent triggered myocardial contrast echocardiography for quantification of coronary stenosis severity and transmural perfusion gradient. *Circulation.* 2001;104:1550-6.

272. Tiemann K, Becher H, Kuntz S, et.al. Real-time perfusion imaging during intravenous contrast echocardiography: First clinical results using the new contrast specific imaging modality Power-Pulse Inversion. *Journal of the American College of Cardiology.* 2000;35:457.

273. Murthy TH, Li P, Locvicchio E, Baisch C, Dairywala I, Armstrong WF, Vannan M. Real-time myocardial blood flow imaging in normal human beings with the use of myocardial contrast echocardiography. *J Am Soc Echocardiogr.* 2001;14:698-705.

274. Lambertz H, Bonhof J, Brechtken J, Stein T, Tries HP, Lethen H. [Noninvasive determination of coronary flow reserve with signal enhanced high resolution transthoracic Doppler color echocardiography]. *Herz.* 1998;23:516-25.

275. Kern MJ. Coronary physiology revisited : practical insights from the cardiac catheterization laboratory. *Circulation.* 2000;101:1344-51.

276. Bekeredjian R, Hansen A, Filusch A, Dubart AE, Da Silva KG, Jr., Hardt SS, Korosoglou G, Kuecherer HF. Cyclic variation of myocardial signal intensity

in real-time myocardial perfusion imaging. *J Am Soc Echocardiogr.* 2002;15:1425-31.

277. Tiemann K, Ghanem A, Schlosser T, Ehlgen A, Kuntz-Hehner S, Haushofer M, Bimmel D, Borovac M, Nanda NC, Omran H, Becher H. Subendocardial steal effect seen with real-time perfusion imaging at low emission power during adenosine stress: replenishment M-mode processing allows visualization of vertical steal. *Echocardiography.* 2001;18:689-94.